



Cite this: *Sustainable Energy Fuels*, 2025, 9, 4793

## Advancements in gasification technologies: insights into modeling studies, power-to-X applications and sustainability assessments

Sonu Kumar,\* Rupesh Palange  and Cataldo De Blasio

The paper presents a comprehensive overview of the latest biomass gasification technologies discussing various configurations like fixed bed, entrained-flow, and fluidized-bed gasifiers along with advanced systems like plasma, multistage biomass, supercritical water and solar gasifiers. The article gives a comparative analysis by examining the performance levels, operational efficiency, and technical parameters within each gasification system. Additionally, the review delves into various gasification modeling approaches which include thermodynamic equilibrium models, kinetic models, computational fluid dynamics and data-driven models using machine learning. These modeling techniques are assessed in terms of their governing equations, solution methods, and accuracy in predicting gasification outcomes. The study also investigates the conversion of syngas and power into green fuels such as methane, hydrogen, and ammonia, with a focus on their techno-economic feasibility and sustainability through life cycle assessment. The review highlights multiple synthesis pathways for green fuel production and evaluates the most efficient methods for maximizing output while maintaining cost-effectiveness. Key research gaps and challenges within gasification technology, modeling methodologies, and green fuel synthesis are identified, emphasizing the need for improvements in gasifier operational efficiency, tar reduction, and model precision.

Received 10th April 2025

Accepted 20th July 2025

DOI: 10.1039/d5se00504c

rsc.li/sustainable-energy

## 1 Introduction

Contemporary research places the development of sustainable technologies at the forefront of its priorities, as scientific evidence consistently indicates that current environmental conditions are deteriorating at an alarming rate.<sup>1</sup> Emissions Database for Global Atmospheric Research (EDGAR) revealed that 53.0 gigatons of carbon dioxide equivalent (Gt CO<sub>2</sub>eq) made up greenhouse gas (GHG) emissions during 2023. The Finnish government remains focused on achieving carbon neutrality by 2035 before striving toward carbon negativity. The average annual decrease in carbon emissions in Finland totals 4–5 percent yet emissions reached about 40 million tons during the year 2023. Multiple emerging technological frameworks offer promising alternatives for transitioning power systems currently dependent on coal, petroleum, and natural gas resources.<sup>2</sup> Thermal conversion techniques such as hydro-thermal liquefaction, pyrolysis, carbonization, torrefaction, combustion, and gasification are actively being explored for biomass processing.<sup>3,4</sup> Among these, biomass gasification stands out as one of the most viable solutions to current environmental challenges.<sup>5</sup> The effectiveness of the gasification

process is highly influenced by the choice of gasifying agent and the composition of the biomass feedstock, which together determine the reactivity of the system and the kinetic behavior of the gasifier design.<sup>6</sup> Gas yield during gasification increases with temperature, with stable syngas production yields reaching up to approximately 90% at elevated operating temperatures.<sup>7</sup> Additionally, the gasification process contributes to the mitigation of municipal solid waste, resulting in a 70–80% reduction in mass and an 80–90% decrease in volume of the feedstock.<sup>8</sup> This process consists of four distinct stages which include drying, then proceeds through pyrolysis (also named as devolatilization) after which oxidation (combustion) and reduction (char gasification) take place.<sup>9</sup> Operational conditions and the improvement of syngas production performance together with carbon conversion efficiency optimization are directly affected by gasification reactivity.<sup>10</sup> The gasification process transforms carbon-based compounds into syngas that mostly consists of H<sub>2</sub> (hydrogen), CH<sub>4</sub> (methane) and CO (carbon monoxide) by introducing a limited amount of oxidizer. The main purpose of gasification differs from traditional combustion and pyrolysis because it targets the generation of efficient syngas for electricity production.<sup>11</sup> Technology obtains acclaim because it can generate products through technology applications using effective emission trapping strategies and processing multiple sources of raw materials.<sup>12</sup> For instance, the low energy materials like refinery byproducts, biomass and

Laboratory of Energy Technology, Faculty of Science and Engineering, Åbo Akademi University, Rantakatu 2, 65100 Vaasa, Finland. E-mail: sonu.kumar@abo.fi; Tel: +358 466376284



municipal solid waste which were previously not utilized effectively are today understood as sustainable energy sources.<sup>13</sup> Gasification differs from combustion and pyrolysis in terms of the amount of oxidant required and the nature of the resulting products.<sup>14</sup> Gasification operates with a varied range of raw materials split across six fundamental groups that include coke, natural gas, coal, petroleum, along with waste and biomass. Among these, coal remains the predominant feedstock, with total syngas production capacities of 130 GWth in operation.<sup>15,16</sup> Between 1999 and 2021, the total energy power for gasification installations, including planning and construction, grew from 42 GWth to 400 GWth, which keeps on raising every year.<sup>1</sup> The gasifying agent used in the process can be steam, air, oxygen, carbon dioxide, or a combination of these.<sup>17</sup> Across the world, large amounts of agricultural residues are produced each year, including fruit shells, straws, seeds, nutshells, plant stalks, molasses, with green leaves, and stover, which serve as biomass sources.<sup>18</sup> According to USDA Foreign Agricultural Service almost 85 million tons of rapeseeds produced per year globally.<sup>19</sup> Moreover, current global production of municipal solid waste (MSW) is estimated to range between 1.3 and 1.9 billion tons annually and is projected to rise to 4.2 billion tons by 2050.<sup>20</sup> The syngas generated from biomass gasification has a wide range of applications like, combustion at elevated temperatures to produce heat or energy, it can also be used as a fuel source for hydrogen-based fuel cells, and utilized in the production of methanol and other valuable liquid fuels as shown in Fig. 1.<sup>21</sup> Gasification leads to the creation of two additional outputs including biochar and tar. Besides serving as agricultural fertilizer biochar acts as an industrial filter absorbent and functions as an energy carrier.<sup>22</sup> The different stages of gasification occur at specific temperature ranges: drying takes place below 150 °C and completes around 250 °C, pyrolysis follows, occurring between 250 °C and 700 °C. Oxidation then occurs within the 700 °C to 1500 °C range, while reduction proceeds from 800 °C to 1100 °C.<sup>23</sup> Multiple parameters influence gasifier operation, including feedstock selection, gasifying agent type, gasification temperature, feeding ratios, reactor

configuration, and overall operational conditions.<sup>24</sup> Gasifiers exist in three principal categories which differ by gas flow mechanisms: fixed bed also named as moving bed and fluidized bed along with entrained flow gasifiers.<sup>25</sup> Gasification technology has advanced through the development of plasma gasifiers, supercritical water gasifiers, and solar-driven gasifiers. Co-gasification approaches, as well as the integration of gasification with anaerobic digestion, have also been explored to enhance overall gasification efficiency and performance.<sup>1</sup>

Mathematical modeling plays a crucial role in design and analysis of industrial and pilot gasification systems. Popular modeling approaches include thermodynamic equilibrium models, kinetic models, and artificial neural network (ANN) models.<sup>26</sup> A majority of biomass gasification investigations depend on equilibrium models with these models accounting for close to 60% of reported studies. Analysis using CFD or ANN methods remains minimal throughout the research.<sup>27</sup> System analysis through CFD modeling uses primarily mass, heat and momentum conservation principles to provide powerful insights into fluid dynamics and heat transfer besides examining energy flows and chemical reactions and mass and momentum conversions within a system.<sup>24</sup> Approximately 72.5% of studies related to gasification modeling have utilized the non-stoichiometric approach in equilibrium model.<sup>28</sup> Numerical solutions of gasification for multiphase flows can be categorized into Eulerian formulations, for instance the two-fluid, and Lagrangian formulations including the discrete element method and the multiphase particle-in-cell method.<sup>29</sup> Also, the data driven model based on ANN proved very accurate for predicting syngas production and chemical breakdown throughout the fixed-bed gasifier biomass conversion process.<sup>30</sup>

Gasification using air generates a fuel gas with a low heating value, typically ranging from 4 to 7 MJ Nm<sup>-3</sup>.<sup>31</sup> When O<sub>2</sub> and steam are used in coal gasification, the resulting synthesis gas has a heating value ranging between 10 and 18 MJ Nm<sup>-3</sup>.<sup>32</sup> Despite extensive research and numerous publications on gasification, large-scale commercialization of these technologies remains limited. The highest reported gasification

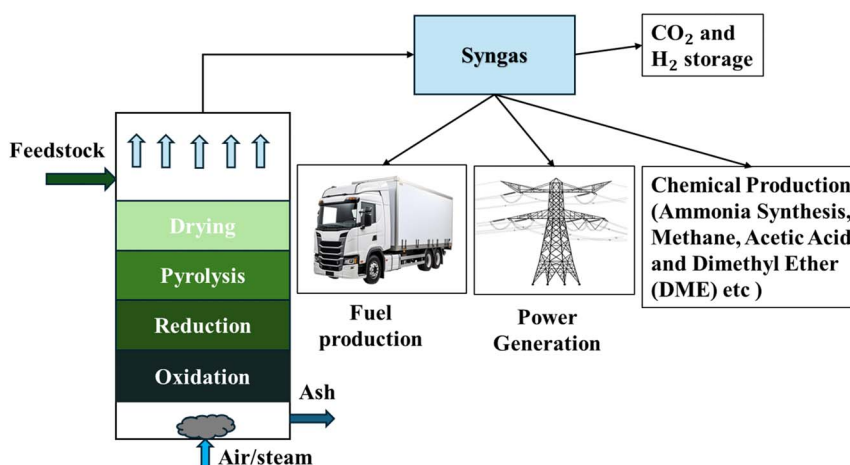


Fig. 1 Basics of gasification process and its applications.



efficiencies for various feedstocks are: coal at 68.5%, pine needles at 76.0%, plywood at 76.5%, and lignite at 74.0%. Additionally, cold gasification efficiency typically ranges between 63% and 66%.<sup>33</sup>

This review explores recent advancements in gasification technology, integrating both traditional and advanced modeling approaches to predict gas composition and assessing the sustainability of green fuel production. It critically evaluates various gasification technologies by analyzing their cold gas efficiency (CGE) and carbon conversion efficiency and also offering comparative insights into different modeling techniques. The study also examines cost-effective biomass-to-energy conversion pathways specializing in hydrogen ( $H_2$ ), methane ( $CH_4$ ), and ammonia ( $NH_3$ ) production. A comprehensive techno-economic assessment is presented, considering factors such as total production cost, capital investment, transportation expenses, energy costs, payback periods, and the carbon-negative potential of green fuel synthesis through life cycle analysis. Additionally, the study investigates the integrated synthesis of ammonia and methanol within gasification systems, identifying operational synergies to enhance process efficiency. By highlighting current research gaps in gasification technology and modeling approaches, this review provides a roadmap for advancing sustainable energy solutions and promoting innovation in green fuel production.

## 2 Gasification reactors and configurations

### 2.1 Fixed bed, fluidized bed and entrained flow gasifier

There are multiple factors influencing biomass gasifier design including available fuel resources alongside the properties of biomass particles, ash contents and the planned application area. The gasifier has been divided into three types based on its design and functionality which are fixed bed, fluidized bed, and entrained flow gasifier. Fig. 2 presents detailed configurations

of the three gasifiers with insight into their working principle. The commercial sector relies on fixed-bed gasifiers primarily because their simple structure allows for reliable operation. Whereas moving bed gasifiers operate under this name because the fuel descends through the plant in a coolant block-like manner. The operating pressure range of these gasifiers' spans from 0 bars up to 70 bars. The three fixed-bed gasifier types are updraft, downdraft and cross draft depending on the movement relationships between the gasifying agent, syngas and feedstock. The fixed-bed gasifier contains solid fuel particles inside a reactor that uses different flows for gasifying agents and reaction products based on reactor design specifications. The updraft design causes the materials to go upward within the reactor while the downdraft directs them downward and cross-draft systems enable horizontal movement across the unit.<sup>9</sup> Gasifiers operating with fixed beds employ three stages of operation that integrate wet scrubbing alongside cyclones followed by dry filtration to cleanse the generated gas. These gasifiers demonstrate a slow descent through the reactor while using concrete or steel components for construction and achieve high carbon conversion rates and long periods of solid residence. Research into tar control has resulted in the development of effective solutions for addressing this challenge.<sup>34</sup> The fixed bed gasification system provides several advantages through its ability to process feedstock with high ash content while generating clean gas and reaching excellent carbon conversion levels together with producing molten slag. These reactors face several operational challenges that hinder their efficiency and broader adoption. Exothermic reactions can create localized hot spots, leading to uneven thermal distribution and potential equipment stress. Ash accumulation on the grate may cause blockages, reducing system efficiency, while channeling where gas flow bypasses portions of the fuel result in incomplete gasification and diminished syngas quality. This technology often exhibits limited specific capacity and slow start-up times, necessitating uniform, large feed materials to ensure consistent operation.<sup>35</sup>

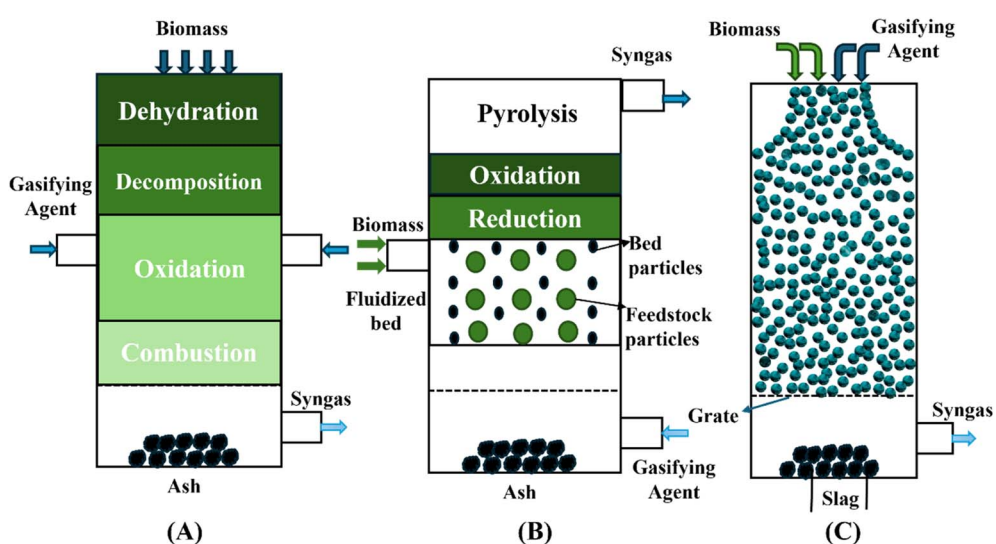


Fig. 2 (A) Fixed bed, (B) fluidized bed, and (C) entrained flow gasifier.



The two types of fluidized bed gasifiers include bubbling and circulating which differ based on their flow characteristics and heat exchange capabilities. A bubbling fluidized bed uses sand or alumina particles to form an inert condition before the gas velocity reaches the minimum fluidization level. Higher gas velocities in circulating fluidized beds create conditions which cause particles to exit the system with the gas stream. The gasifier receives these particles in a cyclone device which acts to return them to the gasifier system.<sup>36</sup>

The solid particles in a cylindrical fluidized bed stay suspended through gas or liquid flow to achieve optimized surface contact for efficient reactions. Excellent heat and material transfer functions together with uniform temperature control alongside the ability to handle various fuel types represent the main advantages of this system. Dust production together with particulate formation represents a significant downside because these pollutants affect equipment in the subsequent stages.<sup>35</sup> Fluidized bed gasifiers deliver several benefits through their perfect temperature control system with excellent heat exchange capabilities and efficient hot spot elimination abilities. The large fuel inventory alongside good gas-solid mixing produces devices with easy operation as well as high reliability. The gasifiers exhibit multiple advantageous characteristics because they achieve high specific capacity by delivering quick reaction rates while maintaining short solid residence times and working at partial load levels between 40–120%. These systems need minimal physical space while accepting various fuel properties and particles together with strong carbon conversion for initial gas filter operations. The product gas obtained from these units contains minimal phenolic substances while requiring lower overall investment costs.<sup>35,37</sup>

The challenges of these gasifiers include dual temperature requirements for different feedstocks together with more complex operations than fixed beds and substantial pressure loss throughout the system and restricted capacity caused by gas velocity effects. Non-molten ash along with elevated energy requirements and abundant dust matter in the gas phase represent different disadvantages of these units.

The studies on existing commercial and near-commercial biomass gasification technologies indicate that directly heated fluidized bed (FB) gasifiers stand as the most frequently

implemented systems as illustrated in Fig. 3.<sup>38</sup> The entrained flow gasifier utilizes oxygen as its gasifying element at temperatures between 1200–1500 °C while maintaining extremely brief residence times of a few seconds. High operating temperatures lead to reduced tar formation and combustible gas concentration while improving the conversion of char materials. The processing capabilities of entrained flow gasifiers now hold greater significance because they combine quick processing and efficient small particle handling with maximum carbon conversion rate. The combination of high capacity with short retention period and strong thermodynamic efficiency makes engineers choose this technology as their primary solution.<sup>39,40</sup> Table 1 has discussed the important differences between the three types of gasifiers and mentioned its limitations also.

## 2.2 Plasma gasifiers

Plasma exists as the fourth state of matter because it contains free electrons and ions along with neutral particles which balance with each other electrically. Its charged particles make it both thermally and electrically conductive.<sup>42</sup> Plasma gasification is an allothermal process that uses external energy to maintain high temperatures, breaking down materials in an oxygen-deficient environment. This high-temperature process enhances conversion efficiency, primarily producing syngas, slag, and ash.<sup>43</sup> Plasma gasification shows promising signs to achieve success as a waste-to-energy technology. Investment at the start of operation remains high but returns substantial economic value.<sup>44</sup> Plasma technology proves best suited for MSW waste management because it achieves 816 kW h energy output per ton along with minimal pollutants and generates the smallest amount of solid waste byproducts. Plasma gasification enables developers to create extensive systems which reach power capacities of thousands of megawatts despite operating at high capital and energy usage levels. Technology's ability to expand at scale improves its economic viability thus making it an attractive option for sustainable waste handling and energy generation purposes.<sup>45</sup>

Fig. 4 describes the detailed working process of the plasma gasifier where it uses plasma torch for heating the feedstock particles to convert into syngas and byproduct like ash. Plasma gasification operates as an innovative technology which utilizes electrically ionized gas that reaches 10 000 °C temperatures produced by plasma torches operating under pressures ranging from 1 to 30 bars.<sup>46</sup> The feedstock enters through the reactor's top section while the gasifying agent is delivered to its sides to start the required reactions. Plasma gasifiers utilize thermal plasmatic systems as their primary mechanism for high-efficiency heat generation.<sup>47</sup> Plasmas inside the reactor establish a hot electrically conductive column which generates incredibly high temperatures. The process completely disintegrates all materials which then transform into gaseous products.<sup>48</sup> The system efficiently deteriorates diverse biomass feedstocks directly through its process without needing pre-processing techniques. The process delivers outstanding decomposition capacity that produces substantial energy output. Its operation produces minimal emissions together

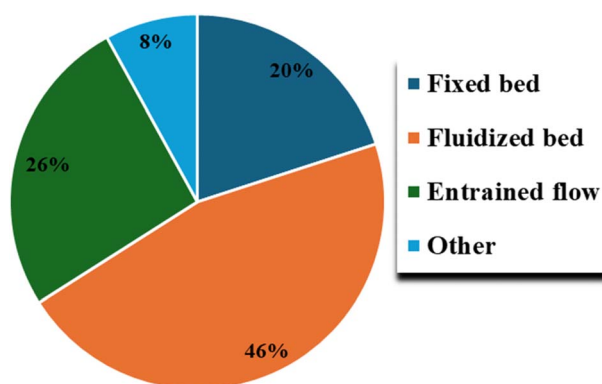


Fig. 3 Reactor configuration in gasification.



Table 1 Difference between three basic gasifiers based on flow<sup>40,41</sup>

Parameters	Fixed bed gasifier	Fluidized bed gasifier	Entrained flow gasifier
Temperature and ash handling	Non-homogeneous temperature distribution, temperature ranges above ash melting point	Homogenous temperature distribution ranging between 800 to 1000 °C. Operating in conditions below the ash-softening point ensures they prevent agglomeration	High operation temperatures reaching 1400 °C while surpassing the ash melting point thus producing molten slag
Particle size and residence time	It uses large size feedstock particles and has high residence time	It accepts wide range of particle size and has less residence time compared to fixed bed	It requires a dry and uniform size biomass particle and has very less residence time
Mixing and reaction characteristics	There is limited mixing between solid and gas	This gasifier allows an excellent mixing of solid and gas phase	This gasifier allows simultaneous mixing and co-current flow of biomass and gasifying agent. Has high carbon conversion efficiency
Capacity and scalability	This is good for small or medium scale production	It is good for industrial or large level of production and has high gasification intensity	Since it operates at very high pressure and temperature, so it is suitable for large scale application
Product gas characteristics	It produces low heating value gas with small amounts of tar	It produces low tar with stable composition and produce gas with high fly ash content	Its yield quality is high, and has tar free syngas with less methane content

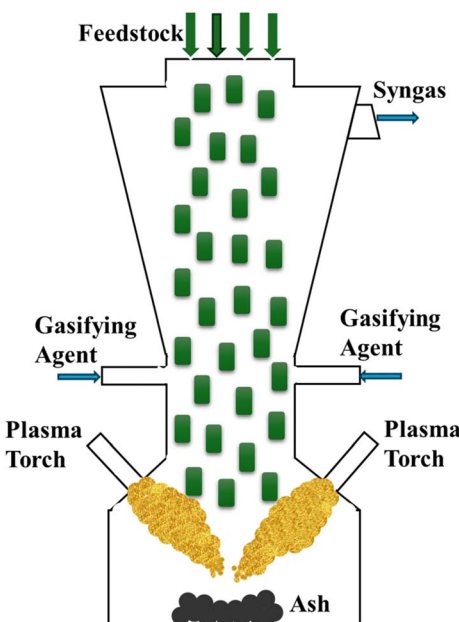


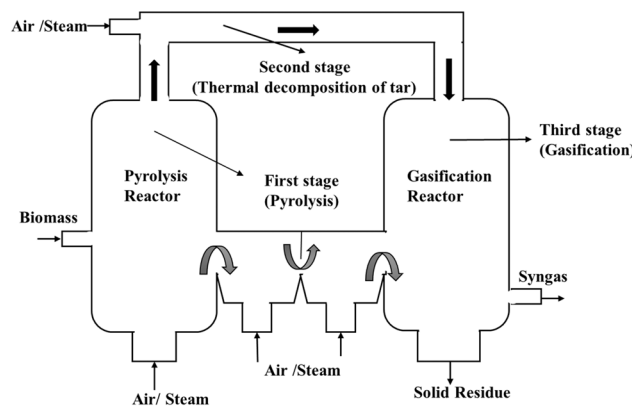
Fig. 4 Schematic diagram for plasma gasification reactor.

with short residence times that result in improved overall environmental advantages and operational performance.<sup>49,50</sup> The high efficiency of plasma gasification requires substantial investments and operation costs. To power the reactor of a 3600 MW plant we need 115 kW h per ton of MSW excluding other system elements. The technology proves commercially worthwhile since research demonstrates that plasma gasification of MSW generates approximately \$3.35 million in annual profit. Through plasma gasification we achieve waste management efficiency and create economic and environmental benefits that enable a circular economy operation.<sup>49,51</sup> Therefore, plasma gasification demonstrates a substantial environmental advantage through its process which produces around  $-31 \text{ kg CO}_{2\text{eq}}$

in negative greenhouse gas emissions. The environmental impact of plasma gasification remains low even when accounting for the small emissions of particulate matter and heavy metals. A long-term waste management and energy production solution becomes possible through plasma gasification because the investment can recover costs within 18 years despite high installation and management expenses.<sup>45,52</sup>

### 2.3 Multistage gasification systems

The two configurations of multistage gasifiers consist of single-reactor systems with controlled zones for pyrolysis and gasification or they utilize separate reactors for these processes in sequence.<sup>53</sup> Compared to single-stage gasification, the efficiency of multistage gasification improves significantly by appropriately increasing the drying zone temperature while reducing the temperatures in the oxidation and reduction zones.<sup>54</sup> Fig. 5 describes the various stage involved in multistage gasification process, during the first stage of a three-stage gasification process biomass particles experience oxidative pyrolysis at 700–

Fig. 5 Line diagram of multistage gasifier.<sup>53</sup>

800 °C temperatures while moving through a fluidized bed device. The decaying pyrolysis gas reaches a thermal decomposition point of 1200 °C in stage 2 to decompose tar. The gasification reactor receives its solid phase from the pyrolysis reactor through a loop gate that functions to divide gases from solids. The third stage of the process includes another gasification unit that continues to process biomass.<sup>53,55</sup>

Through this technology operational efficiency increases while the final syngas product contains decreased amounts of tar. The multiple operating components create substantial operational complexity since their continuous coordination procedures must be maintained. The primary objective in creating multistage gasifiers was developing gas that contained the lowest possible tar quantities. The review demonstrated that temperature levels in the multistage heating and gradient chain gasifier (MHGCG) were highest during the drying phase compared to the subsequent oxidizing and reducing stages. Enhancing drying stage heating while minimizing oxidizing and reducing stage temperatures led to an important elevation of gasification efficiency over standard operational parameters. The gasification process achieved 56% efficiency with a biomass weight loss of 43% when the oxidizing stage equivalence ratio was set to 0.28. Provided gas composition consisted of 4% O<sub>2</sub>, 10% CO<sub>2</sub>, 14% H<sub>2</sub> and 24% CO and the final product concentrations measured at NO: 0.024%, NO<sub>x</sub>: 0.025% and SO<sub>2</sub>: 0.032%.<sup>54</sup> A fluidized bed reactor consisting of multiple stages is simulated through Aspen Plus for *Prosopis Juli flora* air gasification during its pyrolysis, combustion and reduction phases. The semi-detailed kinetic approach uses both reaction rates and hydrodynamic principles for optimized gasifier performance assessment. The computer model indicates gasifier temperature together with air-to-biomass ratio serves as main variables which impact CO gas output. To achieve maximum gas calorific value the system requires a gasifier structure with a 2 m height and 0.5 m diameter and an equilibrium ratio of 0.24 to achieve 65% cold gas efficiency. The reactor technology generates valuable product gas containing high energy value.<sup>56</sup> Saleh *et al.*<sup>57</sup> conducted a study of multistage air inlet modifications to downdraft gasifiers enhanced gas quality through higher heating values and lower tar levels. The evaluation of performance operated through three metrics: equivalent ratio (ER) and pre-heated air temperature and air ratio. The peak performance of the system occurred at an equivalent ratio of 0.4 at 902 °C leading to optimized CO and H<sub>2</sub> production rates and pre-heating the air resulted in increased LHV from 5254 to 5976 kJ kg<sup>-1</sup>. With the optimal ratio of 40:60 the system successfully diminished tar content from 50.02 to 27.82 mg Nm<sup>-3</sup>. Implementation of a multi-stage gasifier operated through variable temperature steam gasification resulted in a 15-fold CO production increase during the second stage with Gasification Carbon (G-C) added substances and produced 2.32 times more total syngas. The addition of G-C enabled researchers to control the H<sub>2</sub>/CO ratio thereby benefiting subsequent synthesis operations. The process achieved both lower energy consumption and reduced CO<sub>2</sub> emissions and performed efficient CO<sub>2</sub> capture and conversion. The method improved the syngas yields for cleaner energy applications.<sup>58</sup> Therefore, the

multistage biomass gasification process decreases syngas tar levels to a point where it becomes usable by internal combustion engines alongside gas turbines without needing expensive deterring equipment. Such gasification systems create cleaner gas outputs than single-stage gasifiers though they become less efficient for wood biomass processing. The technology demands superior quality feedstock which reduces its possible uses. Technology operates against entrained-flow gasifiers when evaluating gas purity.

## 2.4 Supercritical water gasifiers

Supercritical water gasification (SCWG) applies heat decomposition and hydrolytic reaction to convert biomass containing up to 80 wt% moisture into syngas. Energy efficient pre-drying becomes unnecessary, and residence times decrease to seconds or minutes through this process in comparison to traditional gasification technology.<sup>59</sup> SCWG offers several advantages over other gasification technologies, including higher gasification efficiency, greater hydrogen yield, and lower emissions of CO<sub>2</sub>, NO<sub>x</sub> and SO<sub>x</sub>. Reaction temperature plays a crucial role in the process, while extended reaction time further enhances hydrogen production and gasification efficiency.<sup>60</sup> Important process parameters governing SCWG reactions are presented in Fig. 6. Supercritical water gasification (SCWG) is a promising treatment for black liquor, offering high hot gas efficiency and no evaporation requirement. It could enhance non-wood mills and expand product offerings for Kraft mills but requires further investigation on Sulphur balance and feasibility for integration.<sup>61</sup> In supercritical state, water exhibits both solvent and catalytic properties. It combines gas like viscosity with liquid-like density, enhancing mass transfer and solvation. These characteristics enhance biomass penetration and hydrolysis, accelerating reaction kinetics and enabling more efficient gasification. The SCWG gasifier has the potential to produce hydrogen enhanced syngas.<sup>62</sup> At near critical or subcritical temperatures, the presence of H<sup>+</sup> and OH<sup>-</sup> ions catalyze ionic reactions, facilitating biomass hydrolysis. The high pressure in supercritical water gasification removes the need for product gas compression, reducing costs, infrastructure, and resource requirements.<sup>63</sup> By using the SCWG process without a catalyst at 650 °C for 45 minutes the procedure eliminated 75% carbon monoxide and 83% carbon dioxide

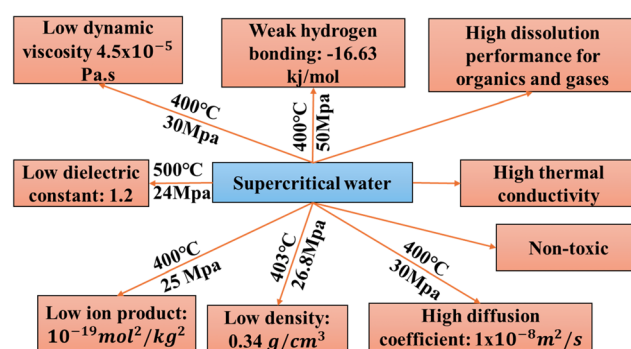


Fig. 6 Unique physicochemical properties of supercritical water.



emissions with respect to MSW processing emissions. An elevated temperature solution reduced the number of released gases during the process.<sup>64</sup> Simulation studies using Aspen Plus demonstrated that peak hydrogen output from the two-stage supercritical water gasification (TSCWG) system occurs when operating temperature reached 603 °C (FGR) and 833 °C (SOR). The efficiency rates measured 54.9% energy and 56.2% exergy.<sup>65</sup>

The 1 ton per h treatment capacity simultaneous saccharification and fermentation (SSF-SCWG) model was used for studying how temperature and reactant concentration influence SCWG product yields.<sup>66</sup> Energy levels increased along with temperature while mass concentration levels decreased the production efficiency of hydrogen and gasification. The combination of maximum hydrogen production reached 0.139 kg kg<sup>-1</sup> accompanied by 108.832 mol kg<sup>-1</sup> gasification yield.<sup>67</sup> The SCWG also allows the production of biofuels and valuable products from Kraft Black Liquor (KBL).<sup>68</sup> Through using a high-heating-rate batch reactor in sewage sludge gasification SCWG operations the process generated considerable higher levels of hydrogen compared to conventional production methods. The reaction temperature influenced all parameters positively and reached their maximum levels of 20.66 mol kg<sup>-1</sup> hydrogen yield at 750 °C and both without and with a catalyst. The combination of steam reforming with water-gas shift and pyrolysis together produced H<sub>2</sub> and CO<sub>2</sub> from 550 to 750 °C with the water-gas shift taking the lead role when reaction time was extended. Higher reaction temperatures combined with prolonged residency duration minimized the production of CO and CH<sub>4</sub>.<sup>69</sup> The research utilizes municipal waste leachate as its focus for creation of Synthetic Natural Gas (SNG) through catalytic improvements using Nickel-based catalytic conversion. The process takes place during the following operational stage beyond the SCWG reactor. The produced syngas consisted of hydrogen and methane gases within a concentration range of 25–47 vol% H<sub>2</sub> and 11–18 vol% CH<sub>4</sub>.<sup>70</sup>

A study developed thermodynamic equilibrium model for pig manure SCWG then investigated how different operating conditions affected heat generation together with system performance.<sup>73</sup> The results demonstrated how lowering pre-heating water temperature while increasing the slurry concentration together with higher gasification temperatures improved both heat production and system efficiency up to 95.53% using 1 : 1 water-to-slurry ratio and 94.90% with 70 wt% slurry concentration. System efficiency reached 39.8% based on exergy analysis and most exergy losses took place in the heat exchange and oxidation stages. Therefore, using SCWG provides an environment-friendly and optimized process to transform coal into hydrogen products compared to conventional gasification systems. High solubility along with reactivity and diffusivity properties in supercritical water allow coal to transform into hydrogen-rich gases at manageable temperatures. At the reactor's bottom natural sedimentation of inorganic salts involving N, S and Hg takes place. Filtration of H<sub>2</sub> from CO<sub>2</sub> occurs effectively through critical point pressure control without the need for specialized separation equipment.<sup>71–73</sup>

## 2.5 Solar gasifiers

Solar energy is a leading renewable resource for future energy needs, but its low density, intermittency, and uneven distribution requires efficient storage solutions.<sup>74</sup> One promising approach is solar-assisted biomass gasification, where concentrated solar energy supplies the heat needed to convert carbon-based materials into high-quality syngas. This syngas can then be processed into valuable hydrocarbon fuels, enhancing solar energy utilization.<sup>75</sup> The combination of H<sub>2</sub> and CO obtained from syngas benefits from solar thermochemical processes through gasification and cracking along with reforming methods allowing their conversion into hydrocarbon fuels using Fischer-Tropsch synthesis. Solar hydrogen production methods can be enabled through two different processes which use the water-gas shift reaction and carbon capture methods.

Fig. 7 shows the detailed operating system of solar gasifiers and describes the utilization of solar thermal energy for the generation of syngas. Solar thermal systems apply focusing mirrors to collect sunlight which produces high-temperature heat exceeding 1273 K. These systems apply optical surfaces to achieve high-temp focal points which operate with efficient heat delivery. The cavity receiver design reduces heat losses to less than 30% which boosts system performance. Solar reactors employ two operational methods to heat their particulate solid feedstock through directly irradiated and indirectly irradiated reactors.<sup>76,77</sup> The eqn (1) and (2) can be helpful to find the energy and thermal energy conversion efficiency as mentioned below.

$$\text{Energy conversion efficiency} = \frac{m_{\text{gas}} \times \text{LHV}_{\text{gas}}}{Q_{\text{solar}} + m_{\text{feedstock}} \times \text{LHV}_{\text{feedstock}}} \quad (1)$$

Thermal energy conversion efficiency

$$= \frac{X_c \times \sum_{x}^{\text{species}} \int_{473\text{K}}^{T_{a,\text{in}}} n_x C_{p,x}(T) dT + X_c \times n_c \times \Delta H_R / T_{a,\text{in}}}{Q_{\text{solar}}} \quad (2)$$

where,  $n_x$  = molar flow rate of species  $x$  (mol s<sup>-1</sup>),  $X_c$  = carbon conversion (–),  $C_{p,x}$  = heat capacity of species  $x$  (J mol<sup>-1</sup> K<sup>-1</sup>),  $\Delta H_R$  = reaction enthalpy (kJ mol<sup>-1</sup>),  $T_{a,\text{in}}$  = temperature inner side of absorber/cavity (K).<sup>78</sup>

Taylor *et al.*<sup>78</sup> constructed a 2 kW solar furnace to operate the first fluidized bed reactor by inserting a silica-glass tube vertically for solar gasification research. The process of fluidizing coconut charcoal using CO<sub>2</sub> flows operated at 2–15 m min<sup>-1</sup> resulted in a 10% energy conversion efficiency but lost significant power due to heat escaping through radiation and conduction and gas escape. The packed-bed reactor operated at 40% efficiency because of its performance improvement over other configurations. A study combines a solid oxide fuel cell (SOFC) which runs on hydrogen–carbon monoxide syngas with a coal-fired combined cycle and concentrated solar energy. The combination of energy systems yielded enhanced performance characteristics by reaching energy efficiency ranges from 70.6% to 72.7% and exergy efficiency rates between 35.5% and 43.8%. The utilization of different coal types resulted in CO<sub>2</sub> emission levels between 18.31 kg s<sup>-1</sup> while using 10 kg s<sup>-1</sup> fuel.<sup>79</sup>



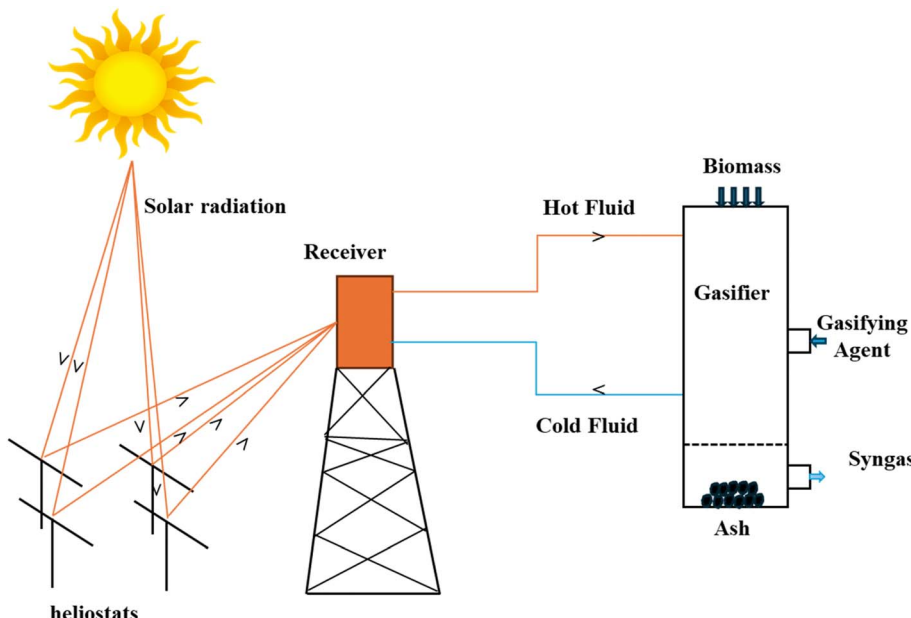


Fig. 7 Diagram of solar gasification process.

Moreover, the rise in power and chemical sector need for solid carbonaceous feedstocks including coal and biomass with waste materials drives fast development of gasification technologies. The alternative solar-driven gasification system corners process heat from concentrated solar radiation to supply high-temperature requirements. The process both improves gas synthesis efficiency and cuts down  $\text{CO}_2$  emission rates through solar-energy-driven calorific value enhancements of raw materials. The elimination of air separation units increases economic viability and makes solar gasification an efficient technique for storing solar energy through mobile chemical compounds.<sup>80</sup>

Additionally, it can be seen that the gasification technologies are shifting towards the green energy operated plant, and more

research has been done in the field of solar based energy system (See Fig. 8). Since the electricity cost has a huge impact on the total investment cost of the gasification system. Therefore, making gasification system more economical and reducing the carbon emission there is necessity to explore the green source of power supply.

### 3 Modeling approach in gasification

Modeling the gasification process is essential for optimizing biomass conversion into syngas, enabling efficient design and operation of gasifiers. Various modeling approaches have been developed to predict gas composition, efficiency, and environmental impact. These models range from traditional thermodynamic equilibrium models to advanced kinetic and computational fluid dynamics (CFD) simulations. Additionally, artificial intelligence methods, such as machine learning and artificial neural networks, have emerged as promising tools for capturing the complex, nonlinear behaviors inherent in gasification processes. Selecting an appropriate modeling approach depends on factors like desired accuracy, computational resources, and specific process conditions. The thermochemical gasification process produces three products including biochar, ash and tar during operation. The high-temperature process depends on a gasifying agent to facilitate the conversion.<sup>81</sup> Table 2 presents the important reaction (R.1)–(R.13) taking place during the gasification process along with the heat of reaction data for the reactions. The positive sign shows that the reaction is endothermic, and negative sign implies as exothermic process.

#### 3.1 Thermodynamic equilibrium models

The thermodynamic equilibrium model offers a thermodynamic framework for simulating gasification processes,

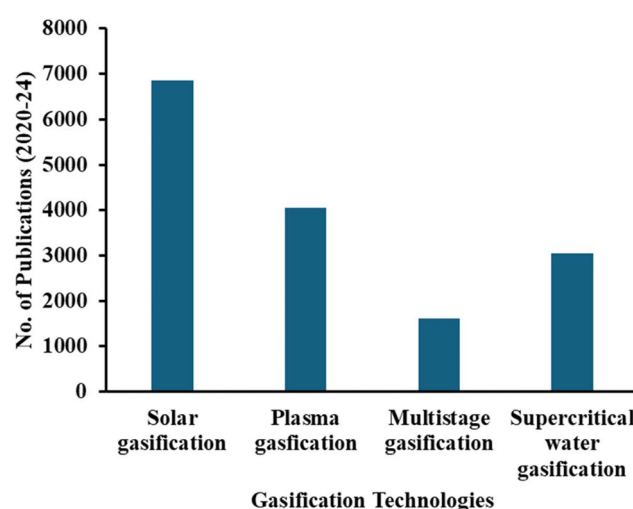
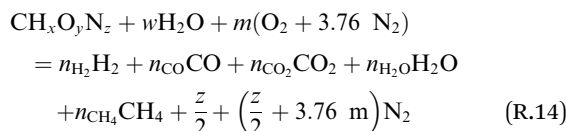


Fig. 8 Number of publications of various gasification technologies in between 2020–24 years.

Table 2 Important chemical reactions take place inside gasification process<sup>82</sup>

Name	Chemical reaction	Heat energy (MJ kmol <sup>-1</sup> )
Boudouard reaction	$C + CO_2 \leftrightarrow 2CO$ (R.1)	+172
Water gas or steam	$C + H_2O \leftrightarrow CO + H_2$ (R.2)	+131
Methane reaction	$C + 2H_2 \leftrightarrow CH_4$ (R.3)	-74.8
Oxidation reaction	$C + O_2 \rightarrow CO_2$ (R.4)	-394
	$CO + 0.5O_2 \rightarrow CO_2$ (R.5)	-284
	$CH_4 + 2O_2 \leftrightarrow CO_2 + 2H_2O$ (R.6)	-803
	$H_2 + 0.5O_2 \rightarrow H_2O$ (R.7)	-242
Shift reaction	$CO + H_2O \leftrightarrow CO_2 + H_2$ (R.8)	-41.2
Methanation	$2CO + 2H_2 \rightarrow CH_4 + CO_2$ (R.9)	-247
	$CO + 3H_2 \leftrightarrow CH_4 + H_2O$ (R.10)	-206
Steam reforming reactions	$CO_2 + 4H_2 \rightarrow CH_4 + 2H_2O$ (R.11)	-165
	$CH_4 + 0.5O_2 \leftrightarrow CO + 2H_2$ (R.12)	-36
	$CH_4 + H_2O \rightarrow CO + 3H_2$ (R.13)	+206

enabling the prediction of syngas composition and assessment of biomass conversion potential under specified conditions. This model, also known as zero-dimensional model, assumes that all reactions within the reactor reach equilibrium instantaneously, providing a simplified yet insightful analysis of the system's behavior. By applying mass and energy balances, the model evaluates how different processing parameters influence the final gas composition, thereby assisting in optimizing gasifier design and operation.<sup>83</sup> Equilibrium modeling exists as stoichiometric and non-stoichiometric types. Stoichiometric equilibrium modeling requires comprehensive knowledge about reaction mechanisms which includes all relevant chemical processes and substances. The stoichiometric equilibrium model uses gasification reaction equilibrium constants while the non-stoichiometric equilibrium model finds minimal value of Gibbs free energy to describe gasification equilibrium.<sup>84,85</sup> The model assumptions in this case typically include uniform pressure, steady state operation, uniform temperature along with chemical reaction at infinite residence time. Gas phase elements are considered to have the ideal gas behavior with single step chemical reaction. It is also assumed that produced gas consists of CO, H<sub>2</sub>, CO<sub>2</sub>, CH<sub>4</sub> and N<sub>2</sub> and H<sub>2</sub>O as major species where nitrogen acts inertly while oxygen remains absent. Depending on the modeling approach, tar may be included or excluded from the gas-phase formulation, whereas ash is often omitted from energy balance calculations.<sup>86</sup> The stoichiometric modeling approach involves mass and stoichiometric coefficient balancing, along with the application of equilibrium constants, and calculations for enthalpy and specific heat of reacting species. The generalized biomass gasification reaction can be represented by the following eqn (R.14) given below.<sup>87</sup>



Here,  $x$ ,  $y$  and  $z$  coefficients refer to the number of hydrogen, oxygen and nitrogen atoms for one mole of carbon in biomass. The coefficients  $w$  and  $m$  refer to moisture and oxidant supply

respectively per kmol of biomass feed. In this approach a set of nonlinear equations are solved obtained by elemental balance of different species in the global gasification reaction and correlating the equilibrium constant to the mole fractions of reacting species during different reactions in the gasification process. The expressions for equilibrium constants are presented in eqn (3) and (4) where the symbols  $x_i$  and  $v_i$  represent the mole fractions and stoichiometric number of  $i$ th species. The equilibrium constants are a function of the standard Gibbs function which are calculated for a specific reaction temperature using eqn (5) and (6). Finally, the gasification temperature is calculated by solving the energy balance eqn (7) and (8) iteratively.<sup>87,88</sup>

$$K_i = \prod_i (x_i)^{v_i} \left(\frac{P}{P_0}\right)^{\sum_i v_i} \quad (3)$$

$$\ln K = -\frac{\Delta G_T^0}{RT} \quad (4)$$

$$\Delta G_T^0 = \sum_i v_i \Delta g_{f,T,i}^0 \quad (5)$$

$$\begin{aligned}
 \Delta g_{f,T,i}^0 = h_f^0 - a' \ln(T) - b' T^2 - \left(\frac{c'}{2}\right) T^3 - \left(\frac{d'}{3}\right) T^4 + \left(\frac{e'}{2T}\right) \\
 + f' + g' T \quad (6)
 \end{aligned}$$

$$\sum_{i=\text{reactant}} h_{f,i}^0 = \sum_{i=\text{products}} n_i (h_{f,i}^0 + \Delta h_{T,i}^0) \quad (7)$$

$$\Delta h_{T,i}^0 = \int_{298}^T C_p(T) dT \quad (8)$$

Another approach for thermodynamic equilibrium modeling of gasification process is the non-stoichiometric method which is based of minimization of Gibbs free energy. It also includes the calculation of chemical potential, and Lagrange function and the related eqn (9)–(13) are given below.



$$G_t = \sum_i n_i \mu_i \quad (9)$$

$$\mu_i = \Delta G_{f,i}^0 + RT \ln y_i \quad (10)$$

$$G_t = \sum_i n_i \Delta G_{f,i}^0 + \sum_i n_i RT \ln y_i \quad (11)$$

$$\sum_{i=1}^N a_{ij} n_i = A_j, j = 1, 2, \dots, k \quad (12)$$

$$\frac{\partial L}{\partial n_i} = \frac{\Delta G_{f,i}^0}{RT} + \sum_{i=1}^N \ln \left( \frac{n_i}{n_{\text{total}}} \right) + \frac{1}{RT} \sum_{j=1}^k \lambda_j \left( \sum_{i=1}^N a_{ij} n_i \right) = 0 \quad (13)$$

where,  $R$  = universal gas constant,  $T$  = temperature,  $y_i$  = mol fraction of gas species  $i$ ,  $\Delta G_{f,i}^0$  = standard Gibbs free energy,  $a_{ij}$  =  $j$ th element present in each molecule of chemical species,  $A_j$  is the total atomic mass of  $j$ th element,  $k$  total number of atoms,  $L$  Lagrange function,  $\lambda_j$  Lagrange multipliers.

The total Gibbs energy can be calculated using eqn (9) (called Gibbs–Duem equation) where  $n_i$  and  $\mu_i$  represent the number of moles and chemical potential of species.<sup>88</sup> This modeling approach is based on the principle that, at equilibrium, the total Gibbs free energy of the system reaches a minimum under specified temperature and pressure conditions. This method does not require a predefined reaction pathway, instead, it considers all possible species and phases and determines their equilibrium composition by minimizing the system's Gibbs free energy, subject to elemental mass balance constraints. As a result, it offers a robust and comprehensive framework for predicting the composition of the syngas in complex gasification systems.

The accuracy of both stoichiometric and non-stoichiometric equilibrium models in biomass gasification can be significantly enhanced by incorporating actual reaction conditions observed during operation. Various modified equilibrium models have been developed, which consider factors such as equilibrium constants, experimentally determined gas compositions, specific reaction stages, operating parameters, and empirical correlations. These refinements enable more realistic predictions of product distribution and process performance under practical gasification conditions. Mountouris *et al.*<sup>89</sup> developed a model based on equilibrium constants used water–gas shift and steam reforming reactions with partial mass balance system for carbon, hydrogen, oxygen alongside heat balance. The model accounts for solid carbon formation and provides exergy data necessary for optimizing system processes. Silva and Rouboa<sup>90</sup> presented a two-stage equilibrium model that establishes equilibrium composition in stage one and stage two operations with gases only while omitting solid carbon. The equilibrium constant was corrected through multiplicative factor to improve equilibrium modeling. Additionally, Aydin *et al.*<sup>91</sup> developed a semi-empirical equilibrium model that integrates two correction variables to enhance the equilibrium constant of the methanation and water–gas shift reactions. The corrections which rely on gasification temperature, equilibrium temperature and equivalence ratio (ER) measurements resulted

from comparing theoretical models to downdraft woody biomass experimental data through the Levenberg–Marquardt method. The modified model shows improved ability to predict concentrations of gaseous species along with tar yield in producer gas. This modified mathematical framework can produce a better estimation of both producer gas composition and obtained tar content.<sup>92</sup> Table 3 summarizes different studies which implemented TEQM for simulation of gasification process along with important findings and limitations.

The equilibrium models are still widely used because of their simplicity and computational efficiency. These models are especially valuable for predicting the theoretical maximum syngas yield and establishing thermodynamic feasibility boundaries for gasification processes. Improving equilibrium models is essential for enhancing the accuracy and reliability of biomass gasification simulations, particularly under practical, non-ideal conditions. Bijesh *et al.*<sup>96</sup> advanced a stoichiometric thermodynamic model of equilibrium of sewage sludge gasification that accounts for sulfur content, char transformation, and four classes of tar compounds. The model showed strong agreement with experimental data, achieving  $R^2$  values above 0.90 and  $p$ -values below 0.05. The results demonstrated that hydrogen ( $H_2$ ) and carbon monoxide (CO) concentrations increased with temperature, while carbon dioxide ( $CO_2$ ), hydrogen sulfide ( $H_2S$ ), and tar concentrations decreased. In another example, a recent review by Carine *et al.*<sup>103</sup> demonstrates how these models are often applied to carry out fast screening of feedstocks and operating conditions. However, a fundamental limitation of these models is their assumption of complete chemical equilibrium, which overlooks reaction kinetics, intermediate species, tar formation, and char reactivity. As shown by Ahmed *et al.*<sup>104</sup> there is always an overestimation of the hydrogen concentration and underestimation of tar or carbon residue, especially in multistage and low temperature gasifiers by using equilibrium models. After a thorough review, it can be confirmed that fact that although these models are statistically valid they may fail to reflect the dynamic behavior of real systems. To address these problems, hybrid equilibrium approaches are currently being developed in which the cores principles of equilibrium model are combined with either empirical or semi-empirical corrections to address devolatilization, and char-gas effects.

### 3.2 Kinetic model

Unlike equilibrium models, which assume that reactions reach a final balanced state, kinetic models account for the dynamic progression of reactions over time, allowing for more accurate predictions of gas composition and yield under varying operational conditions. These models incorporate parameters such as reaction rate constants, activation energies, and the influence of temperature and pressure, enabling the simulation of complex processes like pyrolysis, oxidation, and reduction within the gasifier. By capturing the temporal aspects of chemical transformations, kinetic models assist in optimizing gasifier design and operation.<sup>24,105,106</sup> Kinetic modeling works efficiently when the reaction rate is slow and has a low



Table 3 TEqM model: summary of relevant research

Reference	Feedstock	Gasification agent	Remark	Future research possibilities
93	Rubber wood	Air and water vapour	Studies demonstrated that water vapor functioned as a gasifying agent to produce superior-quality syngas than when using air. The experiment utilizing air generated a hydrogen yield at 35% by volume but switching to steam as the gasifying agent increased the yield to 65% by volume	The gasifying agents are very limited which need to be explored for getting better conversion of biomass to syngas
30	Almond shells	Air, pure oxygen, steam	The research proves that updraft gasifiers can produce syngas which contain higher hydrogen content than other gasifier designs because of its efficiency. The difference between predicted results and experimental findings remains below 10% on average	The primary disadvantage of the updraft gasifier is the high tar content in the output gas, which reduces its lower heating value
94	Pine sawdust	Air	The study revealed that increasing the $H_2O$ content consistently enhanced the yield of effective gases (CO and $H_2$ ), whereas an excess of $CO_2$ inhibited their production	The removal of carbon completely proved difficult to achieve during entrained-flow gasification under analyzed conditions. The study requires more investigation to establish methods which can both decrease and eliminate carbon formation under these conditions
95	Municipal solid waste	Air	The bioenergy system operated at a production capacity of 3.92 MW electrical power together with 608.8 $m^3 h^{-1}$ hydrogen production when fed with 1.155 $kg s^{-1}$ biomass. The established design parameters resulted in an energy utilization factor of 34.71% together with a total exergy efficiency of 29.44% and overall exergy destruction rate of 11 854 kW	The combustion chamber and gasifier experienced maximum exergy destruction because intense chemical processes occurred within their structure. Boosting system exergy efficiency would result from lowering these exergy destruction rates
96	Sewage sludge	$O_2$ and steam	The model has been adapted to include the sulfur content in sludge, along with char conversion and tar formation. For the temperature range of 900 to 1150 K, the average mole fractions of the primary gas components were determined to be 9.76% for $H_2$ , 11.80% for CO, 9.84% for $CO_2$ , and 2.97% for $CH_4$ . As the temperature increases, the molar concentrations of $H_2$ and CO rise, while those of $CO_2$ and $CH_4$ decline	The AAE, SSE, and RMSE values for all product gas components, PGY, LHVp, CGE, and CCE were found to be below 10%. These errors could be further reduced by utilizing an alternative solving model
97	Polypropylene, polyethylene terephthalate, biomass (straw)	Air	An increase of plastic content in gasification feedstock reaches its maximum heating value at 5.78 $MJ Nm^{-3}$ alongside its highest tar concentration of 72.89 $g Nm^{-3}$	Since the tar content has risen more which reduces the syngas yield which is unwanted. So, this can be reduced further by taking different composition of feedstock
98	Woods & sewage sludge	Air, pure oxygen, steam	This study evaluates syngas composition, tar and char yields, gasification temperature, cold gas efficiency, and the lower heating value for different biomass feedstocks characterized by specific ultimate analysis. The predictions are conducted for varying equivalence ratios and moisture contents	This model determines methane concentration levels without needing correction factors to make predictions which is a strength that equilibrium models often lack



Table 3 (Contd.)

Reference	Feedstock	Gasification agent	Remark	Future research possibilities
99	Pine kernel shells (PKS)	Air, steam	The stoichiometric and non-stoichiometric models received validation through experimental data obtained from a semi-pilot scale bubbling fluidized bed gasifier operating with pine kernel shells (PKS) feedstock. The stoichiometric model proved to be more accurate than the non-stoichiometric model for predicting gas composition along with gasification efficiency	The prediction of CO and methane at a stoichiometric ratio (<0.2) still shows notable deviations from the experimental data, which can be further minimized
100	Waste tires	Steam	The study identified the optimal conditions for maximizing H <sub>2</sub> yield in the supercritical temperature range as 599.8 °C, 23.2 MPa, and 5.5 wt%. Conversely, the ideal parameters for achieving maximum CH <sub>4</sub> yield in the supercritical temperature range were 551 °C, 27.2 MPa, and 18.3 wt%. For the transition temperature range, the optimal conditions for CH <sub>4</sub> yield were determined to be 380 °C, 26.4 MPa, and 7.9 wt%	The predicted H <sub>2</sub> yield differences from experimental results reached significant levels. Percentage errors amounted to 46.5%, 27.1% and 48.3%
101	Napier grass	Air	The research demonstrates that for assigned temperature ranges and ER values the model achieves RMS results of 0.0227 and 0.1108 which verify the precise simulation of gasification behavior	The updated model predicted elevated levels of H <sub>2</sub> , and CO <sub>2</sub> formation with around 16% deviation and ash generation but it calculated reduced concentrations of CO and CH <sub>4</sub>
102	Coal	Air and steam	An optimization process using the Taguchi method and utility concept along with TEQM to maximize syngas calorific value and minimize CO <sub>2</sub> yield during coal gasification. The Taguchi method identified two optimal control variable sets, achieving a calorific value of 3.59 MJ m <sup>-3</sup> and CO <sub>2</sub> yield of 6.25%. The utility concept was used to simultaneously optimize both objectives, with air supply, steam supply, and H/C ratio of coal being the most influential parameters. Results from the utility concept showed a 3.34% and 2.30% difference in calorific value and CO <sub>2</sub> yield compared to Taguchi's findings	The optimized model has assumed ideal gas behavior and does not consider the formation of tar which is an important byproduct formed in the gasification process

temperature inside gasifier because complete conversion requires in additional residence time.<sup>107</sup> The model proves to be more reliable than equilibrium models when operating temperatures remain low. Reaction kinetics use bed hydrodynamic data with the mass and energy balance to predict gas, char and tar quantities under different operating conditions. Hydrodynamic analysis of the reactor describes physical mixing and integrates with reaction kinetics. Different models in hydrodynamic complexity shift from zero-dimensional stirred tank reactors to one-dimensional plug flow models and further advance to complex two-dimensional and three-dimensional models for enhanced prediction accuracy.<sup>24,108</sup>

There are basically two modeling methods in kinetic models which are semi empirical kinetic and comprehensive kinetic model.<sup>28</sup> Semi-empirical kinetic models establish local equilibrium in specific reactions and gasifier regions through their calculations of both kinetic-controlled concentrations and temperatures in other areas. The models provide suitable computational efficiency together with accuracy benefits that allow researchers to understand complex processes in biomass and coal gasification. Experimental data including temperature-dependent reaction rates and feedstock behaviors allows the models to produce accurate predictions regarding the gasification efficiency as well as char reactivity and syngas composition.



Researchers utilize these tools extensively for hydrogen optimization as well as assessment of low-temperature char reactions and reactor phase simulation.<sup>109</sup> The comprehensive kinetic modeling methods account for both volatile and char reactions rates by tracking temperature and species changes during reactor progression through time. The semi empirical models demonstrate higher accuracy compared to comprehensive models when the gas phase achieves equilibrium conditions because they need fewer reaction rate laws and parameters.<sup>110</sup>

Empirical models make reaction kinetics simpler to handle by using polynomial approximations, Arrhenius-type expressions, or power-law equations. A research study developed a flexible polynomial model for following rate changes during CO<sub>2</sub> biomass char gasification as conversion increases.<sup>111</sup> The model received verification through 24 TGA experiments where both modulated and constant reaction rate (CRR) temperature programs were utilized to eliminate thermal deactivation and measurement errors. The model parameters were refined and optimized using the least square method and when compared with experimental data the results demonstrated high reliability. These models excel at determining the influence and structural complexity of minerals and catalytic effects present in biomass chars.<sup>111,112</sup> Other modeling methods include single step, multiple steps, Arrhenius based model, and Langmuir-Hinshelwood model. The Global or single-step kinetic models convert gasification into a single reaction for quick estimations without accounting for intermediate reaction steps. Whereas having separate stages in multi-step kinetic models that include pyrolysis and char oxidation with additional gas-phase reactions results in better predictions regarding gas composition behavior.<sup>113</sup> Another approach is Arrhenius-based models, which have gained widespread use to explain reaction rates through their dependency on activation energy and temperature use of the Arrhenius equation. The prediction of char gasification rates proves most effective when using these models.<sup>114</sup> Similarly, Langmuir-Hinshelwood models provide a useful tool for catalytic gasification processes because they help to explain how gas-solid reactions are influenced by surface coverage and adsorption phenomena. Eqn (14) and (15) show the correlation between the kinetic reaction rate, reaction component concentration and reaction equilibrium constant for the chemical reaction involved in gasification process.<sup>34,115</sup>

The Kinetic model basically works on kinetic reaction rate:

$$r_{i,r} = k_r \prod_{i=1}^N [c_{i,r}]^{\alpha_{i,r}} \quad (14)$$

Arrhenius equation for solving  $k_r$ :

$$k_r = A_r T^\beta e^{-\frac{E_a}{RT}} \quad (15)$$

Different studies on gasification based on kinetics models along with their limitations and future potential are summarized below in Table 4.

Kinetic models aim to represent the actual reaction kinetics involved in biomass gasification by explicitly modeling the rates of individual processes such as pyrolysis, oxidation, and reforming reactions. These models typically employ Arrhenius-type expressions to describe the temperature-dependent behavior of chemical reactions, allowing for a more detailed understanding of reaction mechanisms, particularly in relation to time-resolved phenomena such as tar cracking, pollutant formation, and intermediate species evolution. These models are especially valuable for analyzing the transient behavior of gasification systems and for designing processes where dynamic control is essential. They frequently, however, necessitate large pools of kinetic parameter data that are quite exclusive to the type of feedstock, the particle size and the type of reactor being considered. According to *Sylvia et al.*,<sup>126</sup> this kind of specificity restricts the generality of the kinetic models, and the cost of their calculations becomes excessive when they are included in massive simulations. To address these challenges, recent research has focused on the development of reduced-order and semi-global kinetic models. These simplified frameworks aim to retain essential predictive capabilities while reducing the number of required parameters and overall computational cost. Such models are increasingly being used in real-time optimization, control, and system integration applications where full-scale kinetic modeling is impractical. Another example of advancements in kinetic models can be found in case of simulation of biomass staged gasification technology (BSGT), where an important issue is the accurate modeling of medium temperature devolatilization (MTD) and char gasification. Conventional kinetic models often fail to capture this process accurately due to the omission of catalytic effects particularly the influence of inherent alkali metals like potassium. To overcome this limitation, an improved kinetic approach based on the random pore model (RPM) was developed, incorporating a correction factor to account for the catalytic role of potassium in corn stalk gasification. This enhanced model, referred to as RPM+, significantly improves the accuracy of kinetic predictions and offers more reliable guidance for reactor design and simulation in BSGT systems.<sup>127</sup>

### 3.3 CFD models

Computational Fluid Dynamics (CFD) models are instrumental in simulating the complex interactions of fluid flow, heat transfer, and chemical reactions within gasification processes. Numerically solving the Navier-Stokes equations, CFD models provide detailed insights into the behavior of gasifiers under various operating conditions, facilitating the optimization of design and performance. These tools seamlessly integrate simulations of chemical processes with fluid dynamics, giving insights into temperature distribution within systems and the interactions between solid materials and gas streams. CFD models typically utilize three methods namely Direct Numerical Simulation (DNS), Large Eddy Simulation (LES) and the Reynolds-Averaged Navier-Stokes (RANS) equations to model turbulent processes during gasification and combustion.<sup>38</sup> The analysis of gasification process and its modification can be



Table 4 Kinetic models: summary of relevant research

Reference	Feedstock	Gasification agent	Remark	Future research possibilities
116	Corn stover	Air	The study demonstrates that optimum syngas production could be achieved with gasification settings of 850 °C temperature, an O/C ratio of 0.45 and H <sub>2</sub> O/C ratio of 0.6. The experimental conditions produced 0.77 m <sup>3</sup> kg <sup>-1</sup> of syngas with 66.2% cold gas efficiency. The current results indicated a heat output power measurement of 15.42% and a heat efficiency rate of 60.99%	This paper introduces a model which matches experimental observations better than the thermodynamic equilibrium model does regarding accuracy. The total exergy efficiency level stands at 41.64% but still has potential for development. The system's overall performance could be optimized through improved methods of energy utilization efficiency
117	Pomegranate wood	Air	A power output of 7 kW generated syngas with higher molar ratios of H <sub>2</sub> at 21.5% and CO at 30.08%. The power load increase from 7 kW to 10 kW led to H <sub>2</sub> concentrations decreasing by 13.35% and CO concentrations eroding by 13.76%. The model generated syngas composition results with suitable precision through mean absolute percentage errors reaching 8.91% for H <sub>2</sub> and 1.98% for CO which satisfied the researchers	The CCE and CGE in the model are increasing as electric load of gasifier is increasing so further higher power can be investigated to analysis the syngas quality
118	Sewage sludge	Air/steam	A sensitivity analysis of the proposed hybrid SSG model demonstrated that the syngas compositions together with cold gas efficiency (CCE) are strongly affected by changes in flow rates of both gasifying agents (air and steam) and sewage sludge feedstock and by operational temperature and pressure	The validation approach in this research relies exclusively on experimental measurements obtained from fluidized-bed gasifiers which can be done on different gasifier
119	Sawdust	Air/steam	This study reveals that the dry gas yield increased by 8.1% as the steam-to-biomass ratio rose from 0.61 to 2.7, while the tar yield declined by 7.25%. Additionally, as the temperature increased, the gas yield (DGY) consistently grew from 1.72 to 2.0 Nm <sup>3</sup> kg <sup>-1</sup>	Since for engineering applications, the tar yield should be below 0.5 g Nm <sup>-3</sup> . However, in this study, the lowest recorded tar yield was 8.45 g Nm <sup>-3</sup> . To achieve a significant reduction in tar yield, further investigation into the use of various catalysts is required
120	Almond shells and hazelnut shells	Air and steam	The kinetic model proves a better choice for biomass gasification modeling since it requires parameters that are difficult to satisfy within the thermodynamic equilibrium approach. The current model provides a maximum relative error of 14.6% for CH <sub>4</sub> prediction when used for air gasification and achieves 12.8% maximum relative error during air and steam gasification	The prediction of CO yielded the greatest deviation from experimental data due to an error of 20% which resulted in overestimated values. Absolute errors from maximum CO <sub>2</sub> prediction results reached 29.3% and 26.4% respectively. The model's performance requires additional refinement since current deviations appear unacceptable
121	Lignocellulosic	Steam	Under the tested reaction conditions, residence time had little influence on gas formation during SCWG of both biomass model compounds and real biomass. At temperatures between 450 and 550 °C, the SCWG process for different model compounds and real biomass was almost entirely completed within 10 minutes	In developing the general kinetic model for predicting gas yields from real biomass during SCWG, it was assumed that no interactions occur among the three model components. However, interactions may influence the gasification process when mixtures of different components are involved
101	Wood residue	Air/steam	The optimization model reveals that the highest syngas yield of 78.6 vol% is achieved at a temperature of 900 °C, an ER of 0.23, an S/B ratio of 0.21, and a moisture content of 30 wt%	This study did not account for tar formation and overlooked the non-uniform temperature distribution within the gasifier



Table 4 (Contd.)

Reference	Feedstock	Gasification agent	Remark	Future research possibilities
122	Napier grass	Air	The study shows that the highest syngas yield and higher heating value (HHV) achieved were 69.42 wt% and 8.14 MJ Nm <sup>-3</sup> , respectively, under optimal conditions of 850 °C, an equivalence ratio (ER) of 0.3021, and a moisture content of 15.69 wt%. The syngas yield, HHV, carbon conversion efficiency (CCE), and cold gas efficiency (CGE) were reported as 82.51% and 30.69%. Furthermore, the average RMSE values for process temperature and ER were determined to be 0.025 and 0.033, respectively	The more efficient kinetic model requires evaluation for its performance with different biomass types through future research. It must analyze optimal conditions from an economic standpoint because different cost-effective optimizations exist but have not been determined yet
123	Pet coke	Steam and CO <sub>2</sub>	The paper concluded that CO <sub>2</sub> plays a minimal role in the process and as demonstrated in the following section, the reaction involving CO <sub>2</sub> can be disregarded if the temperature does not substantially exceed 1000 °C	In the research paper, it illustrates that at a temperature of 1000 °C with X(H <sub>2</sub> O) at 0.4, there is a greater discrepancy between the predicted and experimental data, which can be further minimized
124	Pine pellets and chips	Air	They show that the maximum absolute error for H <sub>2</sub> prediction was just 4.4%. Additionally, the predicted tar concentration ranged from 20 to 42 g Nm <sup>-3</sup> and decreased with increasing equivalence ratio, temperature, and biomass particle size	The paper demonstrates the least precise prediction of H <sub>2</sub> gas which shows room for enhancement in accuracy levels
125	Rubber wood and refused devised fuel	Steam	A three-zone kinetic model for evaluating rubber wood and refused derived fuel (RDF) gasification by studying five reduction zone reactions. Taguchi optimization showed that methanation represented the most influential process for RDF because it accounted for 65% of calorific value and 71% of exergy efficiency. In rubber wood gasification the Boudouard reaction accounted for 49% calorific value production and the water-gas reaction directly affected exergy efficiency by 46%	The model has assumption of ideal gas behavior with neglection the formation of the tar as byproduct in the gasification process

done through CFD software including study of biomass vaporization along with devolatilization of reactions and gasification transformation mechanisms. The approach proves beneficial for studying both singular and multiple phase flow processes. Lagrangian modeling techniques examine all multiphase flow parameters that include tracking particle position alongside velocity and temperature with studying particle collisions and frictional forces. The CFD simulation model simulates homogeneous and heterogeneous reactions along with primary and secondary tar decomposition.<sup>128</sup>

CFD modeling plays a vital role in simulating fluidized-bed and fixed-bed downdraft gasifiers. Key parameters analyzed during CFD simulations include drag force, biomass porosity, and turbulence attenuation. Due to the high permeability of the bed, a constant pressure assumption was applied throughout the reactor. Pressure drops calculations incorporated a modified Ergun equation, along with numerical solutions of

transport equations using finite-rate kinetic reactions.<sup>127</sup> Moreover, the established correlations in literature provided transport coefficients and chemical kinetics alongside the implementation of a finite volume method for accurate simulation of the gasification process. CFD software allows different gasification projects to guide optimal setup selection while performing budget-friendly evaluation of configurations and operating conditions at different scales.<sup>129</sup>

The governing equations essential for the CFD modelling of the gasification process include the generalized forms of the mass, momentum, and energy conservation equations. These equations are employed to determine the syngas composition, velocity and pressure fields, and temperature distribution within the gasifier. The CFD framework solves the conservation equations separately for the gas phase and the solid phase, acknowledging the distinct physical behaviours of each state. Given the significant interphase interactions between solid



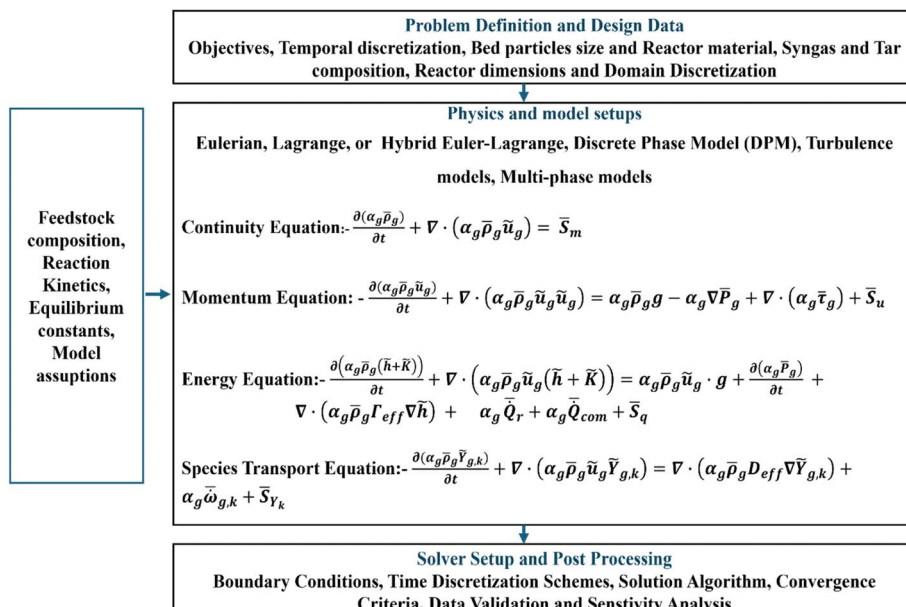


Fig. 9 Mapping data flows for gasification CFD models.

particles and the fluid medium, accurate modelling also necessitates the inclusion of the Energy Minimization Multi-Scale (EMMS) drag model in some cases. Fig. 9 depicts the data flow architecture for the CFD modelling of the gasification process. It encapsulates essential inputs such as feedstock characteristics, syngas composition, reaction kinetics, equilibrium constants, governing transport equations, discretization strategies, numerical solvers, and boundary condition specifications.

Although CFD modeling has proven effective for analyzing the gasification process, its application to commercial fluidized bed systems in combustion and gasification still requires further investigation, particularly when using the Eulerian–Eulerian Two-Fluid Model (TFM) approach. When applying Eulerian–Eulerian modeling to dense fluidized bed combustion and gasification it is difficult to achieve precise results unless assumptions spanning wide ranges of biomass particle sizes are made. A comprehensive investigation of CFD simulations analyzing bed and freeboard together is absent from current research and so are investigations using the same technique for both dense bed and riser/freeboard in commercial units. Limited CFD modeling has been used to study the tar formation process in gasifiers leading researchers to identify new investigation opportunities in this field. CFD models include multiple operation and design parameters but studying their impact on syngas production requires additional scrutiny. The shortage of comprehensive CFD simulations in biomass gasification stems from two primary reasons which include the expensive computational needs and the complex anisotropic characteristics of biomass materials. Table 5 summarizes key research studies on the application of CFD models to gasification processes, along with their major findings. This review encompasses a wide range of feedstocks, including coal, municipal solid waste, biomass pellets, Miscanthus briquettes,

palm kernel shell, softwood pellets, and almond pruning. Various gasifying agents such as air, steam, nitrogen ( $N_2$ ), carbon dioxide ( $CO_2$ ), and oxygen have been considered across these studies.

CFD models provide the highest spatial and temporal resolution for simulating biomass gasification processes by integrating fluid flow dynamics with heat and mass transfer, as well as chemical reaction kinetics. These models serve as powerful tools for analyzing in-reactor phenomena such as flow distribution, temperature gradients, and the formation of hot or cold zones, all of which critically influence reactor efficiency and performance. Euler–Lagrangian and Euler–Euler CFD models have also been shown to be able to capture phase interactions, and predict temperature fields very accurately. For example, ZiTeng *et al.*<sup>140</sup> employed a hybrid strategy where the Euler–Lagrangian method was used to model particle-level interactions at the interface of solid and fluid phases, while the Euler–Euler method captured the macroscopic behavior and interpenetration of continuous phases. Such approaches have demonstrated high accuracy in predicting temperature fields, phase behavior, and fluid–solid interactions within gasification reactors. The large number of equations describing the CFD models, particularly in the construction of multiphase systems or models with complex chemistry, is however a major bottleneck and implies that the computational requirement is high.<sup>141</sup> Further, simplified kinetics or empirical correlations are still used by the chemical sub-models nested within most CFD studies, which limits the ability to accurately predict the formation of secondary species such as tar and soot. To address these challenges, ongoing research is exploring the development of reduced-order CFD models and hybrid modeling platforms that combine CFD with kinetic or data-driven sub-models. These emerging approaches aim to balance the trade-off between model fidelity and computational efficiency,



Table 5 CFD models: summary of relevant research

Reference	Feedstock	Gasification agent	Remark	Future research possibilities
130	Coal	Air and oxygen	The research demonstrates computational fluid dynamics (CFD) to be essential for modeling underground coal gasification processes as a research tool during system design	A discrepancy between experimental measurements and predicted results for $\text{CH}_4$ and $\text{CO}_2$ amounts to 16% to 30% thus suggesting further tests should be conducted to reduce this variation
131	Municipal solid waste	Air	The study demonstrates that the hydrogen yield is minimal at the bottom of the reactor, around 1%, but increases to a peak of approximately 23% near the top. Conversely, the CO molar fraction is highest at the reactor's bottom, reaching about 22%. The relative error for the four main syngas components stays below 12%	Mathematical models need extensive research with development efforts to improve their application scope and precision for process enhancement and plasma gasification implementation
132	Coal	Air and steam	Increasing the tapered angle of fluidized bed gasifier reduces the LHV and HHV of gas products but enhances the CCE, with the CGE improving from $3^\circ$ to $5^\circ$ and stabilizing between $5^\circ$ and $11^\circ$ . Higher velocities of the gasifying agent lower the LHV and HHV while boosting the CCE. Moreover, increasing the steam-to-air ratio reduces the concentrations of $\text{H}_2$ , $\text{CO}$ , and $\text{CO}_2$	The experimental validation performs well yet the predicted $\text{H}_2$ results show lower values than observational measurements. At an 11-degree angle both CGE and CCE reach maximum levels of 30% and 50% indicating areas for possible enhancement
133	Ecoshakti biomass pellet	Air	This research indicates that boosting equivalence ratio (ER) results in diminishing carbon monoxide (CO), hydrogen and methane concentrations together with growing concentrations of carbon dioxide ( $\text{CO}_2$ ) and nitrogen ( $\text{N}_2$ ). During the process of changing ER from 0.25 to 0.60 the air composition shifts to augment nitrogen mole percentage from 41.48% to 66.63%	Average errors from the measurements of CO gases hydrogen and $\text{CO}_2$ concentrations reached 5.21%, 10.55% and 24.63% respectively. The model predicts $\text{CO}_2$ values with a substantial error showing that additional improvements are needed to match actual experimental results
134	Miscanthus briquettes	Combination of air, steam and oxygen	According to the paper, increasing the equivalence ratio (ER) results in a decrease in the concentrations of carbon monoxide (CO), hydrogen, and methane, while the concentrations of carbon dioxide ( $\text{CO}_2$ ) and nitrogen ( $\text{N}_2$ ) increase. The presence of nitrogen in the air, along with oxygen, causes the nitrogen mole percentage to rise from 41.48% to 66.63% as the ER increases from 0.25 to 0.60	Simulation results predict CO and $\text{H}_2$ quantities which match experimental results well. The relative error calculations for $\text{CH}_4$ show substantial variation while producing higher numbers from 6.5 to 64.7. The $\text{CH}_4$ prediction accuracy requires additional simulation model enhancements for better performance
135	Coal	$\text{O}_2$ , steam, $\text{N}_2$	The research model demonstrated a carbon gas efficiency between 45% and 66.78% and carbon conversion efficiency from 40% to 50%. Laboratory tests proved that the fluidized bed gasifier with circulating mode operated better than a bubbling fluidized bed gasifier for carbon conversion performance. The highest production rate of 55% emerged when CRC 701 received an O:C ratio of 0.7	There is still significant deviation in yield percentage prediction of $\text{H}_2$ and $\text{CO}_2$ compared to experimental data for coal CRC704
136	Palm kernel shell	Steam and $\text{CO}_2$	Higher gasification temperatures combined with S- $\text{CO}_2$ -R influence both $\text{H}_2$ production rates as well as tar formation to a significant extent. $\text{H}_2$ production increased by 21.4% and 20.5% during S- $\text{CO}_2$ -R operations at the	Research shows that while the amount of tar decreases during gasification compared to the earlier devolatilization stage, the overall reduction in tar at higher reaction



Table 5 (Contd.)

Reference	Feedstock	Gasification agent	Remark	Future research possibilities
137	Softwood pellets	Steam	higher values of 2.0 and 1173 K respectively relative to 0.4 S-CO <sub>2</sub> -R at 973 K temperature Research through the hybrid Euler-Lagrange approach of DDPM demonstrated the biomass-to-char conversion process takes approximately 40 seconds which indicates viability for laboratory-scale reactor implementation. When initialization methods implement partially converted fuel particles the calculation time decreased because it brought simulations closer to actual reactor operating points	temperatures during both stages is not very significant Further research needs to investigate the complete mechanisms of tar development and breakup because tar impairment remains a fundamental barrier to fluidized bed biomass gasification expansion on industrial scales
138	Almond pruning	Air and steam	An increase in gasifier temperature and steam-to-biomass ratio (S/B) generated better syngas production (CO + H <sub>2</sub> ) with higher hydrogen content in producer gas. Air supply in the dual fluidized-bed system had a minimal effect on biomass gasification because it did not influence the actual process	The current model does not account for tar formation, and the CFD results need to be enhanced, particularly for the cases involving CH <sub>4</sub> and CO <sub>2</sub> . The model underestimates the prediction for CO <sub>2</sub> by approximately 28%
139	Rubber wood and neem	Air	A CFD model examined how tar species (benzene, naphthalene, toluene, and phenol) formed in a downdraft gasifier through primary, secondary, and tertiary stages of tar production. Simulation results showed that CO combustion achieved the fastest reaction speed at ER 0.4 and methane formation operated at its greatest rate	Since this paper has already considered some compound presents in the tar which can be explored in further research for better understanding to reduce its formation during the gasification process

enabling more practical and accurate simulations for reactor design, scale-up, and control. Future advances in this area could significantly enhance the predictive capability of CFD tools while maintaining manageable computational costs.

### 3.4 Data driven modeling

Data-driven models (DDM) objective is to establish relationship between system variables and gasification products by utilizing the statistical or numerical analysis of present experimental data. These models can optimize mathematical operations to predict gasification products without relying on predefined conceptual boundaries. It works on machine learning frameworks to enhance predictive accuracy. Several data driven machine learning techniques are employed in gasification modeling, including artificial neural networks (ANN), support vector machines (SVM), along with multiple linear regression, and decision trees. These models are trained using a hybrid database, which allows for improving the performance analysis and optimization of the gasification operations.<sup>142</sup> Moreover, machine learning (ML) together with deep learning (DL) serves as advanced AI techniques which demonstrate exceptional effectiveness and significance for thermochemical conversion system research. These models hold significant value for their use in productivity forecasting as well as real-time monitoring with process control and process enhancement applications.<sup>143</sup>

Among various data-driven techniques, the Artificial Neural Network (ANN) method is the most widely used. The ANN techniques develop predictive models by creating input-output data correlations. The methodology uses input data sets as its complete requirement thus redundancy of mathematical description is not necessary.<sup>17</sup> ANN models are extensively used because they successfully detect complex nonlinear data connections between inputs and outputs. Among the decision-making factors the researchers employ for method selection are the application type and data access along with computational potency and desired model performance outcomes.<sup>144</sup> This model offers the flexibility to incorporate different important process parameters such as tar content, char content, the steam-to-biomass ratio (for steam gasification), and unconverted carbon along with the other relevant variables essential for the precision of the modeling.<sup>145</sup> There are various ANN architectures, including feed-forward back propagation neural network (FFBP), Elman-forward back propagation neural network (EFBP), cascade-forward back propagation neural network (CFBP), along with nonlinear autoregressive neural network (NARX), and layers recurrent neural network (LR). This model is optimized using algorithms such as Levenberg–Marquardt (L–M), Genetic Algorithm (GA), and Particle Swarm Optimization (PSO) methods.<sup>146</sup>

The ANN model varies in terms of architecture, reactor types, operating parameter, application focus and integration with



different data sets of different gasification systems. A study was developed using ANN system which forecasts gas mixtures produced in fixed bed downdraft biomass gasifiers particularly CH<sub>4</sub>, CO and CO<sub>2</sub> as well as H<sub>2</sub> compositions.<sup>143</sup> It processed elemental composition along with ash and moisture content and reduction zone temperature as inputs to reach high accuracy levels of  $R^2 > 0.99$  for CH<sub>4</sub> and CO and  $R^2 > 0.98$  for CO<sub>2</sub> and H<sub>2</sub>. The gas composition prediction model showed reliability through Garson's equation which evaluated the relative importance of input variables. Joel George *et al.*<sup>147</sup> developed an ANN model in MATLAB to simulate the gasification process using available experimental data from the air gasification in a bubbling fluidized bed gasifier taking various biomass types. The model was trained using a multi-layer feedforward neural network with the Levenberg–Marquardt backpropagation algorithm, minimizing mean squared error (MSE) utilizing the supervised learning method. The performance analysis showed a strong agreement between predicted and the actual values, with a regression coefficient having ( $R$ ) of 0.987 and the MSE of 0.71. The model effectively predicted producer gas yield based on seven key input variables, including biomass composition (C, H, O), gasification temperature ( $T$ ), equivalence ratio, together with ash content (AC), and moisture content (MC). The results validate ANN modeling which is a reliable tool for the gasification process simulation. In another study, H. O. Kargbo *et al.*<sup>148</sup> developed an ANN based model to optimize the operating conditions for two-stage gasification, which is aiming for high carbon conversion, together with increased hydrogen yield, and decrease carbon dioxide emissions in nitrogen and carbon dioxide rich environments. This model has aligned well with experimental data, also confirming the accuracy. Here, the optimal conditions (900 °C in stage 1, 1000 °C in stage 2, with a steam/carbon ratio of 3.8 in nitrogen and 5.7 in carbon dioxide) which resulted in the gas yields of 96.2 wt% (N<sub>2</sub>) and

97.2 wt% (CO<sub>2</sub>), with hydrogen yields of 70 mol% (N<sub>2</sub>) and 66 mol% (CO<sub>2</sub>). The carbon dioxide concentrations were minimized to 16.4 mol% (N<sub>2</sub>) and 12 mol% (CO<sub>2</sub>). Fig. 10,<sup>40</sup> presents the basic framework for development of gasification simulation using ANN. It utilizes experimental and simulation data, various input parameters, reactor dimensions data and output parameter. ANN models simulate a given process by finding correlation between input, hidden and output layer along with reducing the mean square error compared with the experimental or simulated data available in the previous research data.

The ANN model demonstrates strong predictive capabilities for syngas composition; however, further improvements are needed to minimize prediction errors. A key limitation is the scarcity of both simulated and experimental data, which affects the model's flexibility and efficiency. Additionally, it is essential to enhance the model to account for polymeric (lignocellulosic) feedstock compositions, gasifier design parameters, and the formation of tar and char. The data driven model with physics informed neural networks (PINNs) and their derivatives known as Disentangled Representation PINNs (DR-PINNs) are recent data-driven modeling techniques that have provided solutions to predict and model gasification processes. Experimental or simulation data may be used in developing these models and physical limits (conservation of mass and energy) are imposed. Research by Ren *et al.*<sup>149</sup> shows that PINNs can be used to predict syngas composition under a variety of operating scenarios with high accuracy (greater than 0.95  $R^2$ ) and thermodynamic concurrency. These physics-sensitive frameworks are more interpretable and have improved generalization capabilities as opposed to black-box machine learning models. Nevertheless, there still are problems to be solved, especially in the case of handling stiff reaction systems and the extension of the models to previously impervious feedstock/reactor

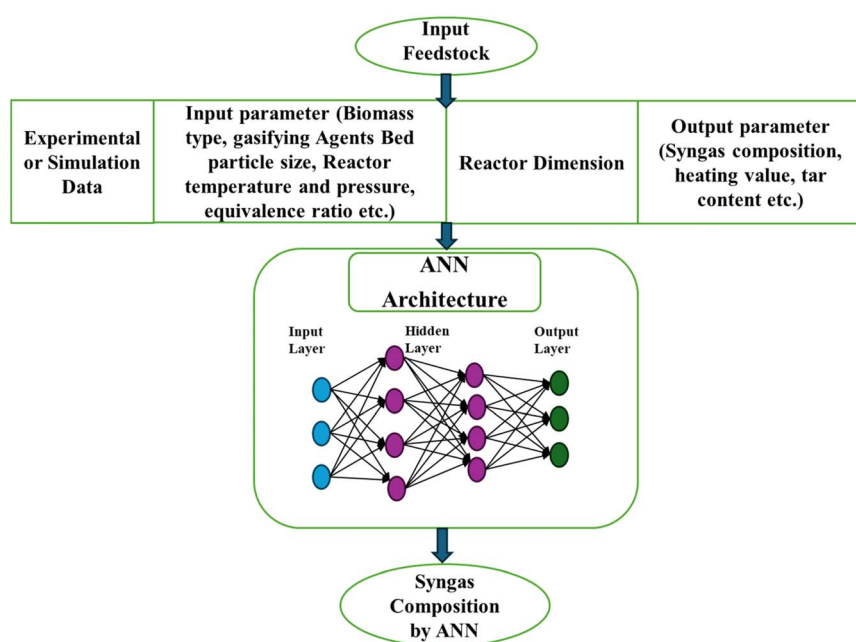


Fig. 10 Flow diagram of data driven modeling.



Table 6 Comparison study between different solving models for gasification process

Comparison between different modeling process<sup>133,146,150-153</sup>

Thermodynamic equilibrium model	Kinetic model	CFD modeling	Data driven modeling
The thermodynamic equilibrium models draw from the second law of thermodynamics by applying equilibrium constants and minimizing Gibbs free energy while optimizing entropy	The foundations of kinetic models rest upon reaction kinetics together with rate of reaction, reactor hydrodynamics and geometry	CFD modeling depends on conservation laws for mass, momentum and species together with energy within predefined boundaries	The modeling methods from data-driven approaches require experimental and simulation data for creating mathematical relationships through regression analysis, tree-based algorithms or support vector machines
This equilibrium model is straightforward to apply and is independent of the gasifier's design	Depends on the gasifiers design	It highly depends on gasifiers designs	Since it is data driven model, so the gasifier designs are their input parameter itself
Time invariant	Time-dependent and can predicts system changes over time	It can perform both steady and time-dependent simulations to analyze the steady and transient behavior	It can handle both static and time-series data
It has relatively simple mathematical calculations	It is more complex due to tough differential equations need to solve for calculation	Highly computationally intensive since it requires fine meshing to capture the physical parameter accurately	It can vary, but can be computationally expensive for large datasets
While the model provides accurate predictions of maximum yield, it tends to overestimate or underestimate the quantities of methane and char produced This is moreover limited to the equilibrium condition	Generally, more accurate for non-equilibrium conditions	This has the capability to deliver comprehensive spatial and temporal predictions	This model is completely depending on the quality and quantity of
The main purpose of this model is to estimate syngas yield while lacking the ability to accurately model complex events including tar formation and char production, minor hydrocarbon generation and heat loss	It can be used for modeling non-equilibrium states and transient behavior	The CFD model is highly adaptable to different reactor designs and operating conditions	It is versatile and can be applied to various types of data and prediction tasks; however, there remains a lack of sufficient data for all types of gasifiers and gasification processes
	Kinetic models use basic methods to simplify the processes involved in tar formation as well as cracking dynamics while handling complex fluid dynamics especially in fluidized bed systems. The precise modeling of char reactivity changes during the gasification process proves difficult to achieve	The computational constraints stop researchers from running direct CFD simulations that require modeling all particle and turbulence scales extending from micrometers to meters	Gasification data driven modeling faces limitations due to its requirement for good data quality and its susceptibility to overfitting as well as its inability to explain what is happening. The system faces difficulties when dealing with uncertainties while providing small information about actual physical processes

combinations. Moreover, stability of the models at saturation extremes and the requirement of large and good quality datasets is still a concern. Current research is tackling these shortcomings with integration of conservation laws as hard constraints and integration of PINNs with mechanistic reactor sub-models to provide additional robustness and flexibility.

Each of the four modeling approaches used to address gasification problems has its own strengths and limitations. Table 6 provides a detailed comparison, outlining the advantages, disadvantages, and key features of each modeling method.

In summary, while each modeling approach offers unique advantages, no single method sufficiently captures the full scope of physical, chemical, and operational complexity inherent in biomass gasification. A forward-looking strategy

should focus on integrating these models such as coupling reduced-order kinetics with CFD insights or embedding mechanistic understanding into physics-informed machine learning models. By doing so, the field can move beyond descriptive modeling and toward predictive, scalable tools that support reactor optimization, techno-economic evaluation, and commercial deployment.

## 4 Gasification integration to P2X: methane and ammonia, hydrogen utilization

This section explores the integration of gasification technologies with Power-to-X (P2X) and other clean energy processes to

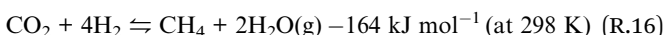
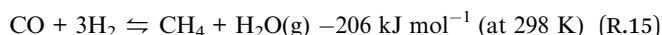


produce clean fuels such as methane, ammonia, and hydrogen within a unified process engineering framework. The primary objective is to evaluate existing models, assess their feasibility, identify limitations, and propose future research directions. Specifically, the discussion is aimed at the integration of gasification with methanation, green hydrogen, and ammonia production. For instance, integrating biomass gasification with renewable energy sources has been proposed to enhance methane production, promoting the chemical storage of renewable energy. Additionally, coupling gasification with the Haber–Bosch process allows for the synthesis of ammonia, utilizing hydrogen derived from gasification. Furthermore, biomass gasification presents a promising pathway for sustainable hydrogen production, offering a renewable alternative to fossil fuel-based methods.

#### 4.1 Methanation

Methanation is a chemical process that hydrogenates  $\text{CO}_x$  to produce methane. The CO methanation and  $\text{CO}_2$  methanation process is mostly used to convert these gases into  $\text{CH}_4$ . Gasification is a sustainable method for producing syngas, which primarily consists of carbon monoxide (CO) and carbon dioxide ( $\text{CO}_2$ ). Converting this syngas into methane not only increases its energy value but also contributes to negative carbon emissions by transforming CO and  $\text{CO}_2$  into green fuel.<sup>154</sup> From 1  $\text{m}^3$  of methane almost 1.8 to 2.3 kW of heat can be produced per hour at standard conditions. The variable gas volumes appear during methanation since CO methanation can reduce up to 50% of carbon monoxide and  $\text{CO}_2$  methanation can reduce 40% of carbon dioxide.<sup>155,156</sup> The methanation of syngas along with  $\text{CO}_2$  can be beneficial for the conversion of renewable energy into practical, transportable, and high-density fuels. The syngas obtained from the gasification can be further utilized to produce valuable chemicals using the Fischer–Tropsch synthesis (reaction (R.15)). Whereas there is need to prevent catalyst deactivation due to the sulfur poisoning with  $\text{H}_2\text{S}$  generated during the gasification that must be removed before the methanation process starts. Since methanation is a reversible exothermic reaction, optimizing the catalyst design is crucial for achieving maximum conversion at approximately 350 °C.<sup>157</sup> The catalysts play an important role for optimization of the reaction condition. There are Nickel-based catalysts, along with noble metal catalysts such as platinum, rhodium, and ruthenium have demonstrated effectiveness in  $\text{CO}_2$  methanation process. The materials include  $\text{TiO}_2$ ,  $\text{SiO}_2$ ,  $\text{ZrO}_2$ , with hydrotalcites and zeolites provides support in reaction.<sup>158–160</sup> According to the study by Liu *et al.*<sup>161</sup> the catalytic performance of  $\text{Ni}-x\text{CeO}_2/\text{Al}_2\text{O}_3$  for methanation is significantly influenced by the  $\text{CeO}_2$  content. Their findings revealed that the catalyst containing 2 wt%  $\text{CeO}_2$  exhibited the most effective catalytic activity and achieved the highest methane ( $\text{CH}_4$ ) selectivity. Moreover, the key operating parameters for syngas methanation utilizing  $\text{Ni}/\text{Al}_2\text{O}_3$  ratio, including the  $\text{H}_2/\text{CO}$  ratio,  $\text{NiO}$ , reaction pressure with  $\text{MgO}$  loading, and space velocity. The incorporation of 2 wt%  $\text{MgO}$  is found to reduce the carbon deposition and enhance the catalyst stability. At 400 °C,

the formation of  $\text{NiO}$  with reducible  $\beta\text{-NiO}$  was promoted in the catalyst containing 20 wt% Ni. The optimal conditions for achieving 100% CO conversion and high  $\text{CH}_4$  selectivity were observed at 3.0 MPa, with 20–40 wt%  $\text{NiO}$  and 2–4 wt%  $\text{MgO}$  supported on  $\text{Al}_2\text{O}_3$  within a temperature range of 300–550 °C. It can contribute to the development and optimization of  $\text{Ni}/\text{Al}_2\text{O}_3$  catalysts for syngas methanation process.<sup>162</sup> The reversible CO adsorption reaction occurred prominently during CO methanation but barely happened during  $\text{CO}_2$  methanation as listed in reaction (R.15) and (R.16).<sup>163</sup> Another study has been analyzed to produce methane rich gas stream from air gasification of low-quality nitrogen diluted syngas. It has considered kinetic as well as thermodynamic aspects with reactor dimensions and its performance. It utilized four adiabatic fixed-bed reactors with an intermediate cooling and the effective water removal has been shown to provide an optimal balance between the efficiency and cost. Therefore, while operating at a pressure of 5 bars it proved sufficient to minimize catalyst usage and suppress the carbon formation. This setup has delivered a strong performance metrics, achieving 99.4% CO conversion,  $\text{CH}_4$  yield of 95.6%, and 89.3%  $\text{CO}_2$  conversion. The resulting methane had a molar concentration of 26.4% with a calorific value of 8.62 MJ  $\text{Nm}^{-3}$  under standard conditions.<sup>164</sup>



The methanation reactors usually face three major challenges like the presence of catalyst poisons (especially the sulfur compounds), carbon deposition, and the highly exothermic nature of the reactions.<sup>165</sup> To ensure a catalyst lifespan of at least one year, which is considered economically viable, the sulfur content present in the feed gas must be kept at below 1 ppm.<sup>166</sup> Secondly, the carbon deposition is particularly problematic at temperatures above 500 °C. Since CO absorbs strongly on nickel-based catalysts, which can decompose into carbon atoms. If it is not rapidly hydrogenated, this carbon can lead to the formation of polymeric carbon with carbon nanofibers, nickel carbides or, all of these can block active catalytic sites.<sup>167</sup> Additionally, the exothermic nature of reaction causes significant temperature increases within the reactor, which potentially can create a hot spot between 550 °C and 750 °C, which can result in the catalyst sintering and loss of activity.

Moreover, the modeling of methanation reactors relies also on fixed-bed, fluidized-bed systems and specialized designs including fixed-bed tube-bundle and structured fixed-bed reactors. The models integrate multiple elements which include time resolution alongside reactor dimensions, phase representation and temperature behavior together with kinetic approach and software simulation tools. The researcher needs to boost the efficiency of methanation combined with improved catalyst performance and sustainable operations while generating pure  $\text{CH}_4$  during low-temperature extended operations. Currently operating methanation systems exist commercially yet researchers must conduct additional studies about catalyst mechanisms and feed gas composition variations. The research



emphasis stands on catalyst enhancement while working to develop better reactor models with optimal temperature control systems. There is necessity to focus on improving three main performance areas that include operational flexibility and dynamic performance with cost efficiency.

## 4.2 Hydrogen production

Several approaches exist for producing green hydrogen, including process integration with technologies like solar PV systems, geothermal energy, wind technology, and biomass gasification systems. The implementation of geothermal power-based hydrogen production requires a combination of production well along with turbine, generator, converter, reinjection well and PEM electrolyzer. The geothermal fluid streams into the system under 240 °C temperature and 33.47 bar pressure conditions.<sup>168</sup> The energetic efficiency rate of biomass gasification reaches 53.6% while its exergetic efficiency rate is 49.8%. The efficiency rate for geothermal-based hydrogen production stands at 10.4% energetic and 10.2% exergetic. The hydrogen production rate reaches 1.13 mol s<sup>-1</sup> through a solar PV-based system which has energetic and exergetic efficiency of 16.95% and 17.45% respectively.<sup>169</sup> A study investigated three PV generators of 6 kW rated power for hydrogen production assessment.<sup>170</sup> The S-DPOH (Solar-Driven Production of Hydrogen) solar-driven process generated 43.75 mmol hydrogen throughout 50 hours of solar irradiation. This photocatalyst produced hydrogen at a rate of  $38.66 \pm 0.655$  mmol h<sup>-1</sup> g<sup>-1</sup> and maintained a production level 1.5 times greater than previous reports using pure TiO<sub>2</sub> photocatalysts.<sup>171</sup> The various techniques available for produce hydrogen are presented in Fig. 11.<sup>172</sup> Water electrolysis is the most used technique among all, and the gasification process is at second position because of its complex operation and developing stage.

Gasification technology is basically a reliable and green source to produce hydrogen since we can utilize various biowaste to convert into rich hydrogen syngas. The recent technologies for producing hydrogen from the biomass include pyrolysis with gasification and various methods for converting biomass into liquid fuels such as hydrolysis, along with liquefaction and supercritical extraction. Sometimes these processes are followed by reforming to enhance the generation of hydrogen yield.<sup>173</sup> When air is used in the gasification system, it can produce a gas

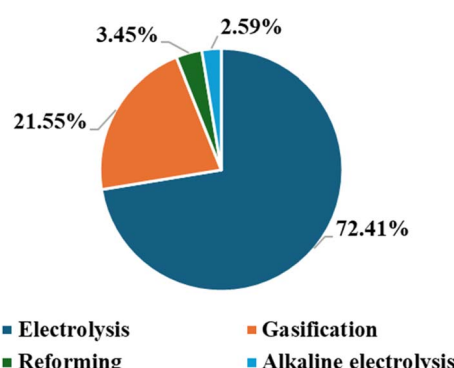
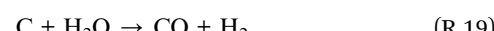
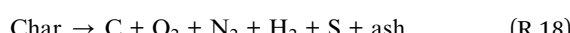
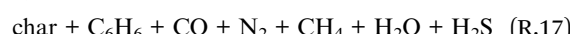


Fig. 11 Popular routes for hydrogen production.

mixture that contains approximately 20% hydrogen, 10% carbon dioxide, 5% methane, along with 20% carbon monoxide and 45% nitrogen. This gas stream can be modified further through a reaction with steam to convert the carbon monoxide into additional hydrogen utilizing the water-gas shift reaction.<sup>174</sup> Whereas supercritical water gasification is also an efficient thermochemical process which enables moist biomass feeding directly to the gasifier along with pressure-induced hydrogen storage cost reductions.<sup>175</sup> Another method to produce hydrogen via biomass gasification with calcium oxide (CaO) serves as a potential viable method for hydrogen generation. This eco-friendly biomass gasification approach enables large-scale production of hydrogen while utilizing widely available and affordable CaO catalyst to generate hydrogen-rich gas products.<sup>176</sup> While the solar based gasification technology is reliable as it provides green source of power to the gasifier. This can also improve the effectiveness of feedstock and overall energy by 30% and 40% respectively.<sup>177</sup> The chemical reactions below illustrate different pathways for syngas reformation produced from biomass gasification. This syngas, composed mainly of CO and H<sub>2</sub>, is directed into a turbine, where it generates power under high-temperature and high-pressure conditions. After exiting the turbine, the syngas passes through a heat exchanger, where it is cooled to a suitable temperature for water heating, enabling steam generation for the electrolysis process. Subsequently, the syngas enters a multi-stage water-gas shift reactor (MWGSR), where steam is used to convert CO into CO<sub>2</sub> while producing additional hydrogen, as represented by reactions (R.17) to (R.20).<sup>28</sup> Additionally, a portion of the syngas can be directly combusted in a Brayton cycle to produce power.<sup>178</sup>

Biomass →



Owing to high carbon dioxide production, hydrogen production by steam reformation is classified as gray hydrogen. Hydrogen production coming from sources like natural gas, biogas or syngas is classified as blue hydrogen. In case of blue hydrogen, the CO<sub>2</sub> emissions can be brought down through carbon capture methods and subsequent reuse practices while grey hydrogen plans lead to atmospheric carbon release. Biomass gasification produces environmental benefits through lower greenhouse gas emissions that range between 405–896.61 g CO<sub>2</sub> per kg H<sub>2</sub> while wind-powered electrolysis produces 600–970 g CO<sub>2</sub> per kg H<sub>2</sub> emissions.<sup>179,180</sup> The worldwide hydrogen manufacturing amounts to 75 million tons per year split into blue hydrogen produced through natural gas that uses 205 billion cubic meters of gas from natural sources while making up 6 percent of all gas use on a global scale. A total of 23% represents grey hydrogen fuel which is derived from coal to generate 107 million tons corresponding to 2% of worldwide

coal consumption.<sup>181</sup> Moreover, the efficiency level for hydrogen gas production can be improved by integrating biomass torrefaction with densification and gasification operations.

### 4.3 Ammonia

Renewable-powered ammonia production offers a net-zero emission solution by enabling energy storage, clean fuel generation, and potential carbon capture. Containing 17.6 wt% hydrogen, ammonia serves as a promising medium for hydrogen storage. Although its energy density is approximately 4.32 kW h per liter about half that of liquid hydrogen it remains an efficient and practical option for hydrogen storage and transportation due to its ease of handling and existing infrastructure.<sup>182</sup> Most of the worldwide ammonia production at 70% serves the fertilizer industry while ammonia functions critically across multiple sectors including carbon-free fuel production, minerals extraction, medicine manufacturing, water purification alongside polymer and textile manufacturing. Main catalytic approaches for ammonia manufacturing consist of electrocatalysis, photocatalysis, photo electrocatalysis and biocatalysis. The analysis of photocatalytic ammonia synthesis concentrated on bismuth-based materials combined with noble metal-modified photocatalysts through metal-free semiconductors and metal sulfide-based materials resulting in research opportunities for green ammonia applications.<sup>183,184</sup> The three primary ammonia technology systems include centralized with modified methane-based Haber–Bosch and electrolysis-driven Haber–Bosch (shown in reaction (R.21)) and distributed ammonia production methods. Traditional Haber–Bosch production runs with both high pressure (15–25 MPa) and elevated temperatures (400–450 °C) through wüstite Fe-based catalysts which use separated air nitrogen with generated methane-derived hydrogen. Current methods for ammonia production use steam methane reforming (SMR) as the most efficient approach to make hydrogen for synthesis.<sup>185</sup>

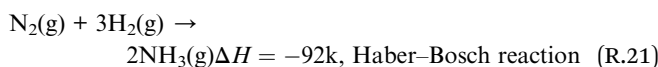


Fig. 12 describes the two-process integration methods to produce green ammonia utilizing renewable sources like syngas gas produced from biomass and renewable power sources inside the electrolysis. Green ammonia functions as a storage solution and transport method for hydrogen to resolve hydrogen storage and transportation issues. Whereas the cracking process transforms stored ammonia back to hydrogen along with nitrogen by applying heat (750–850 °C) and a proper catalyst which is again

a costly process since it requires high heat energy. Through biomass gasification processes agricultural waste together with crop residues turn into syngas by transforming into H<sub>2</sub>, CO<sub>2</sub>, H<sub>2</sub>O, CH<sub>4</sub>, CO, N<sub>2</sub> and air mixture. The synthesized syngas provides a suitable raw material for ammonia production which substitutes fossil fuels while enabling environmentally friendly ammonia manufacturing.<sup>186</sup> Weng *et al.*<sup>187</sup> have simulated hybrid biomass conversion process into ammonia by using chemical looping with solar and wind power system. This system consists of a biomass gasification system, chemical looping air separation (CLAS), water electrolysis with chemical looping ammonia production (CLAP) and power generation sources. Parametric optimization and feasibility assessments were carried out using Aspen Plus simulations. The cascading utilization of the biomass made the simultaneous production of N<sub>2</sub>, H<sub>2</sub> and NH<sub>3</sub>. The standard operating conditions with a biomass feed rate of 1 kg s<sup>-1</sup>, made system to achieve an ammonia selectivity of 79.36%, with an ammonia concentration of 65.65 vol% and a production rate of 34.1 kmol h<sup>-1</sup>. These outcomes demonstrate the viability of the HBCAS approach and offer valuable insights for the practical application. Another study, Nejat Tukenmez *et al.* modeled a multigeneration plant based on solar and biomass power generation. It has utilized a gasifier, hydrogen compressor, cooling unit, parabolic dish collector, Rankine cycle, ammonia storage tank, ORC cycle, hot water production unit, along with PEM electrolyzer and ammonia reactor unit. This integrated plant's total electrical energy output has been determined to be 20 125 kW. Whereas its energy efficiency with exergy efficiency is evaluated at 58.76% and 55.64%, respectively. And the production rates of hydrogen and ammonia are calculated to be approximately 0.0855 kg s<sup>-1</sup> and 0.3336 kg s<sup>-1</sup>, respectively.

The production of green ammonia utilizes alternative sources of renewable energy consisting of solar power and wind energy as well as hydroelectric power to operate electrochemical reactors integrated with biomass gasifier which has potential to decrease carbon pollution. Where the prices for electrolytic ammonia production stands at \$680–900 per ton but experts predict, it will drop to \$400 per ton by 2030.<sup>188</sup> The widespread implementation of ammonia as a commercial fuel faces difficulties because of its low energy content alongside high ignition requirements and NO<sub>x</sub> emissions when burned. The main obstacle in this method occurs when researchers seek an efficient catalyst to perform ammonia synthesis under low temperature and pressure conditions. A suitable catalyst plays a vital role in overcoming the high energy requirements of nitrogen reactions while improving the process viability.<sup>189,190</sup> The stationary power sector currently accepts ammonia as a renewable fuel with support from extended purchase agreements. The advancement of technology is anticipated to lead to better electrochemical processes while reducing costs which will make its implementation more possible.

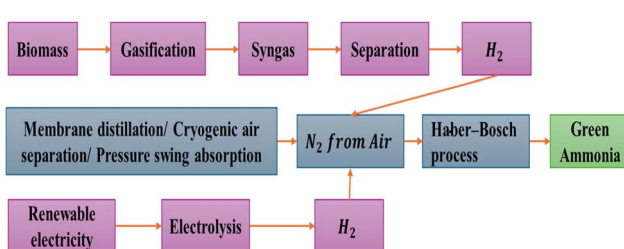


Fig. 12 Process integration to produce green ammonia.

### 4.4 Opportunities and bottlenecks in the future of power-to-X

The Power-to-X (PtX) pathways that incorporate biomass gasification, commonly referred to as Power and Biomass-to-X



Table 7 The possible advances for PBtX

Challenge	Required advances
CAPEX reduction	Scaling up the electrolyzer/SOEC capacity; homogeneous biomass gasification system; supply chain optimization to lower logistics and shared infrastructure expenses
Efficiency under flexibility	Electrolyzers/gasifying reactors that can be partially loaded and cycled without any performance drawback; better thermal integration
System integration	Achieving optimal integration of electrolysis, biomass gasification, and scaled-up renewable electricity infrastructure; completing full process integration including water-gas shift (WGS) and synthesis; and developing advanced syngas purification techniques adaptable to dynamic operating conditions
Demonstration scale	Pilot plants can be established to demonstrate Power-and-Biomass-to-X (PBtX) pathways, and to validate Technology Readiness Levels (TRL) 7–8 through comprehensive techno-economic analysis and life cycle assessment (LCA)
Policy & incentives	Increases in carbon prices, renewable hydrogen credits and subsidies to high-capital PtX infrastructure to fill in cost gaps

(PBtX) systems, offer several compelling advantages, particularly in terms of feedstock flexibility and the potential for carbon circularity. Nevertheless, the deployment of them at scale has critical techno-economic or systemic challenges. Listed below is a quantitative overview of key performance indicators for Power and Biomass-to-X (PBtX) system.

- Carbon efficiency: PBtX systems can achieve carbon efficiencies exceeding 90%, which is significantly higher compared to 25–40 percent reported for conventional biomass-to-X systems.<sup>191</sup>

- Product yields compared to dry biomass feed: recent studies have reported that such systems can produce between 0.31 and 0.79 kg of syngas, 0.70 to 1.28 kg of methanol, and 0.20 to 0.57 kg of Fischer-Tropsch (FT) liquids per kilogram of biomass feedstock.<sup>192</sup>

- Efficiency of electrolyzer: electrolyzer efficiency is another critical determinant of PBtX system performance. Low-temperature electrolyzers such as alkaline electrolysis (AEL) and proton exchange membrane (PEM) systems typically operate at efficiencies of 50–58%, while solid oxide electrolysis cells (SOECs) can theoretically achieve up to 80% efficiency under optimal conditions.<sup>193</sup>

- Specific capital costs: integrated PBtX systems demonstrate approximately 30% lower capital expenditure than standalone PtX plants, with reported costs around €3580 per kW<sub>lhv</sub>, this is large due to yield improvements achieved by system level integration.<sup>191,194</sup>

The economic feasibility of PBtX systems, even with the substantial efficiency metrics, is very dependent on electrolyzer capital expenditures and the costs of renewable electricity. Research highlights that firstly to be competitive electrolyser capacity factors need to be maintained above 82–94%.<sup>191</sup> This requirement is difficult to meet when relying solely on intermittent renewable energy sources, which necessitate backup power solutions or energy storage infrastructure, both of which introduce additional capital and operational expenditures. Secondly, economic modeling shows that PBtX systems based on surplus electricity alone cannot be made to work unless they are kept in non-stop operations. Biomass gasification offers stabilization, allowing a more predictable utilization of capacity. However, ensuring a reliable biomass supply chain

and managing the complex interface between electricity fluctuations and gasification operations remain persistent technical barriers.<sup>195</sup> The third is efficiency losses & heat management, at theoretical efficiencies of nearly 80%, SOEC-enhanced systems hold promise, but, in many instances, device efficiencies are much lower as presented by the auxiliary loads and system losses. As an example, methanol PBtX chains may have declined exergy efficiencies of ~70 to ~58% under real conditions.<sup>193</sup> Hence, a combination of heat recuperation and process maximizing is a priority. Finally, is Technology Maturity & Scale-Up Risk. Most of PBtX ideas remain on simulation or pilot phase. Demonstrations on the TRL 7–8 scale are necessary to confirm integration of electrolysis into a gasification system, dynamically testing at variable electricity, syngas conditioning and removal of tar systems.<sup>196</sup> Otherwise, commercial investors will be hesitant about investing in it when there are doubts about the scalability of it. The further possible advances to improve the PtX system discussed in Table 7 in terms of CAPEX, efficiency, integration, scaling up infrastructure and favorable policies.

## 5 Sustainability assessment

This section investigates the practical implications of the previously discussed energy systems from both economic and environmental perspectives. It is important to analyze the feasibility, durability and total operation cost of the engineering systems to understand their scalability and sustainability. Furthermore, ensuring that these conversion processes should be economical, environmentally friendly, reduce carbon footprints, and have minimal environmental impact is of paramount importance.

### 5.1 Technoeconomic studies

In this section we discuss the economic feasibility of thermochemical energy conversion systems integrated with the gasification process. The focus is to examine the efficiency of these technologies alongside their production capability, expense structure and earnings potential. Renewable hydrogen (H<sub>2</sub>) serves as a sustainable energy carrier through its development



while renewable methane stands as an alternative to fossil-based natural gas that derives from  $\text{CO}_2$  or syngas methanation. The analysis assesses different systems which produce renewable methane through technical, economic and environmental performance assessments. The expansion of the solid oxide electrolysis (SOE) from 1 MW to 10 MW capacity leads to a substantial 23.3% decrease in methane production expenses. The overall cost assessment for renewable methane production involves separate analysis of capital investment and operational expenditure. The methanation reactor, along with the compressor, turbine with drum, and methane upgrading system, constitutes the major share of capital expenditures, while the operating expenses comprise the cost of deionized water, captured  $\text{CO}_2$  together with electricity usages, labor, maintenance and miscellaneous fees. The International Renewable Energy Agency reports that renewable power sources including onshore wind, offshore wind and solar PV generate energy at rates of \$0.039, \$0.084 and \$0.057 per kW h respectively.<sup>197</sup> Economic production costs of renewable methane make it unaffordable against standard natural gas supplies. Industrial production expenses heavily depend on electricity prices especially for electrochemical syngas generation because the process requires high electricity use for heating gasifier and  $\text{CO}_2$  separation unit. The experience rates of renewable methane production can compete with natural gas prices by technological refinements of electrolysis efficiency coupled with declining electricity charges according to a case study analysis. The effectiveness of electrolysis systems along with reduced power expenses creates essential conditions for renewable methane to succeed as a fossil-fuel natural gas replacement. Quite notably the switch from conventional natural gas to renewable methane holds the potential to remove 11.36 Gton of  $\text{CO}_2$  emissions from the atmosphere. A projection shows that renewable energy will dominate the world's primary energy supply to the extent of around 65% in 2050 as opposed to the initially forecasted 24%. Europe sets the pace through Denmark and Germany, but China and India experience fast-paced solar and wind expansion which grows by more than 30% yearly.<sup>198,199</sup> Fig. 13 shows an in-depth look at worldwide renewable energy

transition forecasts for 2050 according to four major organizations including International Energy Agency (IEA), International Renewable Energy Agency (IRENA), British Petroleum (BP) and Shell. These studies predict the percentage of renewable energy used for power generation in the world till 2050 where IRENA forecasts highest share of renewable energy in energy data mix at 43%.

A study evaluated the thermodynamic and economic feasibility of three synthetic natural gas (SNG) production systems based on biomass gasification integrated with syngas methanation. The three case scenarios included case1 as dual fluidized bed (DFB) gasification with  $\text{CO}_2$  capture (DFB + M + CCS), case 2 as DFB with renewable hydrogen (DFB + EL + M) and case 3 as direct biomass gasification with renewable hydrogen (CFB + EL + M). Case 3 achieved the best performance by recovering over 98% carbon content while maintaining efficient cold gas performance at 77.10% and exceeding the results of Case 2 at 70.92% and Case 1 at 63.27%. A better heat integration approach enabled the system to achieve 14.59% enhanced efficiency performance. To become financially competitive the SNG break-even price for Case 2 should remain between 58–98 € per MWh<sub>SNG</sub> while renewable electricity stays below 57.9 € per MWh. The operational model for Case 3 could thrive when electricity prices remained below 70.5 € per MWh.<sup>200</sup>

Broadly hydrogen is divided into different varieties namely blue, gray, brown, black and green depending on how it is produced, the energy source and environmental effect it generates. Renewable hydrogen is expected to achieve \$225.55 billion in the market by 2030 while maintaining a 6.4% compound annual growth rate. By 2026 the U.S. government wants to produce hydrogen at \$2 per kilogram through efficient low-carbon technology solutions which they expect to achieve \$1 per kilogram production by 2031. The currently employed thermochemical along with electrochemical, biological and photolytic processes do not meet the target cost rates.<sup>201</sup> A study performed on two process models to generate hydrogen and syngas from both coal and natural gas.<sup>193</sup> The first case employs literature-validated entrained flow gasification facilities though Case 2 implements a reforming system which improves hydrogen generation and minimizes carbon output. The Case 2 process achieves an 88% enhanced HCR value of 1.20 which surpasses baseline values by 1.20. Moreover, the two-process model offers 55% more hydrogen production along with an 18.5% enhancement in operational efficiency. Case 2 reduces carbon emissions by 69.6% for each unit of produced hydrogen. The investment for producing each ton of hydrogen and the final hydrogen selling price in Case 2 fall at levels which are 28.9% below Case 1 rates. For each metric ton of fuel, the total production cost amounts to €1892.092 in Case 1 and €1344.984 in Case 2. The calculation of total production cost per ton indicates that the TPC amount in Case 2 shows a lower value than the TPC amount in Case 1. The study demonstrates that the minimum selling price of hydrogen operates at a lower competitive level in Case 2 *versus* Case 1. The equation is used to calculate the fixed cost like equipment cost of process design and the total investment cost per ton of  $\text{H}_2$  as mentioned in eqn (16) and (17).

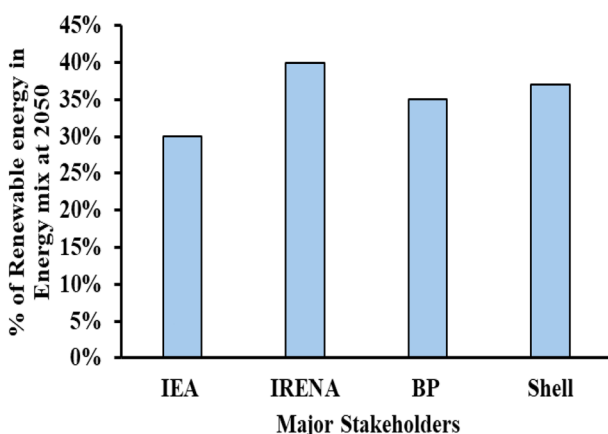


Fig. 13 Percentage of renewable energy in energy mix in 2050 by four major stakeholders.<sup>198</sup>



$$C_E = C_B \times \left( \frac{Q}{Q_B} \right)^M \times \frac{I_E}{I_B} \quad (16)$$

where,  $C_E$  = cost of equipment,  $C_B$  = base case cost,  $Q$  = capacity new,  $Q_B$  = capacity reference,  $M$  = constant(0,6),  $I_E$  = calculating year chemical engineering plant cost index,  $I_B$  = base case chemical engineering plant cost index.

$$\text{TIC per ton of H}_2 = \frac{\text{total investment cost}}{\text{hydrogen generation}} \quad (17)$$

Biofuel sectors face technological challenges along with economic hurdles in generating hydrogen, especially in mini decentralized facilities. Research into a 100 kWth system evaluated production costs by analyzing capital investment expenses and running costs together with efficiency parameters. The research demonstrates that efficiency boosts can decrease total expenses but must be strengthened through additional methods. The Portable Purification Unit (PPS) cost stands as the main cost factor because it requires significant reduction. The specific production cost will fall between 9.5 to 12.75 € per kg when operational costs decrease by 50% and the steam-to-biomass ratio goes from 1 to 1.5.<sup>202</sup> Therefore, the sensitive part of techno-economic analysis for hydrogen production varies by process. Electrolysis studies focus on capital, operating, maintenance costs, and net present value (NPV), while reforming considers production costs, including reactors, membranes, and labor. Gasification mainly evaluates NPV.

Ammonia ( $\text{NH}_3$ ) is synthesized from nitrogen and hydrogen using the Haber-Bosch process, with hydrogen production being the primary economic challenge. A study evaluated the technological feasibility together with economic assessment for producing ammonia through biomass gasification in a pulp and paper facility. Within the integrated system the overall energy efficiency increased by 10%-units above a traditional ammonia production plant. The economic viability needed an increased selling price range of 509–774 € per tons  $\text{NH}_3$  to reach investment return rates between 10–20%. Investment costs representing 45% were allocated to the synthesis loop. The evaluated production capacity at 228 000 tons per year proved unprofitable for current market prices. Plant expansion and cost reduction or increased prices from fossil-based alternatives establish the economic basis for financial feasibility.<sup>203</sup> A technological and financial analysis evaluates the two methods of producing green ammonia against traditional methane-to-ammonia processes alongside heat integration and improved steam cycle management. The 50k ton per year reference production shows different patterns between operational efficiency and cost expenditures. Power-to-ammonia demonstrates the best efficiency at 74% while methane-to-ammonia operates at 61% efficiency, yet power-to-ammonia achieves only 44% efficiency. The biomass-based production methods require high costs at \$450 per ton and need more than six years to break even whereas methane-based products cost \$400 per ton and reach their payback in five years. The power-to-ammonia process exists at present only as an uncompetitive method but advanced

solid-oxide development together with expanded renewable energy usage may lead to its future viability.<sup>204</sup>

## 5.2 Life cycle assessment

The Life Cycle Assessment (LCA) represents a commonplace method which assesses environmental effects. It consists of a comprehensive evaluation method that analyzes every raw material, energy input, product, emission and waste output from the start to end of a product's lifetime. The evaluation stages of LCA are organized into four distinct phases. The goal and scope definition stage of Life Cycle Assessment (LCA) establishes the objectives of the assessment, defines system boundaries, identifies the functional unit, and outlines key assumptions, data allocation methods, and data quality requirements. During the inventory analysis phase of LCA operators must gather information regarding both energy consumption and material inputs alongside product and co-product outputs as well as waste streams, environmental discharges to air, water and soil masses. The stage of impact assessment analyzes environmental impact categories that encompass climate change together with acidification, eutrophication, ozone depletion, human and aquatic toxicity, fossil fuel depletion, water depletion and land use. Improvement analysis verifies that the study's initial goals align with its methodology through a system boundary assessment and data accuracy evaluation and impact assessment model validation. Environmental emissions together with their impacts are provided through essential data generated by the inventory analysis and impact assessment stages. For instance, a study used real data to compare Downdraft Gasifier (DG) and Circulating Fluidized Bed Gasifier (CFBG) as two systems for hydrogen production. The research analyzes three key factors related to energy efficiency, production costs and capital investment efficiency. The assessment indicates that hydrogen production *via* DG would cost \$0.0172 per g but CFBG would cost \$0.24 per g in emission reduction expenses. The Coefficient of Hydrogen Production Performance (CHPP), defined as the ratio of the energy content of the hydrogen produced to the total energy content of the fossil fuels consumed, is calculated to be 5.71 for the CFBG system and 11.36 for the DG system.<sup>205</sup> Another research evaluated the two central gasification techniques for biomass hydrogen production namely fluidized bed (FB) gasification and entrained flow (EF) gasification. Carbon capture combined with liquefaction causes EF-based processes to reach 50% efficiency and FB-based processes to achieve 41%. The combination of \$100 per ton biomass cost and minimum \$115 per ton  $\text{CO}_2$  equivalent price or \$5 per GJ natural gas value produces a cost level comparable to conventional steam methane reforming through natural gas. The biomass-based alternatives can generate negative emissions throughout their life cycle as they have potential to generate green fuels by integrating with multistage operation.<sup>206</sup>

The hydrogen production technologies show that switching from natural gas to biomass as a source reduces GHG emissions by approximately 75%.<sup>207</sup> The analysis of popular gasification process demonstrates that the transformation method presents



an alternative option to conventional natural gas reforming when evaluated at various points in its life cycle. This method reduces GHG emissions by 0.4 kg CO<sub>2e</sub> per kg H<sub>2</sub> more efficiently than natural gas reforming which results in 10.6 kg CO<sub>2e</sub> per kg H<sub>2</sub> emissions and lowers fossil fuel usage.<sup>208</sup> Pyrolysis is also one of the most environmentally friendly methods for hydrogen production. The process produces hydrogen-rich syngas by thermally decomposing biomass in an oxygen-deficient environment.<sup>209</sup> The LCA of the process revealed that it generated decreased greenhouse gases, water usage and energy requirements than alternative hydrogen production approaches. The production of hydrogen through pyrolysis costs almost 2\$ per kg of H<sub>2</sub> production and has 40% of recovery efficiency. Thus, the gasification requires both higher temperatures along with oxygen utilization and produces larger environmental effects than the pyrolysis does. In contrast, dark fermentation generates hydrogen and organic acids from biomass under anaerobic conditions but incurs higher environmental costs compared to the pyrolysis process. Moreover, the steam reforming of biomass demonstrates high-energy requirements and elevated emissions during its processing as a method for hydrogen production. The LCA research demonstrates that using biomass to make hydrogen produces better environmental results than both natural gas reforming and water electrolysis processes. Mass production efficiency from pyrolysis serves as an affordable solution having better performance than gasification, dark fermentation, and steam reforming at reducing energy usage and water demand.<sup>210</sup>

Studies have also examined the various hydrogen production methods based on environmental impacts, including carbon dioxide equivalent emissions, acidification, eco-toxicity, along with the human toxicity, carcinogens, and abiotic depletion.<sup>211</sup> Investigations revealed that the global warming potential of steam methane reforming and coal gasification was 3.03 and 3.85 kg CO<sub>2</sub>-eq per kg of ammonia produced, respectively. In

contrast, biomass gasification had the lowest global warming potential at 0.378 kg CO<sub>2</sub>-eq per kg of ammonia. Additionally, abiotic depletion was highest for steam methane reforming, measured at 0.0264 kg Sb-eq per kg of ammonia produced. Fig. 14 presents the greenhouse gas emissions associated with various ammonia production methods. It indicates that ammonia produced from methane results in the highest CO<sub>2</sub> emissions, while the gasification-based process exhibits the lowest emissions.<sup>211</sup>

Furthermore, the analysis demonstrates that municipal waste incineration together with hydropower techniques produces ammonia with lower environmental impacts when compared against alternative production methods. The quantified greenhouse gas (GHG) emission levels for one kilogram of produced ammonia amount to 0.34 kg CO<sub>2</sub>-eq using municipal waste and 0.38 kg CO<sub>2</sub>-eq using hydropower and 0.84 kg CO<sub>2</sub>-eq from nuclear facilities as well as 0.85 kg CO<sub>2</sub>-eq from biomass generation. The study also performed an energy and exergy analysis to determine sustainability index scores which represented opportunities for improvement. Four types of systems examined for ammonia production efficiency resulted in energy efficiencies of 42.7% for hydropower while nuclear reached 23.8% and biomass achieved 15.4% and the lowest 11.7% was achieved by municipal waste-based systems. The calculated exergy efficiencies for energy production reached 46.4% for hydropower and 20.4% for nuclear and 15.5% for biomass systems while municipal waste-based methods had an exergy efficiency of 10.3%.<sup>212,213</sup> Another study investigated the process integration of the gasification system at olive oil mills with heat and power production through CHP with biochar manufacturing that uses moist olive pomace as fuel source. The system generates electricity with 13.5% efficiency and 32% CHP efficiency which produces 0.88 kW h renewable electricity per kg of olive oil. LCA analysis reveals an 8.25% decrease in environmental effects while achieving a 21% reduction of climate change emissions that fall from 2.21 to 1.74 kg CO<sub>2</sub>eq per kilogram of olive oil. The proposed gasification plant provides responsible methods to manage olive pomace while recovering sustainable energy.<sup>214</sup> Therefore, biomass gasification technologies have the potential to reduce the environmental impact by reducing the emission of carbon and utilizing it for the formation of methane, ammonia and hydrogen. Sustainability assessment including economic viability, such as different biomass gasification technology with its energy efficiency, economic metric emission and economic feasibility considering its cost and technology readiness levels (TRL) scale discussed in Table 8.

## 6 Future scope

This paper has gone through the latest research in relation to various gasification reactors, gasification simulation models, and green fuel production along with its techno-economic and life cycle analysis. Although the gasification models consisting of thermodynamic equilibrium model, kinetic model together with CFD models and data-driven models successfully calculate syngas compositions yet more advancement is needed to

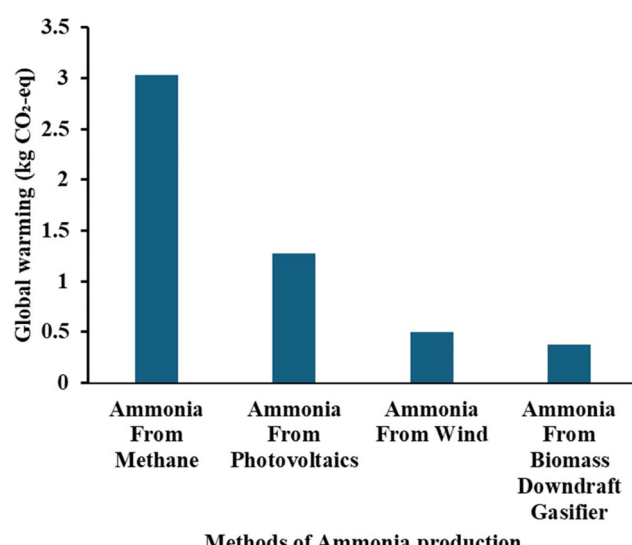


Fig. 14 Carbon emission from various methods of ammonia production.



Table 8 Sustainability overview of biomass gasification technology

Ref. no.	Technology	Energy efficiency	Economic metric	GHG emissions/reduction	CAPEX/OPEX & payback	TRL/scale
2115	Biomass fluidized-bed (FB)	40–50% (LHV)	LCOE (levelized cost of electricity) $\approx$ 0.067 USD per kWh in China Min H <sub>2</sub> price $\approx$ 150 € per t	Near-carbon neutral	Moderate CAPEX; low OPEX	TRL (technology readiness levels) 9, commercial Pilot/demo
2116	Entrained-flow biomass $\rightarrow$ H <sub>2</sub>	~56% (LHV)	BESP (Break-even selling price) $\approx$ € 781–816 per m <sup>3</sup> ; CO <sub>2</sub> avoidance payback	Negative lifecycle GHG possible GHG reduction 79% (no CCS); up to 264% with CCS	High CAPEX; needs $\geq$ 150 € per t H <sub>2</sub> to break even BESP € 781–816; competitive with heat valorisation & CO <sub>2</sub> credits	Demo-scale BtL
2117	Biomass chemical-looping gasification $\rightarrow$ Ftl	52–53% overall biomass to liquid conversion efficiency chain	Low investment –62 458.38k \$	Waste CO <sub>2</sub> fixed ~59.8k t per year	Payback 4.4 year; NPV \$118 M during 20 years of life span	Conceptual/system-level
2118	Medical-waste plasma + SOFC + S + CO <sub>2</sub> cycle + desalination	41.7% net power; 65% energy utilization rate	Operating capacity 1000 t per day with net output 33 MWh Fuel cost = 354 \$ per ton methanol (market range)	Varying; overall lower pollutants than incineration –0.56 kg CO <sub>2</sub> eq per kg methanol (net reduction)	CAPEX 250–450 M USD for 2000–3000 t per d; cost per t drops with scale	Demo-to-commercial
2119	Plasma gasification (general waste-to-energy)	Thermal efficiency 60–80%, net electrical efficiency 18.6–25% 65% total energy conversion	Fixed capital cost = 8 millions CNY (sewage sludge treatment capacity 20 t per h), LCOE-\$0.696 per kWh	Environmentally favorable; subsidies boost ROI	Fuel cost within market; integrated PV reduces system expenses	Model-to-pilot scale
220	Solar-driven biomass gasification hybrid (PV + solar thermal)	System thermal efficiency $\approx$ 63%	–	–	H <sub>2</sub> and power; ROI $\approx$ 24.9%, PP $\approx$ 3.8 year; H <sub>2</sub> cost $\approx$ 17.07 CNY per kg	Pilot-to-demonstration
221	SCWG of sewage sludge for H <sub>2</sub> + power	~81% gasification efficiency; HHV $\sim$ 6.4 MJ Nm <sup>-3</sup>	Complex reactor, pilot to demo scale	–	100 kW to 6 MW pilot/demo	–
222	Multistage biomass FLETG (fixed-bed, low-emission, two-stage gasifier) type gasifier	–	–	–	–	–

minimize experimental discrepancies. The equilibrium model shows significant discrepancies in CO and CH<sub>4</sub> predictions at stoichiometric ratios above 0.2.<sup>36</sup> When empirical correlations are added to equilibrium model it improves downdraft gasification accuracy providing a 52% RMSE reduction relative to baseline models. Within the transition temperature scope researchers noted substantial deviations between simulated and measured H<sub>2</sub> output values which resulted in errors of 46.5%, 27.1% and 48.3%.<sup>100</sup> The advanced model showed a 16% higher value for H<sub>2</sub> and CO<sub>2</sub> production as well as ash formation, yet it generated less CO and CH<sub>4</sub> than anticipated.<sup>223</sup> The kinetic model for gasification significantly overpredicts CO concentrations, resulting in deviations of up to 20% when compared to experimental results. Similarly, CO<sub>2</sub> predictions exhibit substantial errors of 29.3% and 26.4%, indicating that the model requires further refinement and development.<sup>120</sup> Current research on biomass gasification modeling in BFB systems continues to evolve through the integration of factors which include diffusion effects and tar cracking along with reaction kinetics and hydrodynamic principles. The model accuracy and reliability can be improved by involving various parameters in an extended analysis.<sup>224</sup> The accuracy of predicted H<sub>2</sub> gas is the lowest among all the predicted gases demonstrating the necessity to enhance the refinements in kinetic modeling.<sup>124</sup> The existing CFD model lacks systems for tar formation along with requiring better predictions for both CH<sub>4</sub> and CO<sub>2</sub> outcomes. Additional refinement measures are needed to improve CO<sub>2</sub> predictions because the model underestimates this value by 28%. Researchers need to investigate the formation processes of tar and cracking while targeting tar pollution elimination because it will enable the large-scale deployment of fluidized bed biomass gasification systems. Accurate addressing of these issues will boost model accuracy levels which will increase the industrial feasibility potential.<sup>135,137</sup> Data driven modeling is also getting popular in recent years. Whereas numerous barriers exist for data-driven gasification modeling due to data quality demands and complex model fitting and difficult interpretation. The system deals poorly with uncertain data and provides limited clues about actual physical processes at work. Therefore, to enhance the reliability of data-driven systems, it is essential to conduct additional experiments using varied parameters across diverse conditions.

Moreover, there is much potential to improve the gasifier technology to get better cold gas efficiency and carbon conversion efficiency. The updraft gasifier faces the main challenge of producing gas with high tar levels that reduces its heating capacity. Researchers need to explore new methods to remove unburnt carbon in entrained-flow gasification since the approach fails to eliminate the unburnt carbon under all experimental settings. The plasma gasification method also requires enhanced modeling techniques to enable reliable operation and optimize overall performance, including maximizing plasma heat utilization and achieving uniform heating. Also, the commercial application of supercritical water gasification faces difficulties at industrial scale because of varying biomass content and operating parameters. Research into

process improvement remains crucial because biomass variations lead to different responses during different operating temperatures and pressures as well as reaction times and feedstock concentrations and catalyst types. The Concentrated Solar Thermochemical Gasification of Biomass (CSTGB) system increases biomass utilization and power efficiency through producer gas storage by 30% and 40%. Whereas technology faces economic obstacles despite these facts so stakeholders must implement incentive-based policies to overcome this challenge. Practical implementation of the CSTGB process requires additional studies regarding pilot-scale economic models and solar collector materials as well as heat transfer fluid technologies.<sup>225</sup> Therefore, during the conversion process biomass-based systems generate energy outputs which fall 20–70% below what conventional natural gas steam reforming produces.<sup>226</sup> Furthermore, syngas derived from biomass gasification exhibits low H<sub>2</sub> to CO ratios that cause energy usage in upgrading systems to increase substantially because it requires energy-intensive units like water-gas shift reactors along with CO<sub>2</sub> removal systems using amines and PSA. Composition of syngas depends on both gasification temperature and steam-to-biomass ratio, but gasifier technology stands as the main determining element. And there is requirement of complete shifting towards renewable energy and building large infrastructure for green energy production because the energy cost for production of green fuel like H<sub>2</sub>, CH<sub>4</sub> and NH<sub>3</sub> is very high from our conventional resources. There are possibilities to reduce the total capital cost by utilizing the biomass pre-processing methodology integrating with green fuel production system. This can reduce the heterogeneous biomass handling cost and various capital costs.

## 7 Conclusion

This review highlights recent advancements in gasification technologies, alongside simulation methods and process integration strategies for green fuel production, while also evaluating economic feasibility, environmental impact, and future research directions. The development of sustainable energy infrastructure depends on the production of green fuels to effectively address climate challenges. Modern gasifiers such as supercritical water gasification (SCWG), plasma, multistage, and solar gasifiers demonstrate high conversion efficiencies and the potential to significantly reduce greenhouse gas emissions. However, existing modeling approaches for gasification processes still require improvement to achieve more accurate predictions aligned with experimental data. Furthermore, gasification technologies hold strong potential for integration with green fuel production systems in a way that is both economically viable and environmentally beneficial. Important findings are summarized in the following bullet points.

1. Modern gasification technologies have shown efficient performance, with solar gasification standing out for its significant potential. By utilizing renewable energy sources, it can achieve temperatures exceeding 1300 K, with energy efficiencies ranging from 70.6% to 72.7%. Despite challenges related to financial feasibility, solar gasification holds



considerable value with the potential to minimize possible environmental hazards.

2. Modeling methods are fundamental to improve gasification operations and estimate syngas production from biomass. Equilibrium model delivers easy computational operations that predict thermodynamically maximum gas yields through its simple calculations, but kinetic models combine enhanced precision with time-responsive solutions which simplify tar formation processes and fluid movement operations. Among modeling techniques CFD proves most flexible because it can determine flow patterns as well as heat distribution and critical areas. Additional development of these gasification models will be essential for boosting efficiency together with accuracy and general usability.

3. Power production from green fuels, such as hydrogen, methane, and ammonia, offers significant potential for reducing carbon emissions across various industries. The methanation process can help to improve the syngas quality, with potential to reduce CO and CO<sub>2</sub> composition by 50% and 40% respectively. Whereas, ammonia has proven to be an important carbon free hydrogen carrier, and it is expected to become economically viable by 2030, with production costs projected to drop to \$400 per ton, down from the current range of \$680–900 per ton.

4. The overall cost of the gasification process is highly sensitive to electricity prices, particularly in electrochemical syngas generation, which demands substantial green sources of electrical energy. However, integrating direct biomass gasification with renewable hydrogen can significantly enhance efficiency—recovering up to 98% of the carbon content while maintaining a cold gas efficiency of 77.10%. This approach allows electricity costs to remain below 70.5 € per MWh. Moreover, the use of green hydrogen not only contributes to a more sustainable process but also helps reduce the production costs of methanation and ammonia.

5. Transitioning from natural gas to biomass as a feedstock for hydrogen production can significantly reduce greenhouse gas emissions by approximately 75%. Among the evaluated technologies, biomass gasification demonstrated the lowest global warming potential, with an emission value of just 0.378 kg CO<sub>2</sub>-equivalent per kilogram of ammonia produced. Integrating renewable energy and biomass gasification to produce green fuel in a multigeneration plant offers a promising pathway toward achieving negative carbon emissions.

## Abbreviations and acronyms

ANN	Artificial neural network
CFD	Computational fluid dynamics
CGE	Cold gas efficiency
DNS	Direct numerical simulation
GHG	Greenhouse gas
EDGAR	Emissions Database for Global Atmospheric Research
ER	Equivalent ratio
GHG	Greenhouse gas
IEA	International Energy Agency

IRENA	International Renewable Energy Agency
LCA	Life cycle assessment
LES	Large eddy simulation
LHV	Low heating value
MSW	Municipal solid waste
MHGCG	Multistage heating and gradient chain gasifier
NPV	Net present value
RANS	Reynolds-Averaged Navier-Stokes
PBtX	Power and Biomass-to-X
SCWG	Supercritical water gasification
SSF	Simultaneous saccharification and fermentation
SMR	Steam methane reforming
SOE	Solid oxide electrolysis
SNG	Synthetic natural gas
SOEC	Solid oxide electrolysis cells
SOFC	Solid oxide fuel cell
TEqM	Thermodynamic equilibrium models
TRL	Technology readiness level

## Nomenclature

$A_j$	Total atomic mass of the $j$ th element [amu]
$A_r$	Frequency factor [ $\text{mol}^{(1-\alpha)} \text{ m}^{3(1-\alpha)} \text{ s}^{-1}$ ]
$a_{ij}$	Atoms of the $j$ th element in each molecule of $i$ species
$C_p(T)$	Specific heat as a function of temperature [ $\text{J} (\text{kg}^{-1} \text{ K}^{-1})$ ]
$C_v$	Specific heat of particle [ $\text{J} (\text{kg}^{-1} \text{ K}^{-1})$ ]
$c_{i,r}$	Concentration for $i$ th species and $r$ th reaction [ $\text{mol m}^{-3}$ ]
$D_{\text{eff}}$	The effective mass diffusion coefficient for species $k$ [ $\text{m}^2 \text{ s}^{-1}$ ]
$G_t$	Total Gibbs energy [ $\text{kg m}^2 \text{ s}^{-2}$ ]
$\Delta G_{f,i}^0$	Standard Gibbs free energy of species $i$ [ $\text{kg m}^2 \text{ s}^{-2}$ ]
$\Delta G_T^0$	Standard Gibbs function of reaction [ $\text{kg m}^2 \text{ s}^{-2}$ ]
$\Delta g_{f,T,i}^0$	Formation Gibbs free energy at $T$ for species $i$ [ $\text{kg m}^2 \text{ s}^{-2}$ ]
$g$	gravitational acceleration [ $\text{m s}^{-2}$ ]
$h_{f,i}^0$	Formation standard enthalpy for species $i$ [ $\text{kJ kmol}^{-1}$ ]
$\Delta h_{T,i}^0$	Formation standard enthalpy at $T$ for species $i$ [ $\text{kJ kmol}^{-1}$ ]
$h$	Specific enthalpy of the gas [ $\text{kJ kmol}^{-1}$ ]
$I$	The second order unit tensor
$K_i$	Reaction equilibrium constant, dimensionless
$k_r$	Reaction rate coefficient [ $\text{mol}^{(1-\alpha)} \text{ m}^{3(1-\alpha)} \text{ s}^{-1}$ ]
$k$	Turbulent kinetic energy [ $\text{m}^2 \text{ s}^{-2}$ ]
$n_i$	Mole of species $i$ [mol]
$P_g$	Gas pressure [Pa]
$P_o$	Initial gas pressure [Pa]
$\bar{Q}_{\text{com}}$	The mean source term due to radiative heat transfer [W]
$\bar{Q}_r$	Mean source term due to volatile chemical reactions [W]
$r_{i,r}$	Rate of reaction for $i$ th species and $r$ th reaction
$S_m$	Gas formation rate due to thermochemical conversion
$S_u$	Source term due to momentum exchange between the gas and the solid phase
$\bar{S}_q$	The mean source term due to thermochemical conversion of the solid fuel
$\bar{S}_{Y_k}$	The mean formation rate of species $k$ due to thermochemical conversion of the solid fuel particles
$t$	Time instant [s]

$u_g$	Velocity vector of gas [m s <sup>-1</sup> ]
$y_i$	Mole fraction of gas species $i$ [mol]
$\tilde{Y}_{g,k}$	The mass fraction of species $k$ in the gas mixture

## Greek symbols

$\alpha$	Reaction order
$\alpha_g$	Gas volume fraction
$\beta$	Temperature exponent [1/K]
$\bar{\rho}_g$	Gas density [kg m <sup>-3</sup> ]
$\mu_i$	Chemical potential of species $i$
$\mu_g$	Dynamic viscosity [Pa s]
$\tau_g$	The sum of viscous stress and Reynolds stress [s]
$\Gamma_{\text{eff}}$	The sum of molecular and turbulent heat diffusion coefficients [m <sup>2</sup> s <sup>-1</sup> ]
$\lambda_i$	Lagrange multipliers
$\lambda_g$	Gas thermal conductivity [J (m <sup>-1</sup> s <sup>-1</sup> K <sup>-1</sup> )]

## Data availability

No primary research results, software or code have been included, and no new data were generated or analysed as part of this review.

## Author contributions

Sonu Kumar: writing – original draft preparation, conceptualization, data analysis. Rupesh Palange: writing: editing and review, formal analysis, supervision. Cataldo De Blasio: supervision, writing – review and edit, formal analysis, funding acquisition.

## Conflicts of interest

Authors declare no conflict of interest.

## Acknowledgements

Authors acknowledge funding from the following projects: Högskolestiftelsen i Österbotten (Project no: 28600166), EU ERUF: 901449 Mapping CO<sub>2</sub> Streams in Ostrobothnia: Unlocking Potential for the P2X Economy (MAP-UP-P2X), Business Finland, Kumppanuusmalli: 10446/31/2023 Ammonia energy conversion and social acceptance (AINA), Interreg Aurora: 20366523 Carbon-neutral low-processed fuel blending components for existing infrastructure (FOR BLEND).

## References

1. Janajreh, I. Adeyemi, S. S. Raza and C. Ghenai, A review of recent developments and future prospects in gasification systems and their modeling, *Renewable Sustainable Energy Rev.*, 2021, **138**, 110505, DOI: [10.1016/j.rser.2020.110505](https://doi.org/10.1016/j.rser.2020.110505).
2. N. Abas, A. Kalair and N. Khan, Review of fossil fuels and future energy technologies, *Futures*, 2015, **69**, 31–49, DOI: [10.1016/j.futures.2015.03.003](https://doi.org/10.1016/j.futures.2015.03.003).
3. A. Saffe, A. Fernandez, G. Mazza and R. Rodriguez, Prediction of regional agro-industrial wastes characteristics by thermogravimetric analysis to obtain bioenergy using thermal process, *Energy Explor. Exploit.*, 2019, **37**(1), 544–557, DOI: [10.1177/0144598718793908](https://doi.org/10.1177/0144598718793908).
4. S. Azat, A. V. Korobeinyk, K. Moustakas and V. J. Inglezakis, Sustainable production of pure silica from rice husk waste in Kazakhstan, *J. Cleaner Prod.*, 2019, **217**, 352–359, DOI: [10.1016/j.jclepro.2019.01.142](https://doi.org/10.1016/j.jclepro.2019.01.142).
5. K. Srirangan, L. Akawi, M. Moo-Young and C. P. Chou, Towards sustainable production of clean energy carriers from biomass resources, *Appl. Energy*, 2012, **100**, 172–186, DOI: [10.1016/j.apenergy.2012.05.012](https://doi.org/10.1016/j.apenergy.2012.05.012).
6. R. Reschmeier and J. Karl, Experimental study of wood char gasification kinetics in fluidized beds, *Biomass Bioenergy*, 2016, **85**, 288–299, DOI: [10.1016/j.biombioe.2015.05.029](https://doi.org/10.1016/j.biombioe.2015.05.029).
7. S. Wang, D. Kong, R. Shan, J. Gu, H. Yuan and Y. Chen, Comparative study on the effect of H<sub>2</sub>O/air/CO<sub>2</sub> on the gasification results of wheat straw, *Biomass Bioenergy*, 2025, **197**, 107807, DOI: [10.1016/j.biombioe.2025.107807](https://doi.org/10.1016/j.biombioe.2025.107807).
8. Z. Pan, *et al.*, Thermodynamic analyses of synthetic natural gas production via municipal solid waste gasification, high-temperature water electrolysis and methanation, *Energy Convers. Manage.*, 2019, **202**, 112160, DOI: [10.1016/j.enconman.2019.112160](https://doi.org/10.1016/j.enconman.2019.112160).
9. M. Puig-Arnavat, J. C. Bruno and A. Coronas, Review and analysis of biomass gasification models, *Renewable Sustainable Energy Rev.*, 2010, **14**(9), 2841–2851, DOI: [10.1016/j.rser.2010.07.030](https://doi.org/10.1016/j.rser.2010.07.030).
10. J. Wei, *et al.*, A review on reactivity characteristics and synergy behavior of biomass and coal Co-gasification, *Int. J. Hydrogen Energy*, 2021, **46**(33), 17116–17132, DOI: [10.1016/j.ijhydene.2021.02.162](https://doi.org/10.1016/j.ijhydene.2021.02.162).
11. A. Giuffrida, M. C. Romano and G. Lozza, Thermodynamic analysis of air-blown gasification for IGCC applications, *Appl. Energy*, 2011, **88**(11), 3949–3958, DOI: [10.1016/j.apenergy.2011.04.009](https://doi.org/10.1016/j.apenergy.2011.04.009).
12. A. L. Ahmad, N. H. M. Yasin, C. J. C. Derek and J. K. Lim, Microalgae as a sustainable energy source for biodiesel production: a review, *Renewable Sustainable Energy Rev.*, 2011, **15**(1), 584–593, DOI: [10.1016/j.rser.2010.09.018](https://doi.org/10.1016/j.rser.2010.09.018).
13. *Biomass to Renewable Energy Processes*, ed. Jay Cheng, CRC Press, 2nd edn, 2017, DOI: [10.1201/9781315152868](https://doi.org/10.1201/9781315152868).
14. P. Quaak, H. Knoef and H. E. Stassen, *Energy from Biomass: A Review of Combustion and Gasification Technologies*, World Bank Technical Paper 422, Washington, DC: World Bank Publications, 1999, Accessed via World Bank Digital Library, Availability: <http://worldcat.org/isbn/0821343351>.
15. C. Higman, *State of the gasification industry: worldwide gasification and syngas databases*, 2016, <https://www.netl.doe.gov/sites/default/files/2021-04/2016-Wed-Higman.pdf>.
16. J. Ochoa, M. C. Cassanello, P. R. Bonelli and A. L. Cukierman, CO<sub>2</sub> gasification of Argentinean coal chars: a kinetic characterization, *Fuel Process. Technol.*, 2001, **74**(3), 161–176, DOI: [10.1016/S0378-3820\(01\)00235-1](https://doi.org/10.1016/S0378-3820(01)00235-1).



17 T. K. Patra and P. N. Sheth, Biomass gasification models for downdraft gasifier: a state-of-the-art review, *Renewable Sustainable Energy Rev.*, 2015, **50**, 583–593, DOI: [10.1016/j.rser.2015.05.012](https://doi.org/10.1016/j.rser.2015.05.012).

18 J. G. Speight, Feedstocks, in *Gasification of Unconventional Feedstocks*, Elsevier, 2014, pp. 1–29, DOI: [10.1016/B978-0-12-799911-1.00001-7](https://doi.org/10.1016/B978-0-12-799911-1.00001-7).

19 <https://www.agflow.com/agricultural-markets-news/global-rapeseed-demand-to-hit-82-million-tons/>.

20 T.-H. Tsui and J. W. C. Wong, A critical review: emerging bioeconomy and waste-to-energy technologies for sustainable municipal solid waste management, *Waste Disposal Sustainable Energy*, 2019, **1**(3), 151–167, DOI: [10.1007/s42768-019-00013-z](https://doi.org/10.1007/s42768-019-00013-z).

21 J. G. Speight, *Handbook of Gasification Technology: Science, Technology, and Processes*, Wiley-Scribner, Hoboken, NJ, USA, 2020, ISBN 978-1-118-77353-6.

22 J. Hrbek, Past, present and future of thermal gasification of biomass and waste, *Acta Innov.*, 2020, **35**, 5–20, DOI: [10.32933/ActaInnovations.35.1](https://doi.org/10.32933/ActaInnovations.35.1).

23 P. Basu, Design of Biomass Gasifiers, in *Biomass Gasification, Pyrolysis and Torrefaction*, Elsevier, 2013, pp. 249–313, DOI: [10.1016/B978-0-12-396488-5.00008-3](https://doi.org/10.1016/B978-0-12-396488-5.00008-3).

24 D. Baruah and D. C. Baruah, Modeling of biomass gasification: A review, *Renewable Sustainable Energy Rev.*, 2014, **39**, 806–815, DOI: [10.1016/j.rser.2014.07.129](https://doi.org/10.1016/j.rser.2014.07.129).

25 P. Basu, *Combustion and Gasification in Fluidized Beds*, CRC Press, 2006, DOI: [10.1201/9781420005158](https://doi.org/10.1201/9781420005158).

26 J. Warnatz, *Combustion*, Springer Berlin Heidelberg, 2006, DOI: [10.1007/978-3-540-45363-5](https://doi.org/10.1007/978-3-540-45363-5).

27 S. Safarian, R. Unnþorsson and C. Richter, The equivalence of stoichiometric and non-stoichiometric methods for modeling gasification and other reaction equilibria, *Renewable Sustainable Energy Rev.*, 2020, **131**, 109982, DOI: [10.1016/j.rser.2020.109982](https://doi.org/10.1016/j.rser.2020.109982).

28 S. Safarian, R. Unnþorsson and C. Richter, A review of biomass gasification modelling, *Renewable Sustainable Energy Rev.*, 2019, **110**, 378–391, DOI: [10.1016/j.rser.2019.05.003](https://doi.org/10.1016/j.rser.2019.05.003).

29 J. M. de Andrés, M. Vedrenne, M. Brambilla and E. Rodríguez, Modeling and model performance evaluation of sewage sludge gasification in fluidized-bed gasifiers using Aspen Plus, *J. Air Waste Manage. Assoc.*, 2019, **69**(1), 23–33, DOI: [10.1080/10962247.2018.1500404](https://doi.org/10.1080/10962247.2018.1500404).

30 D. Cerinski, J. Baleta, H. Mikulčić, R. Mikulandrić and J. Wang, Dynamic modelling of the biomass gasification process in a fixed bed reactor by using the artificial neural network, *Clean. Eng. Technol.*, 2020, **1**, 100029, DOI: [10.1016/j.clet.2020.100029](https://doi.org/10.1016/j.clet.2020.100029).

31 G. Jankes, M. Trninic, M. Stamenic, T. Simonovic, N. Tanasic and J. Labus, Biomass gasification with CHP production: a review of state of the art technology and near future perspectives, *J. Therm. Sci.*, 2012, **16**(1), 115–130, DOI: [10.2298/TSCI120216066J](https://doi.org/10.2298/TSCI120216066J).

32 H.-K. Seo, *et al.*, Effects of operating factors in the coal gasification reaction, *Korean J. Chem. Eng.*, 2011, **28**(9), 1851–1858, DOI: [10.1007/s11814-011-0039-z](https://doi.org/10.1007/s11814-011-0039-z).

33 M. K. Karmakar and A. B. Datta, Generation of hydrogen rich gas through fluidized bed gasification of biomass, *Bioresour. Technol.*, 2011, **102**(2), 1907–1913, DOI: [10.1016/j.biortech.2010.08.015](https://doi.org/10.1016/j.biortech.2010.08.015).

34 S. Chopra and A. Jain, A Review of Fixed Bed Gasification Systems for Biomass, *Agricultural Engineering International: the CIGR Ejournal*, 2007, **IX**, 5, <https://www.researchgate.net/publication/228668672>.

35 R. Warnecke, Gasification of biomass: comparison of fixed bed and fluidized bed gasifier, *Biomass Bioenergy*, 2000, **18**(6), 489–497, DOI: [10.1016/S0961-9534\(00\)00009-X](https://doi.org/10.1016/S0961-9534(00)00009-X).

36 J. P. Ciferno and J. J. Marano, *Benchmarking Biomass Gasification Technologies for Fuels, Chemicals and Hydrogen Production*, U.S. Department of Energy National Energy Technology Laboratory, Washington, DC, 2002, [https://netl.doe.gov/sites/default/files/netl-file/BMassGasFinal\\_0.pdf](https://netl.doe.gov/sites/default/files/netl-file/BMassGasFinal_0.pdf).

37 S. S. A. Syed-Hassan, Y. Wang, S. Hu, S. Su and J. Xiang, Thermochemical processing of sewage sludge to energy and fuel: fundamentals, challenges and considerations, *Renewable Sustainable Energy Rev.*, 2017, **80**, 888–913, DOI: [10.1016/j.rser.2017.05.262](https://doi.org/10.1016/j.rser.2017.05.262).

38 A. Ramos, E. Monteiro and A. Rouboa, Numerical approaches and comprehensive models for gasification process: a review, *Renewable Sustainable Energy Rev.*, 2019, **110**, 188–206, DOI: [10.1016/j.rser.2019.04.048](https://doi.org/10.1016/j.rser.2019.04.048).

39 P. Gopalakrishnan, *Modelling of Biomass Steam Gasification in a Bubbling Fluidized Bed Gasifier*, 2025, <https://ir.canterbury.ac.nz/server/api/core/bitstreams/2c62a1c1-8424-4de6-8109-4b3c3f43b4c2/content>.

40 A. Kushwah, T. R. Reina and M. Short, Modelling approaches for biomass gasifiers: a comprehensive overview, *Sci. Total Environ.*, 2022, **834**, 155243, DOI: [10.1016/j.scitotenv.2022.155243](https://doi.org/10.1016/j.scitotenv.2022.155243).

41 P. Silva Ortiz, S. Maier, R.-U. Dietrich, A. Pinto Mariano, R. Maciel Filho and J. Posada, Comparative Techno-Economic and Exergetic Analysis of Circulating and Dual Bed Biomass Gasification Systems, *Front. Chem. Eng.*, 2021, **3**, DOI: [10.3389/fceng.2021.727068](https://doi.org/10.3389/fceng.2021.727068).

42 A. Bogaerts, E. Neyts, R. Gijbels and J. van der Mullen, Gas discharge plasmas and their applications, *Spectrochim. Acta, Part B*, 2002, **57**(4), 609–658, DOI: [10.1016/S0584-8547\(01\)00406-2](https://doi.org/10.1016/S0584-8547(01)00406-2).

43 M. T. Munir, I. Mardon, S. Al-Zuhair, A. Shawabkeh and N. U. Saqib, Plasma gasification of municipal solid waste for waste-to-value processing, *Renewable Sustainable Energy Rev.*, 2019, **116**, 109461, DOI: [10.1016/j.rser.2019.109461](https://doi.org/10.1016/j.rser.2019.109461).

44 A. Ramos, J. Berzosa, J. Espí, F. Clarens and A. Rouboa, Life cycle costing for plasma gasification of municipal solid waste: a socio-economic approach, *Energy Convers. Manage.*, 2020, **209**, 112508, DOI: [10.1016/j.enconman.2020.112508](https://doi.org/10.1016/j.enconman.2020.112508).

45 A. Chanthakett, M. T. Arif, M. M. K. Khan and A. M. T. Oo, Performance assessment of gasification reactors for sustainable management of municipal solid waste, *J. Environ. Monit.*, 2022, **24**(12), 2833–2844, DOI: [10.1039/DENV00220A](https://doi.org/10.1039/DENV00220A).



*Environ. Manage.*, 2021, **291**, 112661, DOI: [10.1016/j.jenvman.2021.112661](https://doi.org/10.1016/j.jenvman.2021.112661).

46 S. M. Santos, A. C. Assis, L. Gomes, C. Nobre and P. Brito, Waste Gasification Technologies: A Brief Overview, *Waste*, 2022, **1**(1), 140–165, DOI: [10.3390/waste1010011](https://doi.org/10.3390/waste1010011).

47 A. Molino, S. Chianese and D. Musmarra, Biomass gasification technology: the state of the art overview, *J. Energy Chem.*, 2016, **25**(1), 10–25, DOI: [10.1016/j.jechem.2015.11.005](https://doi.org/10.1016/j.jechem.2015.11.005).

48 E. Gomez, D. A. Rani, C. R. Cheeseman, D. Deegan, M. Wise and A. R. Boccaccini, Thermal plasma technology for the treatment of wastes: a critical review, *J. Hazard. Mater.*, 2009, **161**(2–3), 614–626, DOI: [10.1016/j.jhazmat.2008.04.017](https://doi.org/10.1016/j.jhazmat.2008.04.017).

49 G. C. Young, *Municipal Solid Waste to Energy Conversion Processes*, Wiley, 2010, DOI: [10.1002/9780470608616](https://doi.org/10.1002/9780470608616).

50 H. A. Arafat, K. Jijakli and A. Ahsan, Environmental performance and energy recovery potential of five processes for municipal solid waste treatment, *J. Cleaner Prod.*, 2015, **105**, 233–240, DOI: [10.1016/j.jclepro.2013.11.071](https://doi.org/10.1016/j.jclepro.2013.11.071).

51 C. Ducharme, *Technical and economic analysis of Plasma-assisted Waste-to-Energy processes*, 2010, [https://wttert.org/wp-content/uploads/2020/10/ducharme\\_thesis.pdf](https://wttert.org/wp-content/uploads/2020/10/ducharme_thesis.pdf).

52 B. Assamoi and Y. Lawryshyn, The environmental comparison of landfilling vs. incineration of MSW accounting for waste diversion, *Waste Manage.*, 2012, **32**(5), 1019–1030, DOI: [10.1016/j.wasman.2011.10.023](https://doi.org/10.1016/j.wasman.2011.10.023).

53 A. S. Mednikov, A Review of Technologies for Multistage Wood Biomass Gasification, *Therm. Eng.*, 2018, **65**(8), 531–546, DOI: [10.1134/S0040601518080037](https://doi.org/10.1134/S0040601518080037).

54 J. Cai, S. Wang, Q. Wang and C. Kuang, The characteristics of biomass gasification in multistage heating and gradient chain gasifier, *Int. J. Hydrogen Energy*, 2016, **41**(35), 15674–15681, DOI: [10.1016/j.ijhydene.2016.04.128](https://doi.org/10.1016/j.ijhydene.2016.04.128).

55 R. N. Singh, S. P. Singh and J. B. Balwanshi, Tar removal from producer gas: A review, 2014, [https://wttert.org/wp-content/uploads/2020/10/ducharme\\_thesis.pdf](https://wttert.org/wp-content/uploads/2020/10/ducharme_thesis.pdf).

56 M. Dhrioua, W. Hassen, L. Kolsi, K. Ghachem, C. Maatki and M. N. Borjini, Simulation of Prosopis juliflora Air Gasification in Multistage Fluidized Process, *Processes*, 2020, **8**(12), 1655, DOI: [10.3390/pr8121655](https://doi.org/10.3390/pr8121655).

57 A. R. Saleh, B. Sudarmanta, H. Fansuri and O. Muraza, Improved Municipal Solid Waste Gasification Efficiency Using a Modified Downdraft Gasifier with Variations of Air Input and Preheated Air Temperature, *Energy Fuels*, 2019, **33**(11), 11049–11056, DOI: [10.1021/acs.energyfuels.9b02486](https://doi.org/10.1021/acs.energyfuels.9b02486).

58 H. Liu, Y. Tang, X. Ma and W. Yue, Efficient production of tunable syngas through multistage sorption-enhanced steam gasification of corncobs, *Int. J. Hydrogen Energy*, 2024, **55**, 1242–1253, DOI: [10.1016/j.ijhydene.2023.11.279](https://doi.org/10.1016/j.ijhydene.2023.11.279).

59 C. S. Lee, A. V. Conradie and E. Lester, Review of supercritical water gasification with lignocellulosic real biomass as the feedstocks: process parameters, biomass composition, catalyst development, reactor design and its challenges, *Chem. Eng. J.*, 2021, **415**, 128837, DOI: [10.1016/j.cej.2021.128837](https://doi.org/10.1016/j.cej.2021.128837).

60 J. Chen, *et al.*, Process in supercritical water gasification of coal: a review of fundamentals, mechanisms, catalysts and element transformation, *Energy Convers. Manage.*, 2021, **237**, 114122, DOI: [10.1016/j.enconman.2021.114122](https://doi.org/10.1016/j.enconman.2021.114122).

61 C. De Blasio, *et al.*, A study on supercritical water gasification of black liquor conducted in stainless steel and nickel-chromium-molybdenum reactors, *J. Chem. Technol. Biotechnol.*, 2016, **91**(10), 2664–2678, DOI: [10.1002/jctb.4871](https://doi.org/10.1002/jctb.4871).

62 A. Kruse and E. Dinjus, Hot compressed water as reaction medium and reactant, *J. Supercrit. Fluids*, 2007, **39**(3), 362–380, DOI: [10.1016/j.supflu.2006.03.016](https://doi.org/10.1016/j.supflu.2006.03.016).

63 T. R. Sarker, F. Pattnaik, S. Nanda, A. K. Dalai, V. Meda and S. Naik, Hydrothermal pretreatment technologies for lignocellulosic biomass: a review of steam explosion and subcritical water hydrolysis, *Chemosphere*, 2021, **284**, 131372, DOI: [10.1016/j.chemosphere.2021.131372](https://doi.org/10.1016/j.chemosphere.2021.131372).

64 M. E. M. Soudagar, *et al.*, Organic municipal solid waste derived hydrogen production through supercritical water gasification process configured with K<sub>2</sub>CO<sub>3</sub>/SiO<sub>2</sub>: performance study, *Biomass Bioenergy*, 2024, **190**, 107379, DOI: [10.1016/j.biombioe.2024.107379](https://doi.org/10.1016/j.biombioe.2024.107379).

65 F. Liu, *et al.*, Thermodynamic and environmental analysis of two-stage series supercritical water gasification of biomass for hydrogen production, *Biomass Bioenergy*, 2024, **190**, 107415, DOI: [10.1016/j.biombioe.2024.107415](https://doi.org/10.1016/j.biombioe.2024.107415).

66 M. Akizuki, T. Fujii, R. Hayashi and Y. Oshima, Effects of water on reactions for waste treatment, organic synthesis, and bio-refinery in sub- and supercritical water, *J. Biosci. Bioeng.*, 2014, **117**(1), 10–18, DOI: [10.1016/j.jbiosc.2013.06.011](https://doi.org/10.1016/j.jbiosc.2013.06.011).

67 J. Chen, *et al.*, Thermodynamic, environmental analysis and comprehensive evaluation of supercritical water gasification of biomass fermentation residue, *J. Cleaner Prod.*, 2022, **361**, 132126, DOI: [10.1016/j.jclepro.2022.132126](https://doi.org/10.1016/j.jclepro.2022.132126).

68 C. De Blasio, S. De Gisi, A. Molino, M. Simonetti, M. Santarelli and M. Björklund-Säkiaho, Concerning operational aspects in supercritical water gasification of kraft black liquor, *Renewable Energy*, 2019, **130**, 891–901, DOI: [10.1016/j.renene.2018.07.004](https://doi.org/10.1016/j.renene.2018.07.004).

69 Y. Chen, L. Yi, W. Wei, H. Jin and L. Guo, Hydrogen production by sewage sludge gasification in supercritical water with high heating rate batch reactor, *Energy*, 2022, **238**, 121740, DOI: [10.1016/j.energy.2021.121740](https://doi.org/10.1016/j.energy.2021.121740).

70 A. Molino, *et al.*, Municipal waste leachate conversion via catalytic supercritical water gasification process, *Fuel*, 2017, **206**, 155–161.

71 X. Li, Z. Wu, H. Wang and H. Jin, The effect of particle wake on the heat transfer characteristics between interactive particles in supercritical water, *Chem. Eng. Sci.*, 2022, **247**, 117030, DOI: [10.1016/j.ces.2021.117030](https://doi.org/10.1016/j.ces.2021.117030).

72 Y. Li, H. Wang, J. Shi, C. Cao and H. Jin, Numerical simulation on natural convection and temperature distribution of supercritical water in a side-wall heated



cavity, *J. Supercrit. Fluids*, 2022, **181**, 105465, DOI: [10.1016/j.supflu.2021.105465](https://doi.org/10.1016/j.supflu.2021.105465).

73 L. Guo, H. Jin and Y. Lu, Supercritical water gasification research and development in China, *J. Supercrit. Fluids*, 2015, **96**, 144–150, DOI: [10.1016/j.supflu.2014.09.023](https://doi.org/10.1016/j.supflu.2014.09.023).

74 S. Kumar, P. K. Vijayan, S. Gangwar and S. S. Bhogilla, CFD Analysis of the Steady-State Performance of a Cooktop Integrated Thermosyphon Heat Transport Device With Two Bends, *Heat Transfer Eng.*, 2025, **47**, 1–12, DOI: [10.1080/01457632.2025.2521603](https://doi.org/10.1080/01457632.2025.2521603).

75 D. Xu, X. Gu and Y. Dai, Concentrating solar assisted biomass-to-fuel conversion through gasification: a review, *Front. Energy Res.*, 2023, **10**, DOI: [10.3389/fenrg.2022.1029477](https://doi.org/10.3389/fenrg.2022.1029477).

76 R. Adinberg and M. Epstein, *Development of Solar Coal Gasification Technology*, American Society of Mechanical Engineers, 1996.

77 A. Steinfeld, Solar thermal production of zinc and syngas via combined ZnO-reduction and CH<sub>4</sub>-reforming processes, *Int. J. Hydrogen Energy*, 1995, **20**(10), 793–804, DOI: [10.1016/0360-3199\(95\)00016-7](https://doi.org/10.1016/0360-3199(95)00016-7).

78 R. W. Taylor, R. Berjoan and J. P. Coutures, Solar gasification of carbonaceous materials, *Sol. Energy*, 1983, **30**(6), 513–525, DOI: [10.1016/0038-092X\(83\)90063-4](https://doi.org/10.1016/0038-092X(83)90063-4).

79 A. Karapekmez and I. Dincer, Development of a new solar, gasification and fuel cell based integrated plant, *Int. J. Hydrogen Energy*, 2022, **47**(6), 4196–4210, DOI: [10.1016/j.ijhydene.2021.11.011](https://doi.org/10.1016/j.ijhydene.2021.11.011).

80 N. Piatkowski, C. Wieckert, A. W. Weimer and A. Steinfeld, Solar-driven gasification of carbonaceous feedstock—a review, *Energy Environ. Sci.*, 2011, **4**(1), 73–82, DOI: [10.1039/C0EE00312C](https://doi.org/10.1039/C0EE00312C).

81 Ö. Tezer, N. Karabağ, A. Öngen, C. Ö. Çolpan and A. Ayol, Biomass gasification for sustainable energy production: a review, *Int. J. Hydrogen Energy*, 2022, **47**(34), 15419–15433, DOI: [10.1016/j.ijhydene.2022.02.158](https://doi.org/10.1016/j.ijhydene.2022.02.158).

82 S. Ferreira, E. Monteiro, P. Brito and C. Vilarinho, A Comprehensive Review on Biomass Gasification Modified Equilibrium Models, in *Advances in Energy Research*, Vide Leaf, Hyderabad, 2020, DOI: [10.37247/AER.1.2020.7](https://doi.org/10.37247/AER.1.2020.7).

83 M. La Villette, M. Costa and N. Massarotti, Modelling approaches to biomass gasification: a review with emphasis on the stoichiometric method, *Renewable Sustainable Energy Rev.*, 2017, **74**, 71–88, DOI: [10.1016/j.rser.2017.02.027](https://doi.org/10.1016/j.rser.2017.02.027).

84 A. Źogała, Critical Analysis of Underground Coal Gasification Models. Part I: Equilibrium Models – Literary Studies, *J. Sustain. Min.*, 2014, **13**(1), 22–28, DOI: [10.7424/jsm140105](https://doi.org/10.7424/jsm140105).

85 C. Loha, S. Gu, J. De Wilde, P. Mahanta and P. K. Chatterjee, Advances in mathematical modeling of fluidized bed gasification, *Renewable Sustainable Energy Rev.*, 2014, **40**, 688–715, DOI: [10.1016/j.rser.2014.07.199](https://doi.org/10.1016/j.rser.2014.07.199).

86 M. La Villette, M. Costa and N. Massarotti, Modelling approaches to biomass gasification: a review with emphasis on the stoichiometric method, *Renewable Sustainable Energy Rev.*, 2017, **74**, 71–88, DOI: [10.1016/j.rser.2017.02.027](https://doi.org/10.1016/j.rser.2017.02.027).

87 L. Moretti, F. Arpino, G. Cortellessa, S. Di Fraia, M. Di Palma and L. Vanoli, Reliability of Equilibrium Gasification Models for Selected Biomass Types and Compositions: An Overview, *Energies*, 2021, **15**(1), 61, DOI: [10.3390/en15010061](https://doi.org/10.3390/en15010061).

88 M. Ajorloo, M. Ghodrat, J. Scott and V. Strezov, Recent advances in thermodynamic analysis of biomass gasification: a review on numerical modelling and simulation, *J. Energy Inst.*, 2022, **102**, 395–419, DOI: [10.1016/j.joei.2022.05.003](https://doi.org/10.1016/j.joei.2022.05.003).

89 A. Mountouris, E. Voutsas and D. Tassios, Solid waste plasma gasification: equilibrium model development and exergy analysis, *Energy Convers. Manage.*, 2006, **47**(13–14), 1723–1737, DOI: [10.1016/j.enconman.2005.10.015](https://doi.org/10.1016/j.enconman.2005.10.015).

90 V. B. Silva and A. Rouboa, Using a two-stage equilibrium model to simulate oxygen air enriched gasification of pine biomass residues, *Fuel Process. Technol.*, 2013, **109**, 111–117, DOI: [10.1016/j.fuproc.2012.09.045](https://doi.org/10.1016/j.fuproc.2012.09.045).

91 E. S. Aydin, O. Yucel and H. Sadikoglu, Development of a semi-empirical equilibrium model for downdraft gasification systems, *Energy*, 2017, **130**, 86–98, DOI: [10.1016/j.energy.2017.04.132](https://doi.org/10.1016/j.energy.2017.04.132).

92 S. Ferreira, E. Monteiro, P. Brito and C. Vilarinho, A Holistic Review on Biomass Gasification Modified Equilibrium Models, *Energies*, 2019, **12**(1), 160, DOI: [10.3390/en12010160](https://doi.org/10.3390/en12010160).

93 D. Cvetinović, A. Erić, N. Milutinović, N. Petrov, J. Andelković and V. Bakić, Thermodynamic equilibrium modeling of biomass gasification: effects of operating conditions on gasifier performance, *J. King Saud Univ. Sci.*, 2024, **36**(9), 103370, DOI: [10.1016/j.jksus.2024.103370](https://doi.org/10.1016/j.jksus.2024.103370).

94 L. Liao, J. Zheng, C. Li, R. Liu and Y. Zhang, Thermodynamic modeling modification and experimental validation of entrained-flow gasification of biomass, *J. Energy Inst.*, 2022, **103**, 160–168, DOI: [10.1016/j.joei.2022.06.006](https://doi.org/10.1016/j.joei.2022.06.006).

95 A. Farajollahi, S. A. Hejazirad and M. Rostami, Thermodynamic modeling of a power and hydrogen generation system driven by municipal solid waste gasification, *Environ. Dev. Sustain.*, 2022, **24**(4), 5887–5916, DOI: [10.1007/s10668-021-01690-9](https://doi.org/10.1007/s10668-021-01690-9).

96 R. Bijesh, P. Arun and C. Muraleedharan, Modified stoichiometric equilibrium model for sewage sludge gasification and its validation based on experiments in a downdraft gasifier, *Biomass Convers. Biorefin.*, 2023, **13**(10), 9023–9043, DOI: [10.1007/s13399-021-01916-w](https://doi.org/10.1007/s13399-021-01916-w).

97 D. A. Buentello-Montoya, C. A. Duarte-Ruiz and J. F. Maldonado-Escalante, Co-gasification of waste PET, PP and biomass for energy recovery: a thermodynamic model to assess the produced syngas quality, *Energy*, 2023, **266**, 126510, DOI: [10.1016/j.energy.2022.126510](https://doi.org/10.1016/j.energy.2022.126510).

98 A. Ibrahim, S. Veremieiev and P. H. Gaskell, An advanced, comprehensive thermochemical equilibrium model of a downdraft biomass gasifier, *Renewable Energy*, 2022, **194**, 912–925, DOI: [10.1016/j.renene.2022.05.069](https://doi.org/10.1016/j.renene.2022.05.069).



99 M. Pilar González-Vázquez, F. Rubiera, C. Pevida, D. T. Pio and L. A. C. Tarelho, Thermodynamic Analysis of Biomass Gasification Using Aspen Plus: Comparison of Stoichiometric and Non-Stoichiometric Models, *Energies*, 2021, **14**(1), 189, DOI: [10.3390/en14010189](https://doi.org/10.3390/en14010189).

100 S. Q. Nie, M. Q. Chen and Q. H. Li, Evaluation on hydrothermal gasification of waste tires based on chemical equilibrium analysis, *Int. J. Hydrogen Energy*, 2022, **47**(3), 1435–1448, DOI: [10.1016/j.ijhydene.2021.10.233](https://doi.org/10.1016/j.ijhydene.2021.10.233).

101 Q. Dang, X. Zhang, Y. Zhou and X. Jia, Prediction and optimization of syngas production from a kinetic-based biomass gasification process model, *Fuel Process. Technol.*, 2021, **212**, 106604, DOI: [10.1016/j.fuproc.2020.106604](https://doi.org/10.1016/j.fuproc.2020.106604).

102 R. Palange and M. Krishnan, Coal gasification process optimization for maximum calorific value and minimum CO<sub>2</sub> emission using Taguchi method and utility concept, *Int. J. Energy Environ. Eng.*, 2021, **12**(2), 335–351, DOI: [10.1007/s40095-020-00377-7](https://doi.org/10.1007/s40095-020-00377-7).

103 C. T. Alves, J. A. Onwudili, P. Ghorbannezhad and S. Kumagai, A review of the thermochemistries of biomass gasification and utilisation of gas products, *Sustainable Energy Fuels*, 2023, **7**(15), 3505–3540, DOI: [10.1039/D3SE00365E](https://doi.org/10.1039/D3SE00365E).

104 A. M. A. Ahmed, A. Salmiaton, T. S. Y. Choong and W. A. K. G. Wan Azlina, Review of kinetic and equilibrium concepts for biomass tar modeling by using Aspen Plus, *Renewable Sustainable Energy Rev.*, 2015, **52**, 1623–1644, DOI: [10.1016/j.rser.2015.07.125](https://doi.org/10.1016/j.rser.2015.07.125).

105 R. Palange and M. Krishnan, A novel two-zone sequential optimization model for pyro-oxidation and reduction reactions in a downdraft gasifier, *RSC Adv.*, 2023, **13**(14), 9128–9141, DOI: [10.1039/D3RA00667K](https://doi.org/10.1039/D3RA00667K).

106 R. Palange and M. Krishnan, Three zone kinetic model for characteristic analysis of heat loss parameters in a downdraft gasifier, *Proc. Inst. Mech. Eng., Part E*, 2023, 09544089231190307.

107 P. Evans, T. Paskach and J. Reardon, Detailed kinetic modeling to predict syngas composition from biomass gasification in a PBFB reactor, *Environ. Prog. Sustainable Energy*, 2010, **29**(2), 184–192, DOI: [10.1002/ep.10464](https://doi.org/10.1002/ep.10464).

108 E. Ranzi, M. Dente, A. Goldaniga, G. Bozzano and T. Faravelli, Lumping procedures in detailed kinetic modeling of gasification, pyrolysis, partial oxidation and combustion of hydrocarbon mixtures, *Prog. Energy Combust. Sci.*, 2001, **27**(1), 99–139, DOI: [10.1016/S0360-1285\(00\)00013-7](https://doi.org/10.1016/S0360-1285(00)00013-7).

109 M. S. Eikeland, R. K. Thapa and B. M. Halvorsen, Aspen Plus Simulation of Biomass Gasification with Known Reaction Kinetic, *56th Conference on Simulation and Modelling (SIMS 56)*, Linköping University, Sweden, 2015, pp. 149–156, DOI: [10.3384/ecp15119149](https://doi.org/10.3384/ecp15119149).

110 L. Abdelouahed, O. Authier, G. Mauviel, J. P. Corriou, G. Verdier and A. Dufour, Detailed Modeling of Biomass Gasification in Dual Fluidized Bed Reactors under Aspen Plus, *Energy Fuels*, 2012, **26**(6), 3840–3855, DOI: [10.1021/ef300411k](https://doi.org/10.1021/ef300411k).

111 G. Várhegyi, L. Wang and Ø. Skreiber, Empirical Kinetic Models for the CO<sub>2</sub> Gasification of Biomass Chars. Part 1. Gasification of Wood Chars and Forest Residue Chars, *ACS Omega*, 2021, **6**(41), 27552–27560, DOI: [10.1021/acsomega.1c04577](https://doi.org/10.1021/acsomega.1c04577).

112 M. Beirow, A. M. Parvez, M. Schmid and G. Scheffknecht, A Detailed One-Dimensional Hydrodynamic and Kinetic Model for Sorption Enhanced Gasification, *Appl. Sci.*, 2020, **10**(17), 6136, DOI: [10.3390/app10176136](https://doi.org/10.3390/app10176136).

113 J. Gil, J. Corella, M. P. Aznar and M. A. Caballero, Biomass gasification in atmospheric and bubbling fluidized bed: effect of the type of gasifying agent on the product distribution, *Biomass Bioenergy*, 1999, **17**(5), 389–403, DOI: [10.1016/S0961-9534\(99\)00055-0](https://doi.org/10.1016/S0961-9534(99)00055-0).

114 D. L. Giltrap, R. McKibbin and G. R. G. Barnes, A steady state model of gas-char reactions in a downdraft biomass gasifier, *Sol. Energy*, 2003, **74**(1), 85–91, DOI: [10.1016/S0038-092X\(03\)00091-4](https://doi.org/10.1016/S0038-092X(03)00091-4).

115 J. Yu and J. D. Smith, Validation and application of a kinetic model for biomass gasification simulation and optimization in updraft gasifiers, *Chem. Eng. Process.*, 2018, **125**, 214–226, DOI: [10.1016/j.cep.2018.02.003](https://doi.org/10.1016/j.cep.2018.02.003).

116 M. Dai, T. Guo, X. Hu, J. Ma and Q. Guo, Simulation of a 1MWth biomass chemical looping gasification process based on kinetic and pyrolysis models, *Int. J. Hydrogen Energy*, 2024, **80**, 298–307, DOI: [10.1016/j.ijhydene.2024.07.154](https://doi.org/10.1016/j.ijhydene.2024.07.154).

117 M. HajiHashemi, *et al.*, Combined heat and power production in a pilot-scale biomass gasification system: experimental study and kinetic simulation using ASPEN Plus, *Energy*, 2023, **276**, 127506, DOI: [10.1016/j.energy.2023.127506](https://doi.org/10.1016/j.energy.2023.127506).

118 K. Viswanathan, S. Abbas and W. Wu, Syngas analysis by hybrid modeling of sewage sludge gasification in downdraft reactor: validation and optimization, *Waste Manage.*, 2022, **144**, 132–143, DOI: [10.1016/j.jwasman.2022.03.018](https://doi.org/10.1016/j.jwasman.2022.03.018).

119 Y. Cao, Y. Bai and J. Du, Air-steam gasification of biomass based on a multi-composition multi-step kinetic model: a clean strategy for hydrogen-enriched syngas production, *Sci. Total Environ.*, 2021, **753**, 141690, DOI: [10.1016/j.scitotenv.2020.141690](https://doi.org/10.1016/j.scitotenv.2020.141690).

120 J. Qi, Y. Wang, M. Hu, P. Xu, H. Yuan and Y. Chen, A reactor network of biomass gasification process in an updraft gasifier based on the fully kinetic model, *Energy*, 2023, **268**, 126642, DOI: [10.1016/j.energy.2023.126642](https://doi.org/10.1016/j.energy.2023.126642).

121 H. Li, *et al.*, Supercritical water gasification of lignocellulosic biomass: development of a general kinetic model for prediction of gas yield, *Chem. Eng. J.*, 2022, **433**, 133618, DOI: [10.1016/j.cej.2021.133618](https://doi.org/10.1016/j.cej.2021.133618).

122 H. S. O. Qatan, W. A. Wan Ab Karim Ghani and M. S. Md Said, Prediction and optimization of syngas production from Napier grass air gasification via kinetic modelling and response surface methodology, *Energy*, 2023, **270**, 126883, DOI: [10.1016/j.energy.2023.126883](https://doi.org/10.1016/j.energy.2023.126883).



123 A. Korus, *et al.*, Kinetic parameters of petroleum coke gasification for modelling chemical-looping combustion systems, *Energy*, 2021, **232**, 120935, DOI: [10.1016/j.energy.2021.120935](https://doi.org/10.1016/j.energy.2021.120935).

124 M. Puig-Gamero, D. T. Pio, L. A. C. Tarelho, P. Sánchez and L. Sanchez-Silva, Simulation of biomass gasification in bubbling fluidized bed reactor using aspen plus®, *Energy Convers. Manage.*, 2021, **235**, 113981, DOI: [10.1016/j.enconman.2021.113981](https://doi.org/10.1016/j.enconman.2021.113981).

125 R. Palange, C. De Blasio and M. Krishnan, Energy and exergy analysis of gasification of solid fuels by optimization of chemical kinetics, *Energy*, 2023, **285**, 129487, DOI: [10.1016/j.energy.2023.129487](https://doi.org/10.1016/j.energy.2023.129487).

126 S. Polesek-Karczewska, P. Hercel, B. Adibimanesh and I. Wardach-Świeticka, Towards Sustainable Biomass Conversion Technologies: A Review of Mathematical Modeling Approaches, *Sustainability*, 2024, **16**(19), 8719, DOI: [10.3390/su16198719](https://doi.org/10.3390/su16198719).

127 W. Yi, *et al.*, An improved gasification kinetic model for biochar with high alkali and alkaline earth metals content, *Fuel*, 2023, **342**, 127849, DOI: [10.1016/j.fuel.2023.127849](https://doi.org/10.1016/j.fuel.2023.127849).

128 I. Janajreh and M. Al Shrah, Numerical and experimental investigation of downdraft gasification of wood chips, *Energy Convers. Manage.*, 2013, **65**, 783–792, DOI: [10.1016/j.enconman.2012.03.009](https://doi.org/10.1016/j.enconman.2012.03.009).

129 A. Rogel and J. Aguilón, The 2D Eulerian Approach of Entrained Flow and Temperature in a Biomass Stratified Downdraft Gasifier, *Am. J. Appl. Sci.*, 2006, **3**(10), 2068–2075.

130 C. Hasse, P. Debiagi, X. Wen, K. Hildebrandt, M. Vascellari and T. Faravelli, Advanced modeling approaches for CFD simulations of coal combustion and gasification, *Prog. Energy Combust. Sci.*, 2021, **86**, 100938, DOI: [10.1016/j.pecs.2021.100938](https://doi.org/10.1016/j.pecs.2021.100938).

131 M. Sakhraji, A. Ramos, E. Monteiro, K. Bouziane and A. Rouboa, Plasma gasification process using computational fluid dynamics modeling, *Energy Rep.*, 2022, **8**, 1541–1549, DOI: [10.1016/j.egyr.2022.08.069](https://doi.org/10.1016/j.egyr.2022.08.069).

132 H. Askaripour, CFD modeling of gasification process in tapered fluidized bed gasifier, *Energy*, 2020, **191**, 116515, DOI: [10.1016/j.energy.2019.116515](https://doi.org/10.1016/j.energy.2019.116515).

133 B. Pandey, Y. K. Prajapati and P. N. Sheth, CFD analysis of biomass gasification using downdraft gasifier, *Mater. Today: Proc.*, 2021, **44**, 4107–4111, DOI: [10.1016/j.matpr.2020.10.451](https://doi.org/10.1016/j.matpr.2020.10.451).

134 D. M. Yépés Maya, E. E. Silva Lora, R. V. Andrade, A. Ratner and J. D. Martínez Angel, Biomass gasification using mixtures of air, saturated steam, and oxygen in a two-stage downdraft gasifier. Assessment using a CFD modeling approach, *Renewable Energy*, 2021, **177**, 1014–1030, DOI: [10.1016/j.renene.2021.06.051](https://doi.org/10.1016/j.renene.2021.06.051).

135 R. P, J. K. Singh, A. Sahoo and S. S. Mohapatra, CFD simulation for coal gasification in fluidized bed gasifier, *Energy*, 2023, **281**, 128272, DOI: [10.1016/j.energy.2023.128272](https://doi.org/10.1016/j.energy.2023.128272).

136 K. W. Kuttin, A. Leghari, H. Yu, Z. Xia, L. Ding and G. Yu, Carbon dioxide-steam reforming gasification of carbonized biomass pellet for high syngas yield and TAR reduction through CFD modeling, *Chem. Eng. Sci.*, 2024, **287**, 119716, DOI: [10.1016/j.ces.2024.119716](https://doi.org/10.1016/j.ces.2024.119716).

137 L. von Berg, A. Anca-Couce, C. Hochenauer and R. Scharler, Multi-scale modelling of fluidized bed biomass gasification using a 1D particle model coupled to CFD, *Fuel*, 2022, **324**, 124677, DOI: [10.1016/j.fuel.2022.124677](https://doi.org/10.1016/j.fuel.2022.124677).

138 H. Liu, R. J. Cattolica and R. Seiser, CFD studies on biomass gasification in a pilot-scale dual fluidized-bed system, *Int. J. Hydrogen Energy*, 2016, **41**(28), 11974–11989, DOI: [10.1016/j.ijhydene.2016.04.205](https://doi.org/10.1016/j.ijhydene.2016.04.205).

139 A. M. Salem and M. C. Paul, CFD modelling of spatiotemporal evolution of detailed tar species in a downdraft gasifier, *Biomass Bioenergy*, 2023, **168**, 106656, DOI: [10.1016/j.biombioe.2022.106656](https://doi.org/10.1016/j.biombioe.2022.106656).

140 Z. Yu, Z. Wang, H. Zhong and K. Cheng, Essential aspects of the CFD software modelling of biomass gasification processes in downdraft reactors, *RSC Adv.*, 2024, **14**(39), 28724–28739, DOI: [10.1039/D4RA04886E](https://doi.org/10.1039/D4RA04886E).

141 J. Yu, L. Lu, Y. Xu, X. Gao, M. Shahnam and W. Rogers, Coarse-Grained CFD-DEM Simulation and the Design of an Industrial-Scale Coal Gasifier, *Ind. Eng. Chem. Res.*, 2022, **61**(1), 866–881, DOI: [10.1021/acs.iecr.1c03386](https://doi.org/10.1021/acs.iecr.1c03386).

142 Q. Yang, J. Zhang, J. Zhou, L. Zhao and D. Zhang, A hybrid data-driven machine learning framework for predicting the performance of coal and biomass gasification processes, *Fuel*, 2023, **346**, 128338, DOI: [10.1016/j.fuel.2023.128338](https://doi.org/10.1016/j.fuel.2023.128338).

143 F. Alfarra, H. K. Ozcan, P. Cihan, A. Ongen, S. Y. Guvenc and M. N. Ciner, Artificial intelligence methods for modeling gasification of waste biomass: a review, *Environ. Monit. Assess.*, 2024, **196**(3), 309, DOI: [10.1007/s10661-024-12443-2](https://doi.org/10.1007/s10661-024-12443-2).

144 S. Ascher, I. Watson and S. You, Machine learning methods for modelling the gasification and pyrolysis of biomass and waste, *Renewable Sustainable Energy Rev.*, 2022, **155**, 111902, DOI: [10.1016/j.rser.2021.111902](https://doi.org/10.1016/j.rser.2021.111902).

145 M. Puig-Arnavat, J. A. Hernández, J. C. Bruno and A. Coronas, Artificial neural network models for biomass gasification in fluidized bed gasifiers, *Biomass Bioenergy*, 2013, **49**, 279–289, DOI: [10.1016/j.biombioe.2012.12.012](https://doi.org/10.1016/j.biombioe.2012.12.012).

146 Y. Zhou, W. Li and Y. Song, ANN model of co-gasification process in bubbling fluidized bed: contribution ratio analysis, *Int. J. Hydrogen Energy*, 2024, **73**, 10–19, DOI: [10.1016/j.ijhydene.2024.06.007](https://doi.org/10.1016/j.ijhydene.2024.06.007).

147 J. George, P. Arun and C. Muraleedharan, Assessment of producer gas composition in air gasification of biomass using artificial neural network model, *Int. J. Hydrogen Energy*, 2018, **43**(20), 9558–9568, DOI: [10.1016/j.ijhydene.2018.04.007](https://doi.org/10.1016/j.ijhydene.2018.04.007).

148 H. O. Kargbo, J. Zhang and A. N. Phan, Optimisation of two-stage biomass gasification for hydrogen production via artificial neural network, *Appl. Energy*, 2021, **302**, 117567, DOI: [10.1016/j.apenergy.2021.117567](https://doi.org/10.1016/j.apenergy.2021.117567).

149 S. Ren, S. Wu, Q. Weng, B. Zhu and Z. Deng, Disentangled Representation Aided Physics-Informed Neural Network for Predicting Syngas Compositions of Biomass Gasification,



*Energy Fuels*, 2024, **38**(3), 2033–2045, DOI: [10.1021/acs.energyfuels.3c03496](https://doi.org/10.1021/acs.energyfuels.3c03496).

150 Ö. Ç. Mutlu and T. Zeng, Challenges and Opportunities of Modeling Biomass Gasification in Aspen Plus: A Review, *Chem. Eng. Technol.*, 2020, **43**(9), 1674–1689, DOI: [10.1002/ceat.202000068](https://doi.org/10.1002/ceat.202000068).

151 V. Kirsanovs, Biomass gasification thermodynamic model including tar and char, *Agronomy Research*, 2016, **14**, 1321–1331, [https://agronomy.emu.ee/wp-content/uploads/2016/06/Vol14\\_nr4\\_Kirsanovs.pdf](https://agronomy.emu.ee/wp-content/uploads/2016/06/Vol14_nr4_Kirsanovs.pdf).

152 A. Sharma and R. Nath, Chemical Kinetic Modeling of Air-Steam Gasification of Eucalyptus Wood Sawdust for H<sub>2</sub>-Rich Syngas Production, *ACS Omega*, 2023, **8**(14), 13396–13409, DOI: [10.1021/acsomega.3c00908](https://doi.org/10.1021/acsomega.3c00908).

153 Z. Yu, Z. Wang, H. Zhong and K. Cheng, Essential aspects of the CFD software modelling of biomass gasification processes in downdraft reactors, *RSC Adv.*, 2024, **14**(39), 28724–28739, DOI: [10.1039/D4RA04886E](https://doi.org/10.1039/D4RA04886E).

154 *Coal-to-liquids and polygeneration using low rank coals*, 2017, <https://www.sciencedirect.com/topics/engineering/methanation#:~:text=Methanation%20is%20a%20chemical%20reaction,Sendersens%20in%201902>.

155 H. Hiller, *et al.*, Gas Production, in *Ullmann's Encyclopedia of Industrial Chemistry*, Wiley-VCH Verlag GmbH & Co. KGaA, Weinheim, Germany, 2006, DOI: [10.1002/14356007.a12\\_169.pub2](https://doi.org/10.1002/14356007.a12_169.pub2).

156 J. Kopyscinski, T. J. Schildhauer and S. M. A. Biollaz, Production of synthetic natural gas (SNG) from coal and dry biomass – A technology review from 1950 to 2009, *Fuel*, 2010, **89**(8), 1763–1783, DOI: [10.1016/j.fuel.2010.01.027](https://doi.org/10.1016/j.fuel.2010.01.027).

157 J. Ren, Y.-L. Liu, X.-Y. Zhao and J.-P. Cao, Methanation of syngas from biomass gasification: an overview, *Int. J. Hydrogen Energy*, 2020, **45**(7), 4223–4243, DOI: [10.1016/j.ijhydene.2019.12.023](https://doi.org/10.1016/j.ijhydene.2019.12.023).

158 S. Sharma, Z. Hu, P. Zhang, E. W. McFarland and H. Metiu, CO<sub>2</sub> methanation on Ru-doped ceria, *J. Catal.*, 2011, **278**(2), 297–309, DOI: [10.1016/j.jcat.2010.12.015](https://doi.org/10.1016/j.jcat.2010.12.015).

159 A. Trovarelli, C. Deleitenburg, G. Dolcetti and J. L. Lorca, CO<sub>2</sub> Methanation Under Transient and Steady-State Conditions over Rh/CeO<sub>2</sub> and CeO<sub>2</sub>-Promoted Rh/SiO<sub>2</sub>: The Role of Surface and Bulk Ceria, *J. Catal.*, 1995, **151**(1), 111–124, DOI: [10.1006/jcat.1995.1014](https://doi.org/10.1006/jcat.1995.1014).

160 R. J. Isaifan, M. Couillard and E. A. Baranova, Low temperature-high selectivity carbon monoxide methanation over yttria-stabilized zirconia-supported Pt nanoparticles, *Int. J. Hydrogen Energy*, 2017, **42**(19), 13754–13762, DOI: [10.1016/j.ijhydene.2017.01.049](https://doi.org/10.1016/j.ijhydene.2017.01.049).

161 H. Liu, X. Zou, X. Wang, X. Lu and W. Ding, Effect of CeO<sub>2</sub> addition on Ni/Al<sub>2</sub>O<sub>3</sub> catalysts for methanation of carbon dioxide with hydrogen, *J. Nat. Gas Chem.*, 2012, **21**(6), 703–707, DOI: [10.1016/S1003-9953\(11\)60422-2](https://doi.org/10.1016/S1003-9953(11)60422-2).

162 A. Zhao, W. Ying, H. Zhang, H. Ma and D. Fang, Ni-Al<sub>2</sub>O<sub>3</sub> catalysts prepared by solution combustion method for syngas methanation, *Catal. Commun.*, 2012, **17**, 34–38, DOI: [10.1016/j.catcom.2011.10.010](https://doi.org/10.1016/j.catcom.2011.10.010).

163 D. Schmider, L. Maier and O. Deutschmann, Reaction Kinetics of CO and CO<sub>2</sub> Methanation over Nickel, *Ind. Eng. Chem. Res.*, 2021, **60**(16), 5792–5805, DOI: [10.1021/acs.iecr.1c00389](https://doi.org/10.1021/acs.iecr.1c00389).

164 B. Ciccone, F. Murena, G. Ruoppolo, M. Urciuolo and P. Brachi, Methanation of syngas from biomass gasification: small-scale plant design in Aspen Plus, *Appl. Therm. Eng.*, 2024, **246**, 122901, DOI: [10.1016/j.applthermaleng.2024.122901](https://doi.org/10.1016/j.applthermaleng.2024.122901).

165 T. J. Schildhauer and S. M. A. Biollaz, Reactors for Catalytic Methanation in the Conversion of Biomass to Synthetic Natural Gas (SNG), *Chimia*, 2015, **69**(10), 603, DOI: [10.2533/chimia.2015.603](https://doi.org/10.2533/chimia.2015.603).

166 M. V. Twigg, *Catalyst Handbook*, Routledge, 2018, DOI: [10.1201/9781315138862](https://doi.org/10.1201/9781315138862).

167 R. P. Anderson, J. R. Fincke and C. E. Taylor, Conversion of natural gas to liquids via acetylene as an intermediate, *Fuel*, 2002, **81**(7), 909–925, DOI: [10.1016/S0016-2361\(01\)00188-0](https://doi.org/10.1016/S0016-2361(01)00188-0).

168 F. Wang, S. Deng, J. Zhao, J. Wang, T. Sun and J. Yan, Performance and economic assessments of integrating geothermal energy into coal-fired power plant with CO<sub>2</sub> capture, *Energy*, 2017, **119**, 278–287, DOI: [10.1016/j.energy.2016.12.029](https://doi.org/10.1016/j.energy.2016.12.029).

169 H. Ishaq and I. Dincer, Comparative assessment of renewable energy-based hydrogen production methods, *Renewable Sustainable Energy Rev.*, 2021, **135**, 110192, DOI: [10.1016/j.rser.2020.110192](https://doi.org/10.1016/j.rser.2020.110192).

170 A. Saadi, M. Becherif and H. S. Ramadan, Hydrogen production horizon using solar energy in Biskra, Algeria, *Int. J. Hydrogen Energy*, 2016, **41**(47), 21899–21912, DOI: [10.1016/j.ijhydene.2016.08.224](https://doi.org/10.1016/j.ijhydene.2016.08.224).

171 F. Almomani, M. Shawaqfah and M. Alkasrawi, Solar-driven hydrogen production from a water-splitting cycle based on carbon-TiO<sub>2</sub> nano-tubes, *Int. J. Hydrogen Energy*, 2022, **47**(5), 3294–3305, DOI: [10.1016/j.ijhydene.2020.12.191](https://doi.org/10.1016/j.ijhydene.2020.12.191).

172 Zulphazli, A. R. Keeley, S. Takeda and S. Managi, A systematic review of the techno-economic assessment of various hydrogen production methods of power generation, *Front. Sustain.*, 2022, **3**, 2673–4524, DOI: [10.3389/frsus.2022.943145](https://doi.org/10.3389/frsus.2022.943145).

173 A. Demirbas, Combustion characteristics of different biomass fuels, *Prog. Energy Combust. Sci.*, 2004, **30**(2), 219–230, DOI: [10.1016/j.pecs.2003.10.004](https://doi.org/10.1016/j.pecs.2003.10.004).

174 R. Kothari, D. Buddhi and R. L. Sawhney, Sources and technology for hydrogen production: a review, *Int. J. Glob. Energy Issues*, 2004, **21**(1–2), 154, DOI: [10.1504/IJGEI.2004.004707](https://doi.org/10.1504/IJGEI.2004.004707).

175 S. E. Hosseini and M. A. Wahid, Hydrogen production from renewable and sustainable energy resources: promising green energy carrier for clean development, *Renewable Sustainable Energy Rev.*, 2016, **57**, 850–866, DOI: [10.1016/j.rser.2015.12.112](https://doi.org/10.1016/j.rser.2015.12.112).

176 J. Udomsirichakorn and P. A. Salam, Review of hydrogen-enriched gas production from steam gasification of biomass: the prospect of CaO-based chemical looping gasification, *Renewable Sustainable Energy Rev.*, 2014, **30**, 565–579, DOI: [10.1016/j.rser.2013.10.013](https://doi.org/10.1016/j.rser.2013.10.013).



177 D. B. Pal, A. Singh and A. Bhatnagar, A review on biomass based hydrogen production technologies, *Int. J. Hydrogen Energy*, 2022, **47**(3), 1461–1480, DOI: [10.1016/j.ijhydene.2021.10.124](https://doi.org/10.1016/j.ijhydene.2021.10.124).

178 S. Mukhopadhyay, Solar energy and gasification of MSW: two promising green energy options, in *Green Energy Systems*, Elsevier, 2023, pp. 93–125, DOI: [10.1016/B978-0-323-95108-1.00003-3](https://doi.org/10.1016/B978-0-323-95108-1.00003-3).

179 J. D. Ampah, *et al.*, Investigating the evolutionary trends and key enablers of hydrogen production technologies: a patent-life cycle and econometric analysis, *Int. J. Hydrogen Energy*, 2023, **48**(96), 37674–37707, DOI: [10.1016/j.ijhydene.2022.07.258](https://doi.org/10.1016/j.ijhydene.2022.07.258).

180 M. Wang, G. Wang, Z. Sun, Y. Zhang and D. Xu, Review of renewable energy-based hydrogen production processes for sustainable energy innovation, *Glob. Energy Interconnect.*, 2019, **2**(5), 436–443, DOI: [10.1016/j.gloei.2019.11.019](https://doi.org/10.1016/j.gloei.2019.11.019).

181 Y. Yan, *et al.*, Process simulations of blue hydrogen production by upgraded sorption enhanced steam methane reforming (SE-SMR) processes, *Energy Convers. Manage.*, 2020, **222**, 113144, DOI: [10.1016/j.enconman.2020.113144](https://doi.org/10.1016/j.enconman.2020.113144).

182 S. Ghavam, M. Vahdati, I. A. G. Wilson and P. Styring, Sustainable Ammonia Production Processes, *Front. Energy Res.*, 2021, **9**, 580808, DOI: [10.3389/fenrg.2021.580808](https://doi.org/10.3389/fenrg.2021.580808).

183 S. Joseph Sekhar, A. Said Ahmed Al-Shahri, G. Glivin, T. Le and T. Mathimani, A critical review of the state-of-the-art green ammonia production technologies-mechanism, advancement, challenges, and future potential, *Fuel*, 2024, **358**, 130307, DOI: [10.1016/j.fuel.2023.130307](https://doi.org/10.1016/j.fuel.2023.130307).

184 KBR, *Ammonia & Fertilizers Technologies*, 2025, <https://www.kbr.com/en/what-we-do/technologies/cleanprocess-technologies/ammonia-fertilizers-technologies>, <https://www.sciencedirect.com/topics/engineering/methanation#:~:text=Methanation%20is%20a%20chemical%20reaction,Sendersens%20in%201902>.

185 W. B. Wang, X. B. Cao, W. J. Gao, F. Zhang, H. T. Wang and G. L. Ma, Ammonia synthesis at atmospheric pressure using a reactor with thin solid electrolyte BaCe0.85Y0.15O3- $\alpha$  membrane, *J. Membr. Sci.*, 2010, **360**(1–2), 397–403, DOI: [10.1016/j.memsci.2010.05.038](https://doi.org/10.1016/j.memsci.2010.05.038).

186 J. Tang, L. Kang and Y. Liu, Design and Optimization of a Clean Ammonia Synthesis System Based on Biomass Gasification Coupled with a Ca–Cu Chemical Loop, *Ind. Eng. Chem. Res.*, 2022, **61**(23), 8128–8140, DOI: [10.1021/acs.iecr.2c00616](https://doi.org/10.1021/acs.iecr.2c00616).

187 Q. Weng, S. Toan, R. Ai, Z. Sun and Z. Sun, Ammonia production from biomass via a chemical looping-based hybrid system, *J. Cleaner Prod.*, 2021, **289**, 125749, DOI: [10.1016/j.jclepro.2020.125749](https://doi.org/10.1016/j.jclepro.2020.125749).

188 IEA, *The Role of Low-Carbon Fuels in the Clean Energy Transitions of the Power Sector*, OECD Publishing, Paris, 2021, DOI: [10.1787/a92fe011-en](https://doi.org/10.1787/a92fe011-en).

189 J. H. Montoya, C. Tsai, A. Vojvodic and J. K. Nørskov, The Challenge of Electrochemical Ammonia Synthesis: A New Perspective on the Role of Nitrogen Scaling Relations, *ChemSusChem*, 2015, **8**(13), 2180–2186, DOI: [10.1002/cssc.201500322](https://doi.org/10.1002/cssc.201500322).

190 H. Shen, *et al.*, Electrochemical ammonia synthesis: mechanistic understanding and catalyst design, *Chem*, 2021, **7**(7), 1708–1754, DOI: [10.1016/j.chempr.2021.01.009](https://doi.org/10.1016/j.chempr.2021.01.009).

191 A. Poluzzi, G. Guandalini, F. d'Amore and M. C. Romano, The Potential of Power and Biomass-to-X Systems in the Decarbonization Challenge: a Critical Review, *Curr. Sustainable/Renewable Energy Rep.*, 2021, **8**(4), 242–252, DOI: [10.1007/s40518-021-00191-7](https://doi.org/10.1007/s40518-021-00191-7).

192 M. Dossow, D. Klüh, K. Umeki, M. Gaderer, H. Spliethoff and S. Fendt, Electrification of gasification-based biomass-to-X processes – a critical review and in-depth assessment, *Energy Environ. Sci.*, 2024, **17**(3), 925–973, DOI: [10.1039/D3EE02876C](https://doi.org/10.1039/D3EE02876C).

193 F. Mantei, M. Kraume and O. Salem, Improved Energy Efficiency of Power-to-X Processes Using Heat Pumps Towards Mobility Sector Defossilization, *Chem. Ing. Tech.*, 2023, **95**(6), 912–924, DOI: [10.1002/cite.202200118](https://doi.org/10.1002/cite.202200118).

194 F. G. Albrecht, D. H. König, N. Baucks and R.-U. Dietrich, A standardized methodology for the techno-economic evaluation of alternative fuels – A case study, *Fuel*, 2017, **194**, 511–526, DOI: [10.1016/j.fuel.2016.12.003](https://doi.org/10.1016/j.fuel.2016.12.003).

195 S. Mucci, A. Mitsos and D. Bongartz, Combustion versus Gasification in Power- and Biomass-to-X Processes: An Exergetic Analysis, *ACS Omega*, 2024, **9**(49), 48213–48231, DOI: [10.1021/acsomega.4c05549](https://doi.org/10.1021/acsomega.4c05549).

196 S. Müller, *et al.*, Production of diesel from biomass and wind power – Energy storage by the use of the Fischer-Tropsch process, *Biomass Convers. Biorefin.*, 2018, **8**(2), 275–282, DOI: [10.1007/s13399-017-0287-1](https://doi.org/10.1007/s13399-017-0287-1).

197 C. Choe, S. Cheon, H. Kim and H. Lim, Mitigating climate change for negative CO<sub>2</sub> emission via syngas methanation: Techno-economic and life-cycle assessments of renewable methane production, *Renewable Sustainable Energy Rev.*, 2023, **185**, 113628, DOI: [10.1016/j.rser.2023.113628](https://doi.org/10.1016/j.rser.2023.113628).

198 Q. Hassan, *et al.*, The renewable energy role in the global energy Transformations, *Renew. Energy Focus*, 2024, **48**, 100545, DOI: [10.1016/j.ref.2024.100545](https://doi.org/10.1016/j.ref.2024.100545).

199 A. Evans, V. Strezov and T. J. Evans, Assessment of sustainability indicators for renewable energy technologies, *Renewable Sustainable Energy Rev.*, 2009, **13**(5), 1082–1088, DOI: [10.1016/j.rser.2008.03.008](https://doi.org/10.1016/j.rser.2008.03.008).

200 U. Ahmed, *et al.*, Production of Hydrogen from Low Rank Coal Using Process Integration Framework between Syngas Production Processes: Techno-Economic Analysis, *Chem. Eng. Process.*, 2021, **169**, 108639, DOI: [10.1016/j.cep.2021.108639](https://doi.org/10.1016/j.cep.2021.108639).

201 M. Bibra, Technoeconomic analysis of hydrogen production, in *Renewable Hydrogen*, Elsevier, 2024, pp. 253–279, DOI: [10.1016/B978-0-323-95379-5.00015-8](https://doi.org/10.1016/B978-0-323-95379-5.00015-8).

202 H. R. Sara, B. Enrico, V. Mauro, D. C. Andrea and N. Vincenzo, Techno-economic Analysis of Hydrogen Production Using Biomass Gasification - A Small Scale Power Plant Study, *Energy Procedia*, 2016, **101**, 806–813, DOI: [10.1016/j.egypro.2016.11.102](https://doi.org/10.1016/j.egypro.2016.11.102).



203 J. Andersson and J. Lundgren, Techno-economic analysis of ammonia production via integrated biomass gasification, *Appl. Energy*, 2014, **130**, 484–490, DOI: [10.1016/j.apenergy.2014.02.029](https://doi.org/10.1016/j.apenergy.2014.02.029).

204 H. Zhang, L. Wang, J. Van herle, F. Maréchal and U. Desideri, Techno-economic comparison of green ammonia production processes, *Appl. Energy*, 2020, **259**, 114135, DOI: [10.1016/j.apenergy.2019.114135](https://doi.org/10.1016/j.apenergy.2019.114135).

205 Y. Kalinci, A. Hepbasli and I. Dincer, Life cycle assessment of hydrogen production from biomass gasification systems, *Int. J. Hydrogen Energy*, 2012, **37**(19), 14026–14039, DOI: [10.1016/j.ijhydene.2012.06.015](https://doi.org/10.1016/j.ijhydene.2012.06.015).

206 Y. K. Salkuyeh, B. A. Saville and H. L. MacLean, Techno-economic analysis and life cycle assessment of hydrogen production from different biomass gasification processes, *Int. J. Hydrogen Energy*, 2018, **43**(20), 9514–9528, DOI: [10.1016/j.ijhydene.2018.04.024](https://doi.org/10.1016/j.ijhydene.2018.04.024).

207 C. Koroneos, Life cycle assessment of hydrogen fuel production processes, *Int. J. Hydrogen Energy*, 2004, **29**(14), 1443–1450, DOI: [10.1016/j.ijhydene.2004.01.016](https://doi.org/10.1016/j.ijhydene.2004.01.016).

208 A. Susmozas, D. Iribarren and J. Dufour, Life-cycle performance of indirect biomass gasification as a green alternative to steam methane reforming for hydrogen production, *Int. J. Hydrogen Energy*, 2013, **38**(24), 9961–9972, DOI: [10.1016/j.ijhydene.2013.06.012](https://doi.org/10.1016/j.ijhydene.2013.06.012).

209 T. Kan, V. Strezov and T. J. Evans, Lignocellulosic biomass pyrolysis: a review of product properties and effects of pyrolysis parameters, *Renewable Sustainable Energy Rev.*, 2016, **57**, 1126–1140, DOI: [10.1016/j.rser.2015.12.185](https://doi.org/10.1016/j.rser.2015.12.185).

210 S. Singh, G. Pandey, G. K. Rath, H. P. Veluswamy and N. Molokitina, Life cycle assessment of biomass-based hydrogen production technologies: a review, *Int. J. Green Energy*, 2023, 1–16, DOI: [10.1080/15435075.2023.2245453](https://doi.org/10.1080/15435075.2023.2245453).

211 V. Singh, I. Dincer and M. A. Rosen, Life Cycle Assessment of Ammonia Production Methods, in *Exergetic, Energetic and Environmental Dimensions*, Elsevier, 2018, pp. 935–959, DOI: [10.1016/B978-0-12-813734-5.00053-6](https://doi.org/10.1016/B978-0-12-813734-5.00053-6).

212 Y. Bicer, I. Dincer, C. Zamfirescu, G. Vezina and F. Raso, Comparative life cycle assessment of various ammonia production methods, *J. Cleaner Prod.*, 2016, **135**, 1379–1395, DOI: [10.1016/j.jclepro.2016.07.023](https://doi.org/10.1016/j.jclepro.2016.07.023).

213 Y. N. Kanafin, *et al.*, Anaerobic Membrane Bioreactors for Municipal Wastewater Treatment: A Literature Review, *Membranes*, 2021, **11**(12), 967, DOI: [10.3390/membranes11120967](https://doi.org/10.3390/membranes11120967).

214 L. Fernández-Lobato, R. Aguado, F. Jurado and D. Vera, Biomass gasification as a key technology to reduce the environmental impact of virgin olive oil production: a Life Cycle Assessment approach, *Biomass Bioenergy*, 2022, **165**, 106585, DOI: [10.1016/j.biombioe.2022.106585](https://doi.org/10.1016/j.biombioe.2022.106585).

215 J. Guerrero, S. Sala, A. Fresneda-Cruz, I. Bolea, A. A. Carmona-Martínez and C. Jarauta-Córdoba, Techno-Economic Feasibility of Biomass Gasification for the Decarbonisation of Energy-Intensive Industries, *Energies*, 2023, **16**(17), 6271, DOI: [10.3390/en16176271](https://doi.org/10.3390/en16176271).

216 Y. Qiu, D. Zeng and R. Xiao, Hydrogen Production from Biomass-Based Chemical Looping: A Critical Review and Perspectives, *Energy Fuels*, 2024, **38**(15), 13819–13836, DOI: [10.1021/acs.energyfuels.4c02391](https://doi.org/10.1021/acs.energyfuels.4c02391).

217 V. Gogulancea, *et al.*, Technoeconomic and Environmental Assessment of Biomass Chemical Looping Gasification for Advanced Biofuel Production, *Int. J. Energy Res.*, 2023, **2023**, 1–17, DOI: [10.1155/2023/6101270](https://doi.org/10.1155/2023/6101270).

218 J. Lv, *et al.*, Thermodynamic and economic analysis of a conceptual system combining medical waste plasma gasification, SOFC, sludge gasification, supercritical CO<sub>2</sub> cycle, and desalination, *Energy*, 2023, **282**, 128866, DOI: [10.1016/j.energy.2023.128866](https://doi.org/10.1016/j.energy.2023.128866).

219 V. Nagar and R. Kaushal, A review of recent advancement in plasma gasification: a promising solution for waste management and energy production, *Int. J. Hydrogen Energy*, 2024, **77**, 405–419, DOI: [10.1016/j.ijhydene.2024.06.180](https://doi.org/10.1016/j.ijhydene.2024.06.180).

220 Y. Xin, W. Zhang, F. Chen, X. Xing, D. Han and H. Hong, Integrating solar-driven biomass gasification and PV-electrolysis for sustainable fuel production: thermodynamic performance, economic assessment, and CO<sub>2</sub> emission analysis, *Chem. Eng. J.*, 2024, **497**, 153941, DOI: [10.1016/j.cej.2024.153941](https://doi.org/10.1016/j.cej.2024.153941).

221 D. Hu, *et al.*, Techno-economic analysis of sewage sludge supercritical water gasification for hydrogen and electricity co-generation system, *Energy*, 2024, **313**, 134061, DOI: [10.1016/j.energy.2024.134061](https://doi.org/10.1016/j.energy.2024.134061).

222 V. S. Sikarwar, *et al.*, An overview of advances in biomass gasification, *Energy Environ. Sci.*, 2016, **9**(10), 2939–2977, DOI: [10.1039/C6EE00935B](https://doi.org/10.1039/C6EE00935B).

223 M. S. M. Said, W. A. K. Ghani, H. B. Tan and D. K. S. Ng, Prediction and optimisation of syngas production from air gasification of Napier grass via stoichiometric equilibrium model, *Energy Convers. Manage.:X*, 2021, **10**, 100057, DOI: [10.1016/j.ecmx.2020.100057](https://doi.org/10.1016/j.ecmx.2020.100057).

224 T. K. Tulu, S. M. Atnaw, R. D. Bededa, D. G. Wakshume and V. R. Ancha, Kinetic Modeling and Optimization of Biomass Gasification in Bubbling Fluidized Bed Gasifier Using Response Surface Method, *Int. J. Renewable Energy Dev.*, 2022, **11**(4), 1043–1059, DOI: [10.14710/ijred.2022.45179](https://doi.org/10.14710/ijred.2022.45179).

225 Y. Fang, M. C. Paul, S. Varjani, X. Li, Y.-K. Park and S. You, Concentrated solar thermochemical gasification of biomass: principles, applications, and development, *Renewable Sustainable Energy Rev.*, 2021, **150**, 111484, DOI: [10.1016/j.rser.2021.111484](https://doi.org/10.1016/j.rser.2021.111484).

226 D. B. Levin and R. Chahine, Challenges for renewable hydrogen production from biomass, *Int. J. Hydrogen Energy*, 2010, **35**(10), 4962–4969, DOI: [10.1016/j.ijhydene.2009.08.067](https://doi.org/10.1016/j.ijhydene.2009.08.067).

